The background image shows a wide, flat salt marsh landscape. In the foreground, there is a large amount of weathered, grey driftwood scattered across the green grass. In the middle ground, a long, low dam or dike structure stretches across the horizon. Two tall, thin masts or towers are visible on the dam. The sky is overcast and grey.

Potential Mechanisms for the Salt Marsh Recession on Sturgeon Bank

RICHARD MARIJNISSEN



Boskalis  **TU Delft**

[page left blank intentionally]

Potential Mechanisms for the Salt Marsh Recession on Sturgeon Bank

by

Richard Marijnissen

In partial fulfilment of the requirements

for the degree of

Master of Science

in Civil Engineering

at

Delft University of Technology

20th of January 2017

Graduation committee:

Prof.dr.ir. Stive, M.J.F.	Delft University of Technology	- Chairman
Prof.dr.ir Aarninkhof, S.G.J.	Delft University of Technology	
Dr. ir Borsje, B.W.	University of Twente	
Dr.ir. van Prooijen, B.C.	Delft University of Technology	
Drs. Rijks, D.	Royal Boskalis Westminster N.V.	

[page left blank intentionally]

PREFACE

The thesis would not have been possible without the help of many people who supported me along the way.:

From Canada I want to thank Port Metro Vancouver for their help in this project. Gord Ruffo, Kelsey-Rae Russel and Carolyn Parenteau, it was great working with you during my visit.

Thanks goes out to Sean Boyd and Kathleen Moore from Environment Canada, Brent Gurd from the Ministry of Forests, Lands and Natural Resource Operations, Brad Mason and of course *marsh men* Eric Balke and Derek Hogan. I have had so many wonderful discussions with you and want to thank you for your help out in the marsh.

From the Netherlands I want to thank the people at Boskalis. Also a great thanks to my graduation committee who guided me in this tricky subject.

Delft, December 2016

Richard Marijnissen

SUMMARY

Near Vancouver (Canada) at the mouth of the Fraser River a large amount of intertidal marshland has been lost at an alarming rate. In the area called Sturgeon Bank the marsh has receded 0.5km in the space of just 22 years or less. The marsh is an important part of the Fraser Delta as it supports migratory birds on the Pacific Flyway, it is used for recreation and is part of the coastal protection of the city of Richmond. This study is conducted to identify potential mechanisms for the recession of marsh on Sturgeon Bank.

The physical environment on Sturgeon Bank is characterised by a large tide and with relatively small wind-generated waves. During storms the wind blows from the west, almost perpendicular to Sturgeon Bank. The largest storm events from the past 30 years were identified in the years 2000, 2001 and 2003. The development of the marsh and flats was analysed by air photos and satellite imagery. The marsh had been stable or growing since at least the 1930's. Large-scale recession started only in the 1990's. The rate of retreat decreased exponentially in the 2000's to the point where the marsh appears stable in both the north and south. Furthermore, the satellite study shows a band of about 0.5 km in front of the current marsh edge where sediment has been eroded between 1990 and 2015. Soil investigation and elevation measurements show the north and centre of Sturgeon Bank has become significantly sandier between 2011 and 2016. Earlier samples from 1992 and 1993 imply a similar trend. This signifies erosion of fine particles and/or deposition of fine sand on the inner bank. The models in the study of flows and waves reveals the 0.4 m high, 60m long sandy bed forms named sand swells interact with the flow of the tide and the progression of waves during mean tide level when water depths are small. These features have migrated north-eastward between 1954 and 1979, and between 1986 and 2001.

Several hypotheses have been put forward at the start of the study in an effort to explain the marsh retreat. These hypotheses were evaluated by the results of the analyses carried out during the study of the actual site, satellite and aerial images, modelling, sediment grain sizes, and historic wind and water level records. A sediment deficit was found improbable given that erosion was not observed in recent years. The satellite study suggests erosion was episodic rather than structural. Sea-level rise could not be the primary cause. The amount of retreat that could be accounted for by the rate of sea-level rise was only 3 m/year, one order of magnitude too small to account for 500 m of marsh recession in at most 22 years. A movement of sand swells could initiate retreat of the marsh by blocking the tidal channels. However, the alleged movement of the sand swells by storms would only happen by 2000. At this point the marsh was already receding. Disturbance by algae could cause die-off of marsh locally, but examples in literature show that in most cases the marsh will restore unless other mechanisms are at play. Based on above results, it was clear that the hypotheses could not be substantiated and need to be adapted and/or combined into a more integral hypothesis. Based on the available data and the executed analyses, it remains unclear what the main reason or reasons are for the marsh recession.

TABLE OF CONTENTS

Preface.....	i
Summary	ii
Table of contents	iv
1 Introduction.....	1
1.1 Problem description.....	1
1.2 Research objectives.....	1
1.3 Thesis structure.....	1
2 Literature review.....	3
2.1 The sea of the strait of Georgia	3
2.2 Fraser river and Delta.....	3
2.3 Sturgeon Bank.....	5
2.4 Development of Sturgeon Bank.....	7
2.5 Development of neighbouring marshes.....	9
2.6 Salt marsh dynamics.....	10
3 Statistical Study.....	13
3.1 Tide.....	13
3.2 Waves	14
3.3 Wind and storms	15
4 Aerial Imagery.....	17
4.1 1930.....	17
4.2 1954.....	17
4.3 1979.....	17
4.4 1986.....	18
4.5 2001 to 2003.....	18
4.6 2005 to 2015.....	19
4.7 Summary of observed changes.....	20
5 Satellite study	21
5.1 Background on LandSat images.....	21

5.2	Selection of satellite images	21
5.3	Manual approach.....	21
5.4	Scripted approach.....	22
5.5	Results for tidal flats	23
5.6	Results for the marsh.....	24
6	Field study	26
6.1	Observations.....	26
6.2	Elevation measurements.....	28
6.3	Soil samples	29
7	Model study.....	31
7.1	Flow model	31
7.2	Wave model.....	32
8	Overview of changes on Sturgeon Bank.....	34
8.1	Before 1990	34
8.2	Marsh recession	34
8.3	Erosion and deposition.....	34
8.4	Soil composition	35
9	Potential retreat mechanisms.....	38
9.1	Framework.....	38
9.2	Reduced sediment supply.....	39
9.3	Relative sea-level rise.....	39
9.4	Sand swells.....	40
9.5	Ponding.....	41
9.6	Feedback mechanisms.....	42
10	Evaluation of potential retreat mechanisms	43
10.1	Reduced sediment supply.....	43
10.2	Relative sea-level rise.....	43
10.3	Sand swells.....	45
10.4	Ponding.....	45
10.5	Feedback mechanisms.....	46
11	Summary of potential mechanisms.....	48
12	Recommendations.....	50

12.1	Data collection	50
12.2	Morphological studies.....	50
12.3	Ecological studies.....	51
12.4	Pilot study.....	51
13	References.....	53
A.	Appendix 1: Maps and figures.....	A-1
B.	Appendix 2: Tide analysis, Method & assumptions.....	B-1
C.	Appendix 3: Inundation by the tide.....	C-1
D.	Appendix 4: Storm analysis, method and scripts.....	D-1
E.	Appendix 5: Sattelite study, scripts	E-1
F.	Appendix 6: Report of the fieldwork.....	F-1
G.	Appendix 7: Sediment analysis.....	G-1
H.	Appendix 8: Flow model.....	H-1
I.	Appendix 9: Wave model.....	I-7
J.	Appendix 10: Sand swells on Sturgeon Bank.....	J-1
K.	Appendix 11: Vertical refference datums.....	K-1
L.	Appendix 12: Research approach.....	L-1

1 INTRODUCTION

1.1 Problem description

South of the city of Vancouver (Canada) lies the Fraser delta. Located at the seaward edge between the arms of this river is Sturgeon Bank (Figure 1). It is a vast flat intertidal area that is submerged during high tide and exposed during low tide. On the interface between wet and dry an ecosystem has developed unique to the West Canadian coast.

The marsh on Sturgeon Bank is vital for hundreds of thousands of birds who visit the marsh as part of the Pacific Flyway (Ministry of Forests, Lands and Natural Resource Operations, 2015). It also serves as rearing habitat for salmon. Additionally, the dike trail along the marsh is used for recreation and the site is tourist destination for Richmond (Wood, 2014). Finally, Sturgeon Bank is part of the coastal defence of city of Richmond. The shallow foreshore of Sturgeon Bank reduces the wave height before it reaches the dike that separates the marsh from the city.

The marshes of Sturgeon Bank west of Richmond appear to have receded at an alarming rate. In 2011 a comparative field study on the effects of snow goose feeding brought to light that marsh had receded up to 500m since the earlier study in 1989 (Boyd, McKibbin, & Moore, *Unpublished*). Since then more studies have been conducted to establish the full scale of the retreat (Ilori, 2015; TRE Canada Inc., 2014) yet little is known about the mechanisms responsible for the die-back at the Sturgeon Bank marsh.

1.2 Research objectives

The objective of the research is to:

- identify potential mechanisms for the retreat of the salt marsh on Sturgeon Bank
- determine how they contribute to the retreat
- Provide recommendations for mitigating these processes and restoring the marsh.

The objectives are structured such that it covers the entire process from identifying the problem, determining the causes to finally reaching a solution. As such each objective builds on the previous one to reach the final objective.

1.3 Thesis structure

First the current literature will be reviewed for the current state of knowledge on the processes on Sturgeon Bank as well as documentation for historic salt-marsh development (Ch. 2). This knowledge is expanded by analyses of time series of wind and water levels (Ch. 3), air photos (Ch. 4), satellite images (Ch. 5) and complemented by a field study (Ch.6). The results and implications are summarized in Ch. 8. Based on the results, hypotheses are presented for the marsh recession (Ch. 9) and evaluated (Ch. 10). The results of the recession are summarised in Ch. 11. Finally, recommendations are presented to restore the marsh and suggestions for further research (Ch. 12).

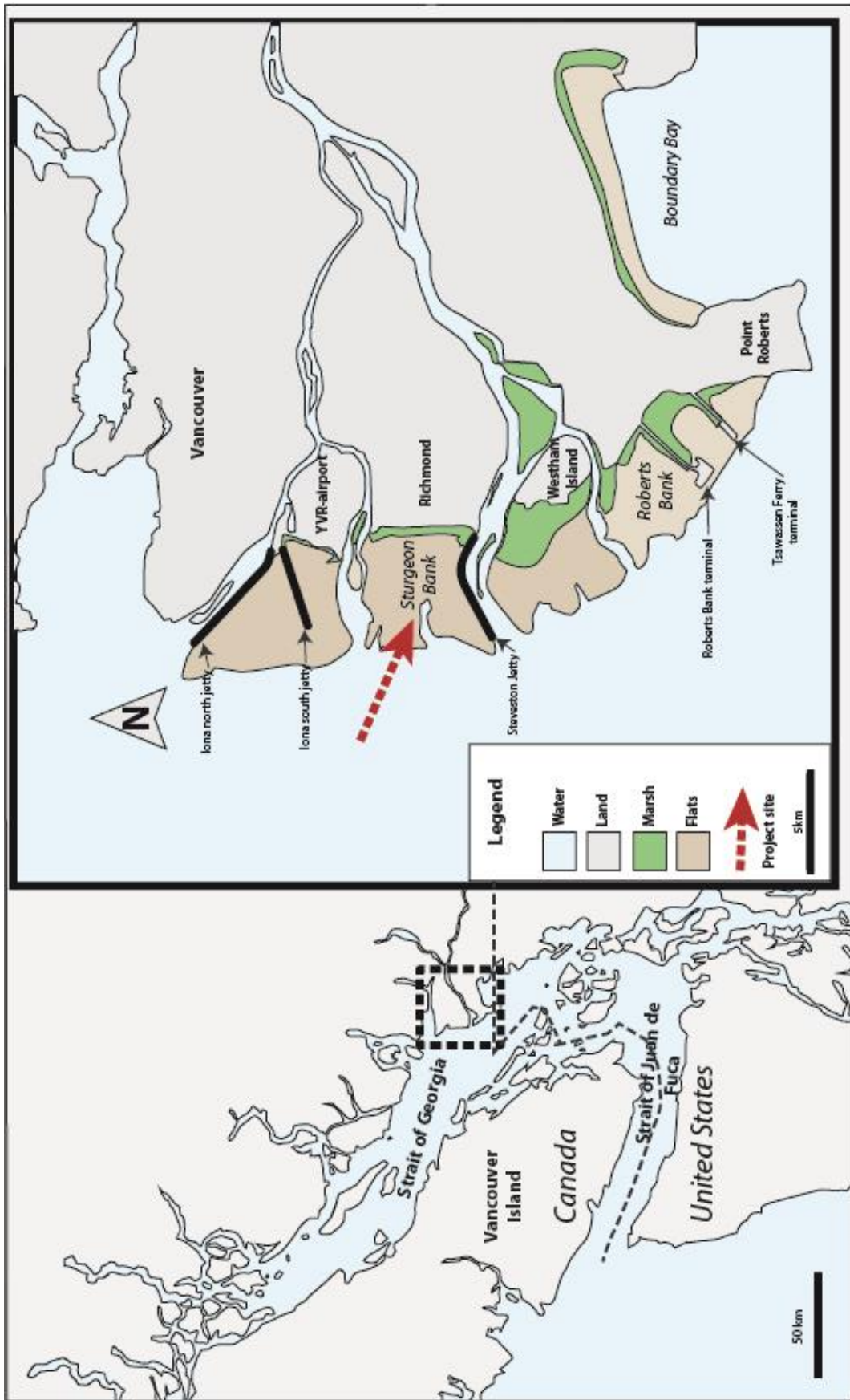


Figure 1 The location of Sturgeon Bank

2 LITERATURE REVIEW

2.1 The sea of the strait of Georgia

The Strait of Georgia is part of a larger system called the Salish sea. It extends from the Desolation Sound in Canada to the Puget Sound basin south in the U.S (depicted in figure 1). The Strait of Georgia is on average 220 km long, 28 km wide and 155 m deep (Thomson, 1981). It is separated from the Pacific Ocean on the west by Vancouver Island. It connects to the ocean through several long narrow channels in the north and the wide channels between the San Juan and Gulf islands in the south that flow through the Juan de Fuca strait into the ocean.

The tide propagates from the Strait of San Juan into the Strait of Georgia and is reflected into the basin in the north. As a result the tide in the Strait of Georgia exhibits a standing wave pattern with the highest range in the north (Sutherland, Garrett, & Foreman, 2005; Thomson, 1981). The tide is semi-diurnal with strong diurnal components. Its main components are M2 and K1 with amplitudes of around 80 cm (Foreman, Sutherland, & Cummins, 2014; Isachsena & Pond, 2000; Marinonea, Pond, & Fyfe, 1996).

Tidal asymmetry induces a net northward transport of sediment as flow velocities during flood exceed those during ebb. The direction of the flow follows the delta front in deep water but is in the direction of the slope in the upper shore. This has resulted in a fine-grained depositional slope off Sturgeon Bank (Hill et al., 2008). The causeways over the inter-tidal zone interrupt the dominant northward flow. Behind the structures the tidal flow separates into large clockwise gyres (Barrie & Currie, 2000).

The waves within the Strait of Georgia are primarily locally generated wind waves. Waves from the Pacific Ocean cannot travel through the Strait of Juan de Fuca and up into the Strait of Georgia unimpeded. Wave heights are bounded further by small islands and other obstructions limiting the fetch (Thomson 1981).

Wave heights are small. Most of the time they are smaller than 1 m. However, steepening of waves can occur when waves propagate in the opposite direction of the current, for example during periods of high discharge from the Fraser river as well as due to shoaling near the river mouth (Thomson 1981).

2.2 Fraser river and Delta

At New Westminster the Fraser river splits into several separate arms to form the Fraser delta. In between these arms the inter-tidal areas of Sturgeon Bank, Westham Island, Roberts Bank and Boundary bay are located. These form the outer edge of the delta. The delta has been advancing for the past 9000 years despite periods of rising sea-levels. For the last 2250 years lateral expansion averaged around 2.4m/year (Williams & Roberts, 1989).

The Fraser river is fed by rainfall and snow melt. As a result, the discharge peaks in spring when the snow melts and is at a low in the winter. The months May through September account for 72.5% of the annual run-off with a mean long-term maximum discharge of 8705 m³/s while the mean long-term minimum for the low-period is only 687 m³/s (Mikhailov, Mikhailova, & Rets, 2007).



Figure 2 The sediment plume as observed with LandSat 8 on the 6th of September 2014, made available by the USGS (<http://landsatlook.usgs.gov/viewer.html>), visualised with Google Earth Engine Explorer (<http://explorer.earthengine.google.com>) and adapted with text for geographic location.

Based on the same calculations the mean annual discharge is 2748 m³/s. All these values were calculated for the Hope station a few kilometres upstream of the delta.

The mean long-term sediment discharge at the Mission station is around 18.5*10⁶ tonnes/year (M. Church & Krishnappan, 1998). Attard, Venditti, and Church (2014) measured that 70% of the sediment load was silt and clay.

Furthermore, they concluded that the threshold for significant sand suspension lies between 5000 and 5700 m³/s which only happens during the period of high discharge.

As the sediment is discharged into the Strait of Georgia, it forms a plume. Normally the plume is characterized by fine- grained sediments from the river flowing on top a layer of dense salt water that extends into the river. During freshets, the salt-wedge is pushed out of the river and coarse sand from the bed is resuspended. In that case the river plume is characterized by a high concentration of coarser sediments (Kostaschuk, Stephan, & Luternauer, 1993). In such conditions turbidity could be high enough for gravity flows off the delta slope transporting sediment into deep water. This is likely the cause of the up-slope

migrating sediment waves at the river mouth of the Main channel which are known to form in such environments (Hill et al., 2008).

The suspended sediment concentration of the plume depends mostly on seaward distance, tidal height and to a lesser extent on river sediment concentration. The direction of the plume is determined by a combination of the tide, wind, and river discharge. Without strong winds the plume travels northward during flood while during ebb it travels southwest, despite the ebb flow being directed southeast. Due to the Coriolis effect the plume turns more northward during flood and resists the ebb current to the southeast (Thomson, 1981).

Sediment is discharged mostly from the Main and North arms of the river while the Middle arm contributes little to the sediment supply of Sturgeon Bank (McLaren & Ren, 1995).

Furthermore, the North and Main arms have been channelized preventing sediment from being discharged onto the flats directly. Sand is transported to the Sand Heads instead where a clockwise gyre transports it to the northeast of Sturgeon Bank and the Iona causeway (McLaren & Ren, 1995). However, due to slope failures at the river mouth sand that could have replenished the sand flats on Sturgeon Bank is being lost to deep water (Kostachuk & Luternauer, 2004).

Sediment is removed from the river by dredging. Dredging of the river has been ongoing as early as 1885. The first estimates of dredged volumes are from 1946 to 1956. In this period 1.4 million m³/year was dredged from the river. In the 60's Public Works Canada (PWC) along with private parties dredged the river with a hopper dredge that disposed material into deep water and a

pipeline dredge that disposed material on-shore. In 1990 the PWC operations were discontinued and taken over by private companies. Between 1978 and 1988 dredging often exceeded the necessary navigation dredging as the dredge spoil was used for land reclamation and construction. Recently 60 to 70% of the bed load in the main channel is being dredged. The dredged sediment is either deposited in a deep water disposal site or pumped onshore to be sold (Northwest Hydraulic Consultants, 2002).

Most dredging takes place along the Steveston North Jetty accounting for 30 to 50% of all dredging activity in the river. A return flow near the river mouth transports sand back into the river which increases the need for dredging (McLaren & Ren, 1995).

2.3 Sturgeon Bank

Sturgeon Bank can be divided into four sections: the sand flats, the mud flats, the marsh, and the dike. Each area has its own habitat and characteristics. The different zones are for a large part the result of the very gradual increase in elevation over the flats. As wave energy disperses shoreward finer sediment is able to settle which leads to the gradual transition from coarse to fine sediment on the flats. The marsh edge can generally be found where the flat is exposed just long enough during each tidal cycle for plants to grow without drowning. The marsh extends to the dike which separates Sturgeon Bank from the city of Richmond.

2.3.1 Sand flat

The sand flat is bordered by the Strait of Georgia in the west. At the fore slope the coarsest sand of about 250 µm can be found (Feeney, 1995; McLaren & Ren, 1995) and transitions gradually

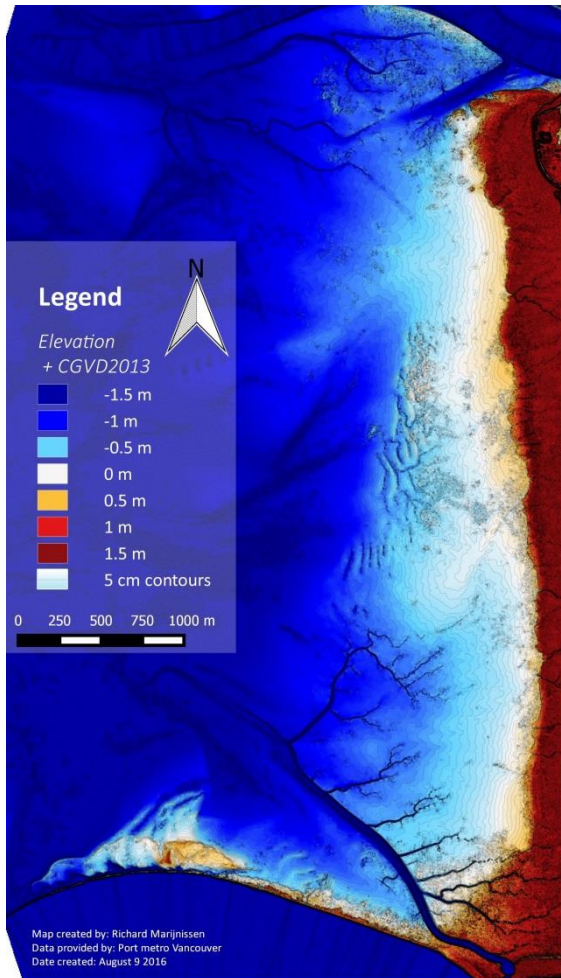


Figure 3 Lidar image of Sturgeon Bank (data provided by Port Metro Vancouver). See Appendix 1: Maps for the big map

into silt over a distance of 4.5km. Flows on the sand flats are bidirectional with tidal velocities at flood exceeding those during ebb. (Feeney, 1995).

Tidal channels dissect the land ward edge of the sand flats in the south and extend further into the mud flats. These too are composed of fine sand due to the concentrated tidal flows. Along the jetty and in the centre of the bank sand swells (also referred to as sand waves) can be found with heights less than 1 m and lengths between 60 and 100 m (Medley, 1978). These are low sand bars likely generated by wave action (J. L. Luternauer, 1980). Some patches of bulrush can

be found on and behind the most shoreward crests of the sand swells.

2.3.2 Mud flat

The mud flat on Sturgeon Bank is between 0.5 to 1.5 km wide. A combination of fine sand, silt and mud is present here (Feeney, 1995; McLaren & Ren, 1995; Wootton & Sarrazin, 2011). Fine sand is found within and near the tidal channels. Mud is dominant close to the marsh edge. In-situ experiments on the sediment by Feeney (1995) and further analysed by Amos, Feeney, Sutherland, and Luternauer (1997) showed the inner bank is quite resilient to erosion of sediments. Flow velocities generally do not exceed the critical shear velocities and erosion would only occur during storms when wind-induced waves reach the bank.

A notable feature on the mud flat is the tidal channel system in the south. It stems from the gap in the Steveston Jetty at Garry Point that connects landward side of Sturgeon Bank to the Main Arm of the Fraser river. On the mud flat there are some small patches of bulrush, most of them close to the sand swells.

2.3.3 Marsh

On the flats patches of pioneering vegetation can be found that transition into the salt marsh. Hutchinson (1982) classified the salt marsh of Sturgeon Bank into different zones. A relation exists between submergence time (directly related to elevation) and vegetation. The zone below 3.65 m+CD (just below MLHW) was classified as low marsh with mostly bulrush (specifically *Schoenoplectus pungens* or *Scripius americanus*).

Bulrush is the pioneering species in this ecosystem. It grows mostly along the tidal creeks

of the mud flat on well-drained sandy soils (Hutchinson, 1982). The dense root system of the bulrush makes the soil more resistant to erosion while the stems attenuate wave energy (Albert, Cox, Lemein, & Yoon, 2013). Fine sediments accumulate between the stems raising the elevation of the mudflat. As inundation reduces and soil stability improves, other marsh species can expand into the colonized patches of bulrush. Through these interactions bulrush acts as a facilitator of marsh growth.

The transition to middle marsh had been identified by a minor scarp. There the marsh consists for the most part of the plants species *Bolboschoenus Maritimus* and *Carex Lyngbyei*. At 4.15 m+CD (just below MHHW) the marsh develops into high marsh where submergence time decreases rapidly and a variety of high marsh species reside Hutchinson (1982).

2.4 Development of Sturgeon Bank

2.4.1 Human interventions

The first settlers arrived in 1868. Diking only began in 1905 when the Lulu West Dyking District was established (Richmond, 2005). Because of the diking the marsh on Sturgeon Bank has been confined. In 1917 to the north of Sturgeon Bank the North Jetty was constructed and extended in 1951. The Iona jetty further bounded the north of Sturgeon when it was constructed in 1961 (Levings, 1980). In the south the construction began on the Steveston Jetty in the 1930's and was completed in 1935. Until 1978 the jetty was a closed structure but in 1978 four openings were made as part of the reconstruction of the jetty (Levings, 1980).

An attempt to create additional marsh habitat was made in 1980 when 40,000 m³ of sand was placed

on the outer bend of the Steveston Jetty. The created egg-shaped island lost as much as 1m of substrate height within the first 3 months due to wave action (Levings, 2004). Burial and exposure of plugs due to dredge spoil drift and high salinities relative to donor sites led to the unsuccessful marsh creation effort (M. A. Adams & Williams, 2004). A few years later additional dredged material was placed (~ 60,000 m³) and surplus concrete pipes were installed to mitigate erosion. Ongoing coastal processes have significantly reworked the island since (Levings, 2004).

Up until 1988 waste water was discharged at the Iona island causeway. This contaminated the soil and reduced bio activity on the bank. Waste water has been discharged in deep water after 1988. Only during storms waste water is discharged onto the flats. Since then the plant growth has recovered (Harrison et al., 1999).

Human interventions in the past 150 years have probably caused a reduction of the natural sediment supply to Sturgeon Bank through diking, dredging and the construction of jetties. The system could have become erosional as a result. In the future interference in the form of sediment delivery could be necessary in order to restore it (Atkins, Tidd, & Ruffo, 2016).

2.4.2 Marsh development until 1990

After the construction of the Steveston North Jetty in 1932, marsh growth was observed at its lee-side. According to Hales (2000), growth of the marsh continued until 1994 possibly due to a peak in dredging activities in the main river suspending more fine sediment in the outflow.

An aerial survey by Medley and Luternauer (1976) found the marsh had been stable between

1950 and 1976. Subsequent fieldwork found that the dendritic network of channels on Sturgeon Bank was expanding, leading to erosion of the tidal flats (Medley, 1978). As noted by Medley, the presence of more channels is not necessarily bad as more flats can be supplied with sediment in turn facilitating future growth. Furthermore, sand swells were observed on the flats which could collect mud in their troughs and set up the conditions for further marsh development. Levings (1980) suggests that the construction of the Steveston North Jetty in 1932 has induced a wave refraction pattern that is ultimately responsible for the sand swells and marsh growth.

2.4.3 Recent marsh development

Both Williams and Hamilton (1995) and Hales (2000) found that sedimentation rates on Sturgeon Bank had decreased by 50% between 1954 and 1994 but differ in interpretation. Williams and Hamilton (1995) related this decrease directly to dredging in the main river whereas Hales (2000) argues that 1) sedimentation rates decrease naturally as the marsh approaches an equilibrium with the hydrodynamic conditions and 2) the dredging removed primarily sand from the river while sediment deposited on the marsh is mud. The decreased supply of sand would however degrade the sandy tidal flats, in turn increasing the water depth and erosion rates by waves.

Additional mapping of the marsh edge with aerial photographs by M. Church and Hales (2004) showed a continued advance of the lower marsh with the exception of the marsh area in the north of Lulu island where significant losses were observed. These losses are localized and could be attributed to goose feeding, plant disease or physical damage.

In contrast to the earlier findings, TRE Canada Inc. (2014) indicated a retreat of the marsh between 2001 and 2013 based on the difference between the observed coastlines on satellite images acquired at water levels between 3.34 m+CD and 4.03 m+CD and a measured bathymetry from 2013.

Ilori (2015) found that the amount of three-square bulrush had decreased from 457 ha in 1987 to only 39 ha in 2015 and was replaced by bare mud flats. Ilori (2015) used LandSat satellite imagery and aerial photographs to detect areas with a similar signature as a selected bulrush-vegetated location.

Another study confirmed this with field measurements in 1988 and 2011 and shows retreat of the bulrush leading edge by as much as 500m (Boyd et al., *Unpublished*). The results of these recent studies suggest a shift has occurred from advancement to retreat of the marsh. The data about how or when a shift to retreat happened is inconsistent.

M. Church and Hales (2004) conclude there is no overall retreat prior to 2004. The use of aerial photography alone is not ideal as sparse vegetation can be hard to spot on the mudflats. However, in combination with sediment core analyses, visits to the marshes in the Fraser Delta and research into the changes in the delta in the last 100 years in Hales (2000) the results are placed into broader context.

TRE Canada Inc. (2014) reports a large retreat combined with erosion, but due to the inaccuracy of determining the water line from satellite images as well as the uncertainties added by weather, seasonal and water pooling effects the

results would benefit from verification.

Ilori (2015) reports a large retreat as well starting as early as 1987. Visual interpretation was combined with trained classifiers of marsh vegetation which makes the results more objective but the use of manually selected training areas for each image still allows subjective interpretation.

The measurements of Boyd et al. (*Unpublished*) are most objective since it based the retreat on physical field observations at the same locations in 1988 and 2011. Although this establishes retreat has occurred in this period, it gives no information about any marsh development in between these years.

The current literature paints a picture of long-term marsh growth on Sturgeon Bank. Only recently do signs of marsh degradation appear. This can either result from the marsh reaching a dynamic equilibrium with the environment or a regime shift that has been initiated by interventions in the past. In the former the marsh retreat would be only temporary and restore after some years. In the latter, there is a permanent loss of salt marsh. A final possibility is that biological factors (e.g. plant disease) are responsible.

2.5 Development of neighbouring marshes

For some of the previously mentioned studies, the marshes on Roberts Bank have been studied either as a reference or to study the Fraser delta as a whole. To put the developments on Sturgeon Bank into perspective the development of the two closest marshes is briefly discussed.

2.5.1 Roberts Bank: Westham Island

The northern part of Roberts Bank is the island

called Westham. The marsh at the banks of Westham Island have seen a large growth of 16% following the construction of the Steveston North and South Jetty in 1932, and the Woodward training wall and Albion jetty in 1935-1936 (Hales, 2000). The first fixed the channel of the main arm across the tidal flats to improve navigation. The second were placed in the middle of the main arm to encourage scouring of the main channel and reduce maintenance dredging. Because no major floods occurred in this period the rapid expansion of the marsh is most probably related to these structures.

Similar to Sturgeon Bank, the sedimentation rates at Westham Island had decreased by around 50%, yet lateral expansion of the marsh continued (Hales, 2000). Ilori (2015) found that, like on Sturgeon Bank, on Westham Island and Roberts Bank the bulrush had retreated as well. However, the retreat on Westham Island and Roberts Bank was far less than on Sturgeon Bank with only a decrease from 294 ha in 1987 to 170 ha in 2015. This retreat occurred between 1987 and 1996 and is primarily on Roberts Bank. The leading edge has remained stable after 1996. Fieldwork on the bulrush in 1988 and 2011 did not show a retreat of the leading edge although a decrease in stem density was observed (Boyd et al., *Unpublished*). All this leads to the conclusion that the banks fronting Westham Island are currently stable.

2.5.2 Roberts Bank: terminals

The southern part of Roberts Bank (from now on simply referred to Roberts Bank) has seen much human activity. From 1958 to 1969 the BC Ferries terminal and causeway and the Roberts Bank causeway and terminal were constructed. A turning basin was dredged on the flats between

1979 and 1982. The latest expansion was completed in 2009 when a third berth was constructed (Northwest Hydraulic Consultants Ltd., 2014). Aerial observation of the channels showed the increased erosion of the tidal flats following the dredging and the shift of the erosion after a crest protection wall was constructed. Different erosion rates at different channels were suggested to be related to the local ponding of ebb water. The ponds retain more fine sediment and organic matter and thus erosion was (partially) mitigated (J. L. Luternauer, Duggan, & Hendry, 1984).

In between the causeways the marsh retreated (J. L. Luternauer, 1976) and stabilised in 1981 (Northwest Hydraulic Consultants Ltd., 2014). On the other hand north of the causeway the intertidal marsh has increased between 1954 and 1974 (Hales, 2000). Between 1974 and 2004 the marsh on Roberts Bank has remained stable with only very limited growth (M. Church & Hales, 2004).

Bathymetries measured in 1976, 2002 and 2011 show very limited morphological activity on the bank. Only some deposition was observed at the lee-side of the causeways between 1976 and 2002 (Northwest Hydraulic Consultants Ltd., 2014). Fieldwork on the bank confirmed there is little sedimentation on the bank as well (Northwest Hydraulic Consultants Ltd., 2014). It is hypothesized that the causeways have effectively cut off the bank from any supply of sediments but also provide shelter from erosive waves and currents.

2.6 Salt marsh dynamics

2.6.1 Salt marsh characterization

Salt marshes are at the edge between the land and

sea. The salt marsh fulfils many ecosystem services. It has a high primary production, it supports a variety of bird and fish species, regulates the impact of storms, filters contaminants in the water, and the landscape is of recreational value (Costanza et al., 1998). The plants within a salt-marsh are submerged daily by the tide. The distribution of marsh species is controlled primarily by the tide (D. A. Adams, 1963). Between mean high water and mean low water plant species that have adapted to the regular submergence by the tide can start to grow (McKee & Patrick, 1988). It is submergence frequency, which oscillates between spring and neap tides, rather than duration that governs the lower limit of the marsh (Balke, Stock, Jensen, Bouma, & Kleyer, 2016). As the elevation increases, the stress of the repeated flooding decreases. Other plant species that were unsuccessful at lower elevations, start outcompeting the lower marsh species and a zonation of different plant species develops along the elevation gradient of the marsh (Levine, Brewer, & Bertness, 1998). These interactions make the salt marsh home to a large variety of species.

2.6.2 Salt marsh growth

The growth of salt marsh is not a continuous process. The establishment of pioneering vegetation on the tidal flats relies on a window of opportunity. Such opportunities arise when the tidal flat is free of physical disturbances (e.g. storms, erosion, or flooding) for a sufficiently long time (Balke, Herman, Bouma, & Nilsson, 2014; Hu et al., 2015). When a critical biomass has been reached, positive feedback reinforces further expansion through trapping of sediments, stabilization of the soil and dampening of wave

forces (Bouma et al., 2009; Corenblit, Tabacchi, Steiger, & Gurnell, 2007). The vegetation obstructs the flow into concentrated streams. This interaction shapes the formation of channels that further improve the physical environment of the plant by draining more water at low tide (Temmerman et al., 2007). Wave forces are a regular disturbance and limit the lateral expansion of the marsh (Silinski, Fransen, Bouma, Meire, & Temmerman, 2016). A marsh that grows seaward becomes more vulnerable to waves and storm events. One such storm can initiate a cascade of plant die-off in an beforehand stable or expanding marsh (van de Koppel, van der Wal, Bakker, & Herman, 2005).

2.6.3 Salt marsh retreat

There are effectively two ways for a salt marsh to develop; either vertically or horizontally. Sea-level rise falls into the first category. When the sea level rises relative to marsh the inundation increases. Unless compensated by deposition of sediment it will lead to a decrease in primary production (Morris, Sundareshwar, Nietch, Kjerfve, & Cahoon, 2002) and drowning of the marsh (Nyman, DeLaunel, Roberts, & Patrick, 1993). In order to maintain the same inundation, the marsh shifts landwards. Without physical barriers like dikes the landward shift does not diminish the size of the marsh and may even expand (Kirwan, Walters, Reay, & Carr, 2016), but when bounded a loss of marsh is inevitable.

Horizontal change can often be attributed to edge erosion by waves. Several studies found a direct link between the wave energy at the marsh edge and the rate of lateral retreat (Marani, D'Alpaos, Lanzoni, & Santalucia, 2011; McLoughlin, Wiberg, Safak, & McGlathery, 2015; Reed, 2001).

On a large scale, wave breaking and bed shear result in the formation of a scarp with a marsh platform above mean sea level and a flat below mean sea level as the marsh retreats (Mariotti & Fagherazzi, 2010). On a local scale the waves cut small incisions in the marsh edge by eroding mud from between the roots until the edge collapses (Reed, 2001).

A combination of sea-level rise and wave-edge retreat can trigger runaway erosion through the formation of ponds (Mariotti, 2016). Ponds are created by disturbances in the marsh and grow if deposition is smaller than the relative sea-level rise (drowning), by biochemical erosion processes (van Huissteden & van de Plassche, 1998) or by surficial flooding of the adjacent marsh (Wilson et al., 2009). The ponds grow until drained at which point the biochemical balance restores and water is drained. Unless there is sufficient deposition to restore the depressions more marsh is exposed to wave edge erosion and the process is amplified (Mariotti, 2016).

The processes described are biophysical. However, there are biological factors that are known to have caused a rapid marsh recession. For example die-off in the south-east of the U.S. has been attributed by pressure from snails following a drought (Silliman, van de Koppel, Bertness, Stanton, & Mendelssohn, 2005). Die-off in New England salt marshes were triggered by increased herbivory from crabs (Holdredge, Bertness, & Altieri, 2009).

Different studies found higher sulphide concentrations as well as higher pH-levels in the soil of die-back areas, both of which are detrimental to plant growth. However, these changes can be the result of the die-off event

rather than the cause (Alber, Swenson, Adamowicz, & Mendelssohn, 2008; Marsh, 2007; McKee, Mendelssohn, & D. Materne, 2004).

2.6.4 Salt marsh restoration

Weinstein, Teal, Balletto, and Strait (2001) summarized the components for successful marsh creation as:

- **Historical ecosystem types:**
The area supported a functioning salt marsh in the past.
- **Hydrology and topography:**
The area must have the right amount of inundation for a salt marsh to establish.
- **Creeks and channels:**
The area should have a sufficient wetting/drying cycle to aerate the soil.
- **Sediment organic content:**
Organic content should be present as a source of nutrients, substrate for the germination of seeds and to support benthic organisms.
- **Colonizer presence and proximity:**
Colonizing plant species should be close to allow rapid colonization.
- **Salinity:**
Salinity levels should not exceed the tolerance of the intended marsh species.
- **Sediment accretion:**
There should be a sufficient supply of sediment in order for the marsh to adapt to rising sea-levels

Most restoration efforts focus on the topography and sediment availability to reverse the effects of subsidence and erosion. The sudden die-back of marsh after a drought in Louisiana was restored with dredge slurry. The altered inundation regime as a result of the higher elevation increased the

rate of recovery (Schrift, Mendelssohn, & Materne, 2008). On a larger scale, terraces can be constructed from the bottom material to create higher elevations for emergent vegetation (Underwood, Steyer, Good, & Chambers, 1991).

Elevation can be enhanced also indirectly by structures. Low stone dams were used to stop the erosion of salt marsh in the Netherlands. The dams reduced the lateral cliff retreat and promoted sedimentation of the hinterland. The mudflats behind the dams were colonized by pioneering vegetation to elevations lower than it had previously (Van Loon-Steensma & Slim, 2012). The same principle was applied in Galveston Bay (Texas) though with temporary sacrificial mounds that double as a sediment source for the marsh (McPherson, Blackmar, & Heilman, 2015).

The elevation can further be raised when the sediment supply to the salt marsh is increased. A pilot is being conducted to deposit dredge spoil from the harbour of Harlingen in the Wadden Sea and let natural currents distribute the material onto the salt marsh (van Eekelen et al., 2016).

Drainage of the marsh might not always be adequate either due to natural processes or by human interference such as diking. To promote the growth of salt marsh an initial drainage network needs to be established which is then allowed to further develop on its own. This method was employed in Delaware where salt marsh was recreated by dredging channels into diked salt hay farms. Thereby the tidal regime was restored (Teal & Weishar, 2005).

3 STATISTICAL STUDY

3.1 Tide

The tide is a key part of the physical environment on Sturgeon Bank. It governs which areas will be flooded, for how long and drives crucial morphological processes. No tide station is currently operational at Sturgeon Bank. The closest one is at Point Atkinson about 20 km to the north. A detailed description of the methods and assumptions used in the analysis can be found in Appendix 2: Tide analysis.

Hourly water levels from 1984 to 2016 at Point Atkinson were analysed with the tidal harmonics analysis procedure described in Pawlowicz, Beardsley, and Lentz (2002). The method separates the tidal signal into its constituents (Table 1). Each constituent represents a different timescale and associated mechanism (e.g. M for lunar tide, S for solar tide).

The tide can be classified by the form factor:

Eq. 1
$$F = \frac{K_1 + O_1}{M_2 + S_2}$$

Where K_1 , O_1 , M_2 and S_2 are the amplitudes of the respective tidal constituents (see Table 1)

The form factor is calculated as 1.19 which signifies a semi-diurnal tide with strong diurnal components. There are two high and low waters per day, but there is a big difference between each.

The mean water level was found at 3.1 m + chart datum (CD). The tide can range between -0.24 m +CD and 5.52 m +CD. Average tides only range about 3.28m, between 4.48 m+ CD and 1.20 m +CD. High tides last longer than low tides. As a result, fine particles will have a long time to settle on the higher elevations of the flats.

The tidal signal shows the largest velocities are at low water. At high water the velocities are smaller. This is reflected in the large difference between the mean water level (MWL) and the mean lowest low water (MLLW) compared to the difference with the mean highest high water (MHHW). The former is 1.9 m while the latter is only 1.3 m. Such an environment encourages deposition onto the tidal flats. Sediment brought in with the tide has a long time to settle at high water when flow velocities are small.

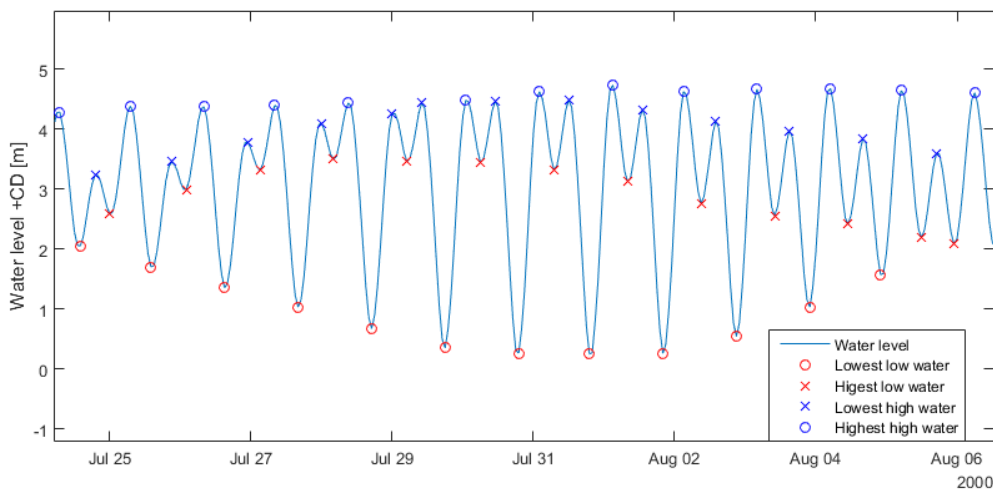


Figure 4 Tide in Point Atkinson showing a strong daily inequality, data from Canadian Hydrographic Service (2015)

Table 1 Tidal constituents calculated from historical water levels at Point Atkinson, data from Canadian Hydrographic Service (2015)

Const.	Frequency [h ⁻¹]	Amplitude [m]	Phase [degrees]
M ₂	0.0805114	0.9050	154.82
K ₁	0.0417807	0.8668	164.36
O ₁	0.0387307	0.4818	150.44
P ₁	0.0415526	0.2709	163.17
S ₂	0.0833333	0.2299	175.12
N ₂	0.0789992	0.1873	132.48

Table 2 Tidal levels calculated at Point Atkinson, data from Canadian Hydrographic Service (2015)

HHW	5.52	m+CD
MHHW	4.48	m+CD
MLHW	3.91	m+CD
MWL	3.10	m+CD
MHLW	2.96	m+CD
MLLW	1.20	m+CD
LLW	-0.24	m+CD

From the time series, the average skewness of the tide was calculated. Skewness reflects the difference in duration of the rising tide compared to the falling tide. A positively skewed signal shows flood is dominant over ebb currents. Skewness was calculated as:

Eq. 2
$$\gamma_1 = \frac{\frac{1}{n-1} \sum_{i=1}^n (\zeta_i' - \bar{\zeta}')^3}{\left[\frac{1}{n-1} \sum_{i=1}^n (\zeta_i' - \bar{\zeta}')^2 \right]^{\frac{3}{2}}}$$

ζ' = Time derivative of the water level

n = Number of records

Source: (Nidziedo, 2010)

The tide is positively skewed with a value of 0.14. Flood velocities will thus generally exceed the ebb velocities. Because of this there will be a net transport of coarser sediment shoreward.

3.2 Waves

There is limited data available for the characteristics of waves at or near Sturgeon Bank. The latest measurements were carried out just offshore with a buoy in the 70's by the ministry of Fisheries and Oceans. However, it is unlikely the conditions have changed much.

The wave heights and periods from the record were ranked and normalised to produce a histogram corresponding to the probability of occurrence. Wave heights are small and rarely exceed 1m. Wave periods are generally short. Only occasionally do longer waves appear. Both wave height and period show that small, short waves are dominant on Sturgeon Bank. Such waves are usually locally generated by the wind.

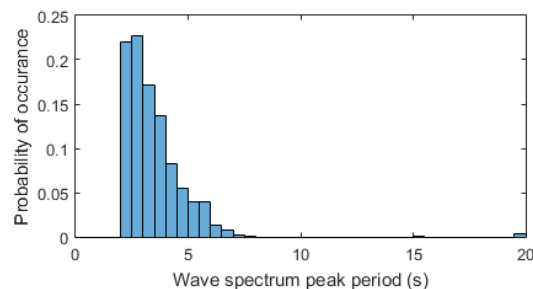
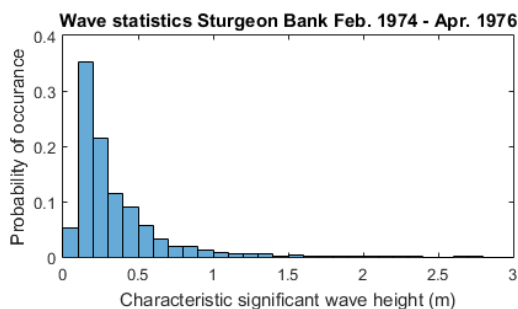


Figure 5 Wave statistics in 1974-1976. Data from Fisheries and Oceans Canada (2013)

Empirical relations between wind speed and wave height exist like the Bertschneider formula or the formula from Young & Verhaegen. Recent wave heights can be estimated using these relations and wind data.

South of Sturgeon Bank at Roberts Bank north of the container terminal, wave heights have been studied across the sandy intertidal flats more recently by Houser and Hill (2010). During 2 months of observations the highest significant waves heights were around 0.25-0.3 m during storms with peak wind speeds between 10-16 m/s. Normally roughly 50% of wave energy is dissipated across 4.5 km of sand flats on Roberts Bank. However during storm winds in particular, wave heights can continue to grow across the sand flats. Wave heights are largest at high tide and during the peak of storms.

3.3 Wind and storms

Located close to Sturgeon Bank is the international airport YVR. At the airport, there is a long record of wind data available. Twenty years of wind speed measurements at YVR airport were analysed by sorting by magnitude and direction.

Winds from the east occur for the majority of the time. Winds from the west to north west are less frequent, but are dominant when it comes to storms. Almost 50% of all wind speeds greater than 10 m/s (36 km/h) came from the west to north west. Since most waves are locally generated by winds, it can be concluded that waves arrive on Sturgeon Bank from the same direction.

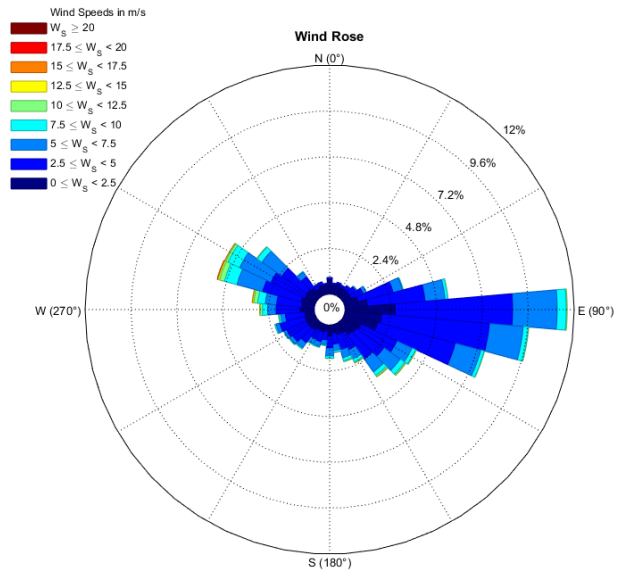


Figure 6 Wind rose of YVR airport between 1992 and 2012 data from: <http://climate.weather.gc.ca>

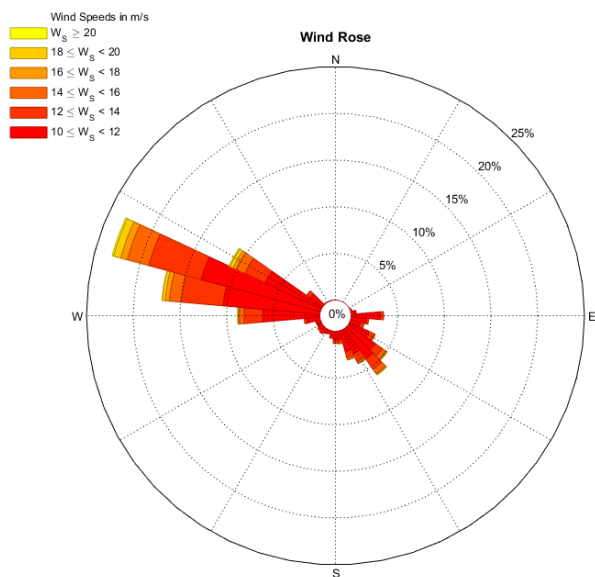


Figure 7 Wind rose of storm winds ($w_s > 10$ m/s) at YVR airport between 1992 and 2012 data from: <http://climate.weather.gc.ca>

Table 3 Return period of storm winds

Return period	Hourly wind speed [m/s]	Hourly wind speed [km/hr]
1 year	17.1	61.6
2 years	18.5	66.6
5 years	20.4	73.4
10 years	21.7	78.1
20 years	22.9	82.4
50 years	24.5	88.2

Table 4 Largest hourly wind speeds at YVR airport between 1985 and 2012, data from: <http://climate.weather.gc.ca>

Date	Max. hourly wind speed [m/s]	Day averaged wind speed [m/s]	Wind direction [degrees north]	Tidal range on date [m]
14-Dec-2001	22.78	14.84	300	3.92
28-Oct-2003	22.78	9.40	290	4.41
15-Dec-2000	22.22	7.66	290	4.19
09-Jan-2007	21.67	9.38	280	3.05
08-Apr-2010	21.67	10.21	290	2.74

Given the strong connection between waves and storms the wind data was analysed to identify the storms events that could have contributed to the retreat of the marsh. The largest wind speeds of each year between 1985 and 2015 were collected to determine the frequency and intensity of storms at Sturgeon Bank. A generalized extreme value distribution was fitted to the highest hourly wind speed of each month to do so. Historic storms were then compared to their respective return periods. Also, the tidal range on that specific day was retrieved to see whether the storm coincided with a spring or neap tide.

The most powerful storms occurred in a brief period between 2000 and 2003. An exceptional series of rare storms (return periods ≈ 20 years) coincided with large tidal ranges. It can be expected that the sudden increased severity of the wave climate generated by the storm winds has left an impact on the flats and marshes of Sturgeon Bank.

4 AERIAL IMAGERY

A great deal of information about the morphological development of Sturgeon Bank can be derived from aerial photographs. The position of the marsh edge shows if/when the marsh retreated or grew. Tidal channels and sand swells can be observed clearly on the photographs as well. Both features have affected the position of the low marsh in the past (Hutchinson, 1982) and were therefore analysed as well.

Other studies have analysed aerial photographs to determine historical changes of the marsh before (M. Church & Hales, 2004; Hales, 2000; Ilori, 2015; J. L. Luternauer, 1980; Medley, 1978; Medley & Luternauer, 1976). All studies agree that interpretation of these images can be challenging as important details may not always be clearly visible. Interpreting a marsh edge can be subjective when present in a gradient from sparse to dense rather than a clear-cut boundary. This might explain the differences in the marsh extent found in the literature. By re-examining the photos, a more consistent evaluation can be made and the difficulties for interpretation highlighted.

4.1 1930

In 1930 the main part of the Steveston South jetty had already been built. Due to the water level the channels in area C were not visible (see Figure 8). In the south part of area D, no channels had developed yet. The main channel entering Garry Slough was also a lot smaller (about 20 m wide) compared to now (40 m wide). In area B, there were already clearly developed channels with marsh in between stretching all the way to the sand swells. Area A was not covered in the photo.

Table 5 Air photos used for the analysis

Sources photos:	
1930	National Air Photo Library. A2238_0761. Ottawa: Natural Resources Canada, 1930
1954	NAPL A13977-18 as found in: J. L. Luternauer (1980)
1979	Province of British Columbia. BCC226 & Ortho BCC227 series. Scale 1:12,000. Victoria: photos: Province of British Columbia, 1979.
1979	Boyd (1979, <i>pers. com.</i>) Oblique photo:
1986	Province of British Columbia. BCC534 & BCC535 series. Scale 1:12,000. Victoria: Province of British Columbia, 1986
2001	Google Earth
2002	FREMP. Photo flight. Scale 1:20,000, made available by Environment Canada, 2002
2003	Google Earth
2005	Google Earth
2015	Google Earth

4.2 1954

The 1954 photo only covers the channels in area C and the sand swells west of the channels. The sand swell in the photo are identical to ones from 1930. These features have remained stable in these 24 years, at least in the area next to the channels.

4.3 1979

The photograph from 1979 is the first one with colours and has good detail. Interpretation was aided by the oblique air photo from the same year. Area B has remained unchanged since the 1930 photo. The channels have remained similar in length while the marsh is still enclosed by the sand swells.

In area C, the channels have expanded in all direction by 50 to 80 m. The sand swells have slightly shifted in the north-east direction since

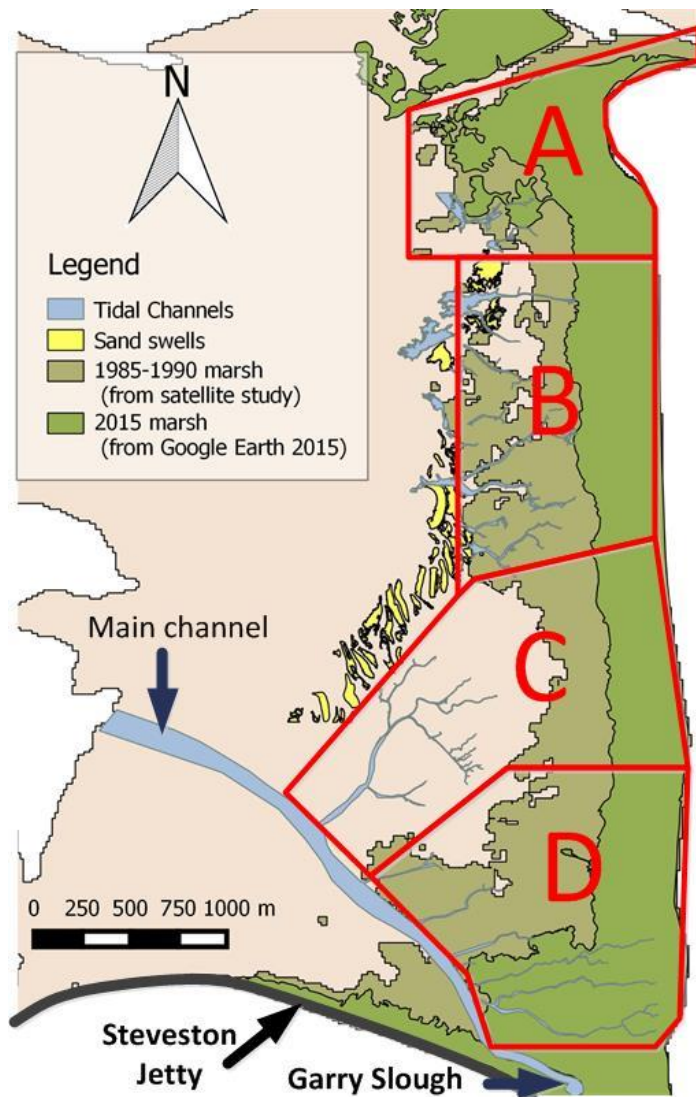


Figure 8 Sturgeon Bank divided in areas and relevant features. (Channels and sand swells in areas A, B, and C from 1986, main channel and channels in area D from 2015)

the 1954 photo. In that photo sand swells were westward from the connection between the main channel and the channels in area C. No sand swells were identified at that location in 1979. Contrasting shades are still visible but the first clear sand swells were found 350 m further to the north east. These crests are still at roughly the same position as in 1954 though their orientation has shifted more north-east ward.

In area D, the main channel near Garry Slough has widened from 20 m in 1930 to 33 m in 1979. Smaller offshoots have developed from the main channel though

these were only about half the length of today. The rapid expansion of channels was documented by Medley (1978) who reported severe head-cutting at the end of the channels in the south of Sturgeon Bank (areas C and D).

4.4 1986

The same trends as identified in 1979 have continued. Areas A and B have remained virtually unchanged while expansion of the channels in areas C and D continued. Channels expanded by 30 to 50m though one channel was found to have grown 110 m in length in the north-east direction. The channel at Garry slough has widened only slightly by about 1 m.

4.5 2001 to 2003

The system has undergone a lot of changes since 1986. In area A and the north of area B the channels are no longer there. The other channels in area B are halved in length and do no longer reach into the (middle) marsh. The old path of the shortened channels can still be seen as darker (i.e. wetter) depressions but in area A the channels have been erased from the mud flat. The ends of the channels can (even today) be found as channels within the middle marsh.

In area B, the marsh has receded by 400m. In contrast, the middle marsh seems to have grown 25 m. The middle marsh is darker due to the higher density of plants there. Possibly sediment has been moved from the terrace in between

the sand swells into the middle marsh.

The sand swells along areas B and C have shifted again. This time they have oriented themselves into an eastward configuration. Channels through the sand swells in area B have changed their paths between them. In area C, the channel that branched off due north was cut short by a sand swell that had moved towards it. Similar to what happened in between 1954 and 1979 the sand swells can only be found further north east. The location along area C where sand swells begin has shifted about 200 m north east.

In area C, the channels directed south east have stopped expanding. The northernmost channel had grown 400 m and reached into area B by curving northward. It appears from the direction of the dark (i.e. wet) patches that this channel took over some of the drainage from the channels in area B.

In area D, some marsh has been lost as well. Whereas before the marsh had extended towards the northernmost channels in area D, it has receded 550m south east. The channels that no longer lie within the marsh have shrunk while the remaining channels



Figure 9 Composite of the marsh in 1979, by Province of British Columbia (1979)



Figure 10 The marsh in 2016 in Google Earth

within the marsh continued expanding into it.

4.6 2005 to 2015

By 2005 the sand swells can only be found along the edge of area B. Their appearance on photos is much fainter as well. Furthermore, in area B the channels that were still visible in 2003 are no longer visible by 2005. The channel that reached all the way into area B has receded at almost the same pace it had grown. By 2005 the channel ends at the center of area C. Between 2005 and 2015 no major changes have been observed. Most of the features

on the mud flats like the sand swells and channels have become fainter over time. The main channel however has become about 2 m wider between 2005 and 2015.

- Features have become fainter on recent air photos. This suggests the features have been smoothed out though this needs confirmation.

4.7 Summary of observed changes

- The marsh and channels in area B have been stable from 1930 to 1986.
- A sudden marsh die-off occurred between 1986 and 2001 along the entire marsh.
- The main channel has widened rapidly from 1930 to 1979 and continued this trend towards 2015 at a slower pace.
- The channels in area C have been expanding since at least 1954. Expansion in all directions continued up to 1986 or later. By 2002 a single channel had expanded into area B while other channels no longer grew. By 2005 this expansion was being reversed.
- In area D channels, had been expanding since 1930. After the recession event between 1986 and 2001 only the channels that remained within the marsh continued to expand.
- Sand swells were stable in the periods from 1930 to 1954 and 1979 to 1986.
- Sand swells have moved north-eastward between 1954 and 1979, and between 1986 and 2001.

5 SATELLITE STUDY

For the analysis of the system LandSat satellite images available from the U.S. Geological Survey are used to examine recent changes on Sturgeon Bank. Since the 1980's there is steady record of imagery that shows Sturgeon Bank. As such it is a good source to investigate the changes that did occur on Sturgeon Bank.

5.1 Background on LandSat images

The orbits of the LandSat satellites allow them to observe any point on earth once every 8 days. The images are produced by measuring the light radiated from the earth's surface over a wide spectrum of wavelengths grouped into bands. The bands can be processed and combined to create the images (U.S. Geological Survey 2015). LandSat images are recorded since 1972 and have become more detailed since.

The best quality images are from 2013 onwards when the latest LandSat8 system was adopted. The precursor LandSat7 suffers from technical issues since 2003 and leaves stripes of missing data. Despite this, the data can still be used for this analysis since the larger features on Sturgeon Bank are still clearly distinguishable. The accuracy of the LandSat measurements themselves is 30 meters (U.S. Geological Survey, 2015).

5.2 Selection of satellite images

Although every 8 to 16 days an observation is made, most of them are not useful for interpretation. Cloud cover is most often the reason to exclude an observation from the analysis. Furthermore, there must be enough daylight reflected from the surface to distinguish the mudflats on Sturgeon Bank from the surrounding water. Cloudless days are associated

with calm weather, which means storms scenes are excluded. Furthermore, most selected images are taken in the summer when the days are longer. Therefore the analysis only reflects Sturgeon Bank under calm conditions associated with deposition, rather than under erosional conditions.

5.3 Manual approach

A crude outline of the flats is mapped on the satellite image and its area is calculated. Flats on the bend of the Steveston Jetty are excluded as they were probably influenced to a large degree by the jetty and thus not representative of the entire stretch. A representative width is also estimated from the image. Dividing the area of the flats by the length of the dyke and comparing it to the estimated width of the flats should result in approximately the same representative width. This is a control to notice when a bad measurement has been taken.

The width of the flats is then related to the water level at the time the satellite image was taken. Historical records were only available for the Vancouver station hence these water levels were used. The width of the flat at a given water level is equal to the position of the profile relative to the landward edge of the flat at that given elevation. With enough images at different stages of the tide a cross-shore profile can be constructed for the period the images are taken. To get enough data for a profile 3 to 5 year periods were made for which the profiles are calculated: 1974-1978, 2003-2007, 2008-2012 and 2013-2015.

Finally, the LandSat images from the end of July and beginning of August between 2013 and 2015 were processed to NDVI values and compared.

The NDVI is a vegetation index between -1 and 1 based on the ratio between the near-infrared radiation and the visible radiation. The underlying assumption is that plants absorb most of the visible light for photosynthesis while reflecting near-infrared. A higher NDVI score would indicate more photosynthesis and thus more plants. A score lower than 0.05 would indicate a bare soil (Parente, 2013) so these values are removed. Comparing the NDVI distribution of satellite images from different years shows whether the amount of vegetation has increased or decreased.

5.4 Scripted approach

In the previous analysis satellite images were processed by hand. However, to include more images the EE-coast application was adapted for this purpose (Friedman, 2015). The program first searches for Landsat images taken at Sturgeon Bank and removes images with too much cloud cover. Then the NDVI is calculated for each image. A NDVI threshold was determined visually that matched the boundary between

marsh, water, and land on most images. The water threshold was easily determined from the Landsat images themselves by looking at the seaward extent and channels. The marsh threshold was determined from the calculated NDVI values on the Landsat images at the marsh edge as visible on air photos from 1986 and 2015. The program searches on each image where the threshold is reached and produces the coast/marsh lines. These are exported for post-processing.

A second program was made to import the coast and marsh lines from the EE-coast application, the acquisition date of the Landsat images used and the measured water level at point Atkinson. As before the water level at the acquisition date is used to determine the elevation of each coastline but no average width or submerged area is calculated. Instead, the script collects all the coast lines with corresponding water levels within 5 years and interpolates a bathymetry. It is assumed that within these 5 years the bathymetry did not change significantly. By comparing the bathymetries of each 5-year period some insight can be gained about the morphological changes in the inter-tidal zone.

The marsh lines were filtered further to those taken in the month August and during low-tide. This reduces the seasonal variability of the plant cover and ensures no parts of the marsh were submerged when the image was taken. Validation of the results with the 1986 air photo showed the area in between parts of the southern tidal channels had the same NDVI values as the marsh despite a lack of visible bulrush on the air photo. Possibly this is due to accumulation of algae in this area at that time. This area was filtered out of the result. The remaining edge had a good fit with

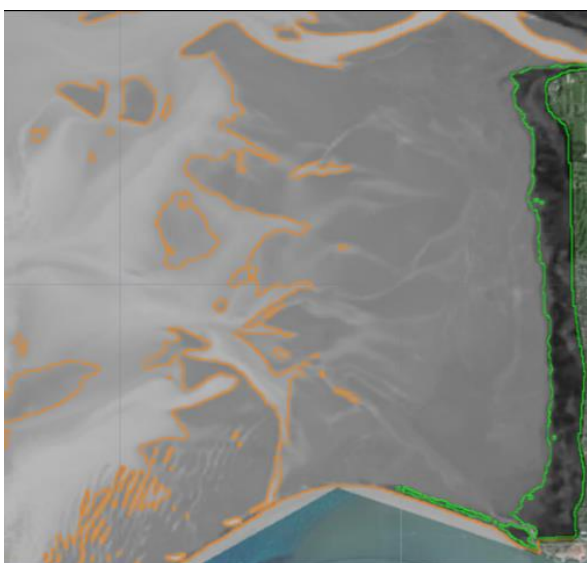


Figure 11 A processed Landsat image with the produced coast line in orange and the marsh line in green

the visible marsh in 1986. Further validation with the marsh edge measured in the field in 2015 (Mason, 2015, pers. com.) showed an almost perfect fit with the LandSat marsh edge.

5.5 Results for tidal flats

From the manually measured width of exposed flats it was found that the averaged cross-shore profile of Sturgeon Bank does not follow a smooth equilibrium profile (Figure 12). Instead there is some variability on the profile. On first sight the curve of 1975-1978 is similar to the other curves and shows no large amounts of sediment have been gained or lost in the last 40 years. In general, a wave like pattern seems to be imposed on all the profiles.

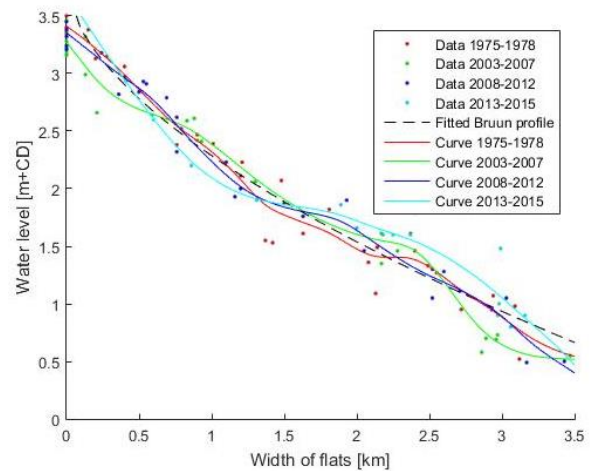


Figure 12 Relation between the width of exposed flats and the water level

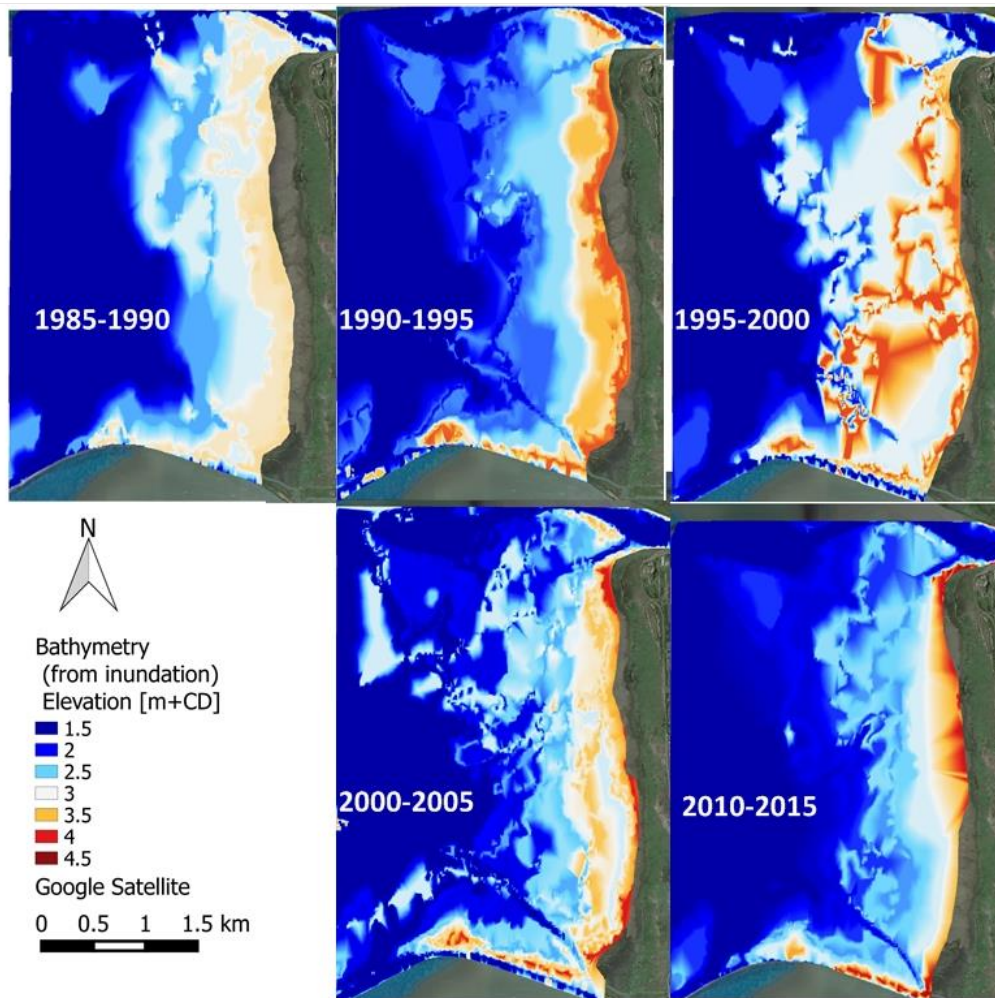


Figure 13 Bathymetries derived from exposed flats and tide levels on LandSat imagery

The initial results from the scripted method needed some cleaning as some coastlines contained ‘specks’ or looped around the border of the image. Weather conditions could have produced these. Most noise was generated by suspended sediment in the water. Suspended sediment could not readily be distinguished from exposed flats with this method. Additional filters were put in place to remove them but artefacts still remain (see 1995-2000 in figure 13).

After the bathymetries were corrected they could be interpreted. Since the bathymetry is interpolated between the coastlines, the minimum and maximum elevations shown on each map do not necessarily correspond to the actual minimum and maximum elevations at that time, but to the minimum/maximum water level at the time a LandSat image was acquired in that period (see 1985-1990 in figure 13).

The bathymetries derived for 1990-1995, 2000-2005 and 2010-2015 show the clearest features. The 1985-1990 bathymetry did not have enough data to generate a bathymetry close to shore while the 1995-2000 had too much noise to be properly interpreted. The 2005-2010 bathymetry could not be produced due to a lack of suitable LandSat images.

In 1990-1995 there used to be a fairly flat section of mud flats. By 2000-2005 this terrace is broken up by a depression in the middle of it. In 2010-2015 both the terrace and the depression within it are no longer visible and there is a smooth profile from the marsh to the mud and sand flats.

The difference in elevation between the bathymetry derived for 1990-1995 and 2005-2010 near the current marsh is between -0.6 and -0.8m. This cannot directly be interpreted as erosion.

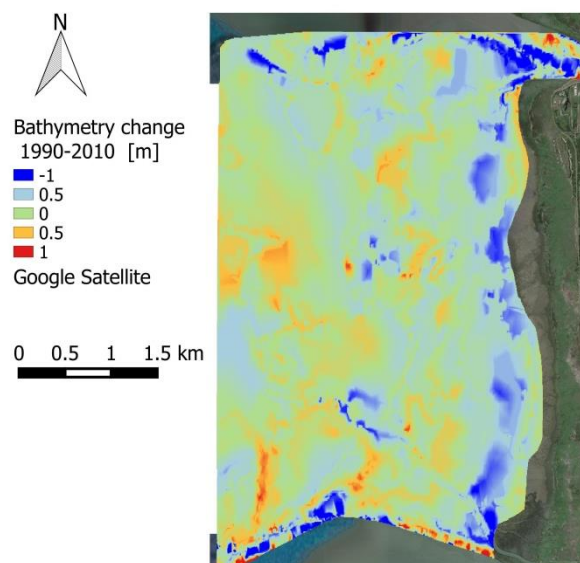


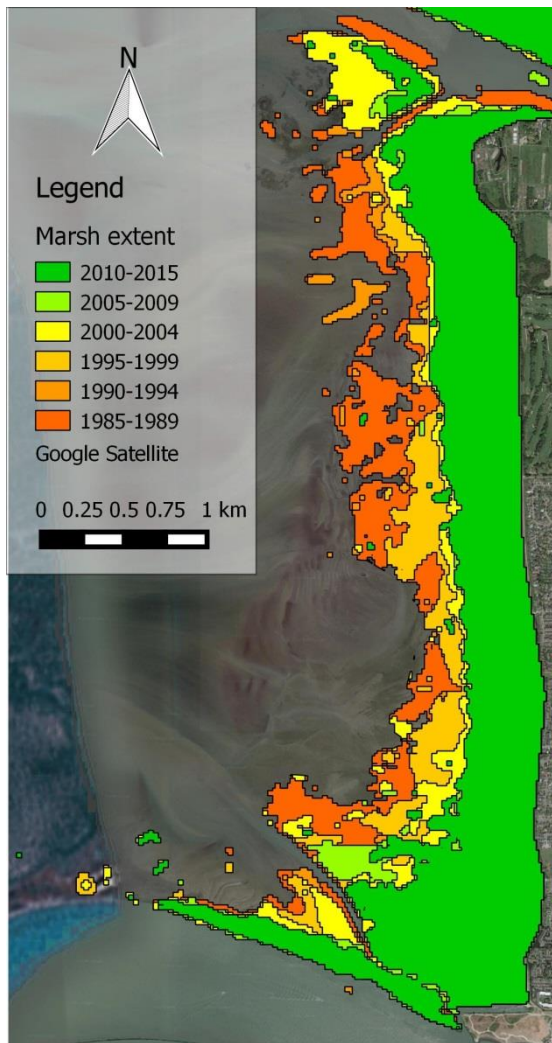
Figure 14 Difference in elevation between the 1990-1995 reconstructed bathymetry and the 2010-2015 reconstructed bathymetry

The method assumes that longer submergence time of the flats is the direct result of a loss in elevation. However, because of the very small elevation gradient a decreased drainage could result in longer submergence as well. Most likely a combination of erosion and poorer drainage did occur.

5.6 Results for the marsh

A large amount of marsh was lost in the past 30 years. The largest retreat occurred in between 1985 and 1990 and the second largest in between 1995 and 2000. The retreat has slowed down after the year 2000. There is only a minor difference between the marsh from the 2005-2010 period and the 2010-2015 compared to the periods before 2000. The marsh appears to have somewhat stabilised.

Most change happened between 1985 and 1989 but within this period the detected marsh extent showed large variation. Some large areas would be identified as marsh in one image, but not on



another from the same year. The low marsh is patchy by nature which makes it hard to distinguish from bare flats, especially on older images. Marshes detected for later years were more consistent. Despite uncertainty of the 1985-1989 marsh, it still supports retreat occurred between 1985 and 1994.

Some signs of retreat are still visible. Comparing the LandSat from august 2013 and 2015 reveals a band of decreased green cover around the marsh edge. On the other hand, the southern and northern parts of Sturgeon Bank appear to have increased in green cover. This suggests that in the central area of Sturgeon Bank a form of retreat is still ongoing while the north and south are already recovering.

Figure 15 Marsh extent between 1985 and 2015 from LandSat images

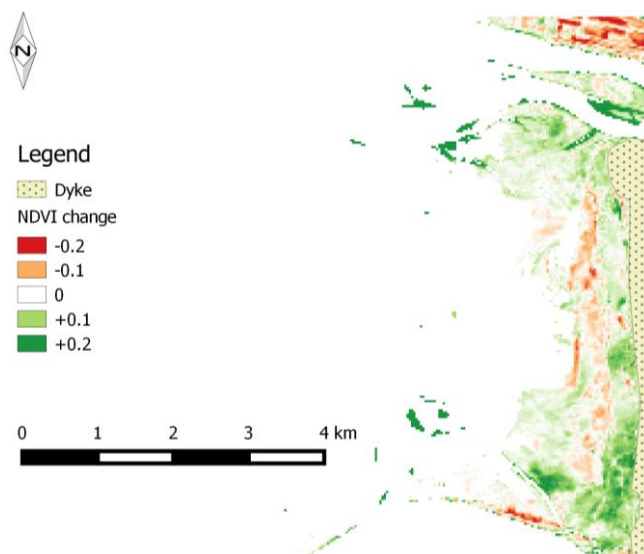


Figure 16 NDVI Change between august 2013-2015, note that slightly higher NDVI values at the seaward end are caused by the different tides on the 2 images

6 FIELD STUDY

6.1 Observations

In the beginning of June 2016, a field study was conducted on Sturgeon Bank (see Appendix 6: Report of the fieldwork). The entire length of the current leading marsh edge was inspected and observed for signs of erosion and or retreat.

Some key differences had been observed between the north, the middle and south end of the marsh. The north didn't show signs of retreat or erosion like scarps. There is an edge of dense marsh vegetation but a large part in front is covered by sparser patches.

Moving south these patches made way to clumps of mud that were filled with dead roots. Some scarps about 30 cm high were observed as well as small creeks and pools that formed behind the leading-edge vegetation. All these are clear indications of marsh retreat.

In the far south of Sturgeon Bank south of the CBC radio tower pier the marsh appears healthier. There are no clumps or scarps observed like in the middle of Sturgeon Bank. There is also a monoculture of bulrush (*Schoenoplectus Pungens*) whereas the leading edge elsewhere had been mixed.

Observations had also been made further from the leading edge. About 500m from the leading edge in the north and middle of Sturgeon Bank small islands of bulrush were found. These islands were noticeably sandier than the muddy leading edge. Seaward of the islands the low sand swells were found. In the south such features were not found. This area was covered by a system of branching tidal channels. Both the sand swells and tidal channels can also be seen on the Lidar map (Figure 2).



Figure 17 The marsh edge in the north of Sturgeon Bank



Figure 18 The marsh edge in the middle of Sturgeon Bank



Figure 19 The marsh in the south of Sturgeon Bank



Figure 20 A sand swell in the north of Sturgeon Bank



Figure 21 A tidal channel in the south of Sturgeon Bank



Figure 22 Algae covering several bulrush islands



Figure 23 Algae covering a large portion of the marsh edge at the middle of Sturgeon Bank

During the fieldwork, a lot of algae (ulva species) were encountered. These were found covering part of the leading edge of the marsh in the middle of Sturgeon Bank and on some of the bulrush islands. Some of these algae layers were thick. The algae pose several problems for the bulrush. Firstly, the algae flatten the stems to the ground damaging them and secondly the covered bulrush does no longer receive any sunlight. When the algae dry, it forms brittle white layer on top of the plants.

On the 3rd of July, strong wind blew from the west with speeds up to 40 km/h. Despite the low tide, a large portion of Sturgeon Bank from the leading edge up to 1.4 km from the dike remained inundated. Most of the water was pooling about 100 to 200m from the leading edge. When moving further offshore the water depth gradually decreased. Inundation was not only related to elevation, but also to wind and drainage patterns. Storm winds (see section 3.3) thus affect inundation as well as waves.

6.2 Elevation measurements

As part of the Fraser River Estuary Management Program (FREMP) transects were established and monitored. The previous analyses showed most retreat occurred at the center of Sturgeon Bank. Hence at the two middle transects the elevation was measured again using a GPS receiver. As described in the previous section it was observed that at most areas water was still present and only some parts were dry or almost dry (layer of water ≈ 1 cm). The satellite study relies on these observations of the water line. Using elevation measurements erosion can more accurately be determined by comparing new measurements with previous ones (see section 8.3).

Sturgeon Bank is almost flat. The gradients measured were only 1.2×10^{-3} for transect J and 0.6×10^{-3} for I. On transect I one section 600 to

1000m away from the dike was found to be flat. In contrast, transect J has sand swells that are 20cm higher than the flats. These features were 50-70m long and asymmetric. They lean forward in shoreward direction (Figure 25). Because of their resemblance to swell waves in the sea they are referred to as sand swells as coined by J. L. Luternauer (1980).

Behind the sand swells the islands of bulrush were slightly elevated as well. Several of them between transects I and J have been measured. The elevation was found to be 6 to 17 cm higher at the centre of the island than at the seaward edge of the island.

At 8 points on the leading edge of the marsh the elevation was measured. The leading edge varied in elevation between 0.38m and 0.55m



Figure 24 Locations of transects I and J © 2016 Google

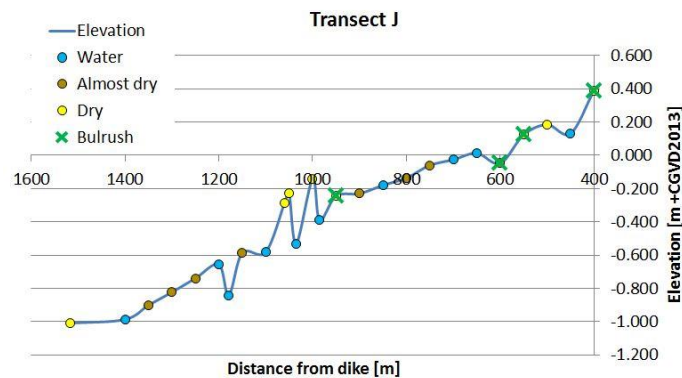


Figure 25 Elevation and observations at J

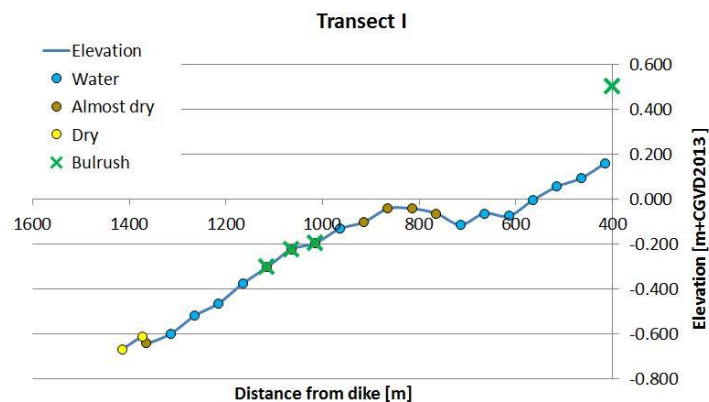


Figure 26 Elevation and observations at I

+CGVD2013 for the entire length of Sturgeon Bank. Only in the southernmost part of the marsh slightly lower elevations of about 0.31 m were measured. South on Westham Island bulrush can still grow at lower elevations (-0.7 m) (Boyd & Mason, *pers. com.*). Thus, elevation alone does not explain the current position of the marsh edge.

6.3 Soil samples

The top soil reflects the morphological processes acting at Sturgeon Bank. Fine sediment can only settle under little wave action and small flow velocities. A change in grainsize of the top soil from previous measurements will thus reflect a change in these processes. The process and results from this study are briefly presented in this section but the full method and results can be found in Appendix 7: Sediment analysis. The results are compared to other studies in section 8.4.

The top soil was sampled to a depth of 16 cm to get enough material for testing. This was done at

13 locations across Sturgeon Bank from the marsh edge to 1.5 km away from the dike. Sampling was carried out at FREMP sites Z4, Z6, H2, H5, H8, I2, I4, I6, J1, J5, L1, L3 and L5 (see Appendix 1: Maps FREMP Locations) so these can be compared with previous measurements.

The top soil was taken with a piston sampler. The core was then inspected and photographed before being sent to the laboratory in plastic containers. When the samples arrived in the laboratory each one was photographed again and weighed. It was found that some of the soil had oxidised and some water had leaked during transport. Nevertheless, no soil was lost during transport.

Each sample was mixed before soil was taken for testing. The samples for testing were dried overnight in an oven at 107 °C. Mud samples lost 30% of weight of evaporated water, slit samples around 22% and sandy samples about 20%.

Organic content had to be removed from samples

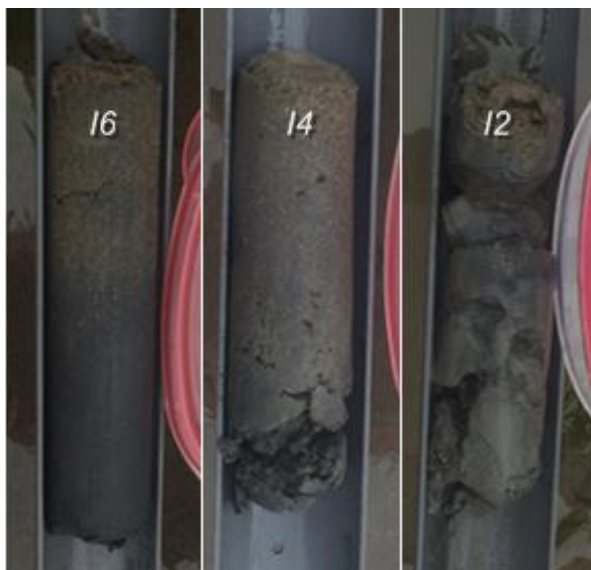


Figure 27 Cores taken at transect I



Figure 28 Cores taken at transect J

before grain sizes could be measured while also providing insight into the presence of (dead) roots at the site. From the fine samples close to the marsh (J1, L1, Z4 and Z6) and one silt sample (H5) representative for flats further out organic content was removed with a solution of hydrogen peroxide (300 g/l). Every hour 25 ml of the solution was added for a total of 6 times. After the treatment, the samples were dried and weighed. The samples from within the marsh (J1, L1) had an organic content of 4% while other samples only had 1% of organic content.

The grainsize distributions of all samples were measured by sieving and/or a hydrometer test. The southernmost samples (Z) were all predominantly mud. In the north, a combination of mud and fine sand was found (L). In the area dominated by the tidal channels (transect H) mud

and silt were found as well as sand at the most seaward location. The samples on transect I contained mud, silt, and a top layer of sand. This top layer was thickest seaward (I6) and small at the marsh edge (I2). The most varied transect was J where on the sand swells only sand was found (J5) and near the marsh edge only mud (J1).

Typical grain sizes for Sturgeon were determined from the samples. Near the marsh edge where mud is dominant the median grain size is only 9-12 μm . At the centre of the bank close to the marsh I2 had a median grain size of 40 μm . Very fine sand was found in the north and south ranging from 62 to 77 μm while in the middle there is fine sand of 125 μm . The coarsest sample was taken at the sand swells with a mean grain size of 210 μm .

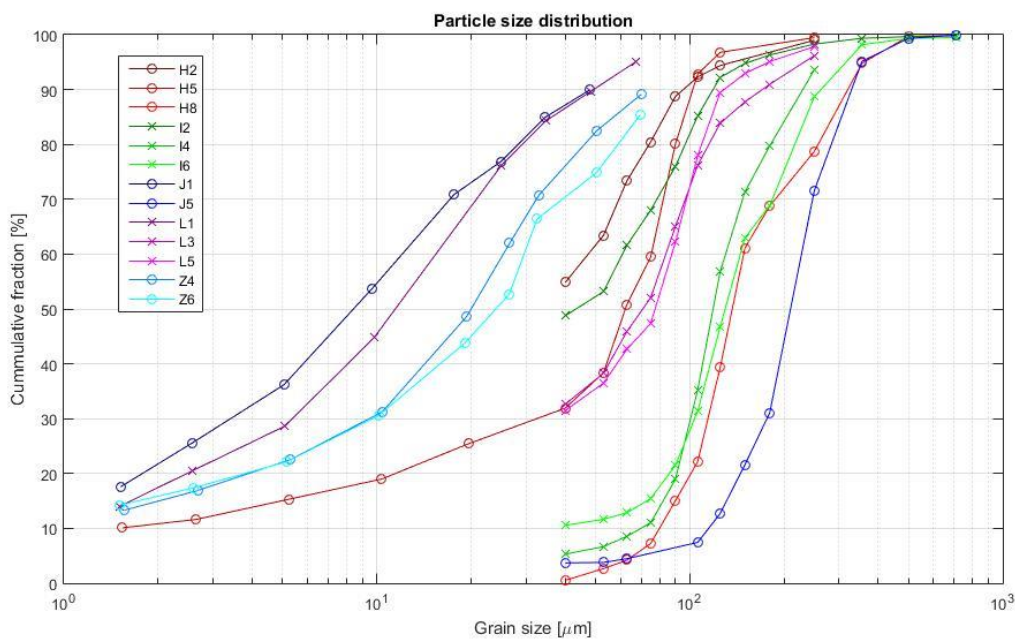


Figure 29 Particle size distributions of samples

7 MODEL STUDY

As part of the study of the governing processes on Sturgeon Bank models were developed to simulate the flow and the tide. The results are presented in this chapter.

7.1 Flow model

Delft-3D is a numerical program that simulates the flow of water by solving the depth-averaged Navier-Stokes equations at different points in time. The rigid vegetation module in Delft-3D was used to simulate the roughness imposed by the marsh and bulrush islands. A detailed description of the model can be found in Appendix 8: Flow model.

After testing the model could only be validated for the progression of the tidal flow on the flat. It was unable to calculate flows at water depths smaller than 7.5 cm. The model was therefore only used to determine the general flow paths on the bank while ponding effects and surficial draining at low tide were omitted.

The flows are concentrated around the tidal channels as could have been expected. The tide does also follow the remnant of the tidal channel in front of the sand swells identified in from the air photo from 1986. Flows are funnelled in between the sand swells and bulrush islands.

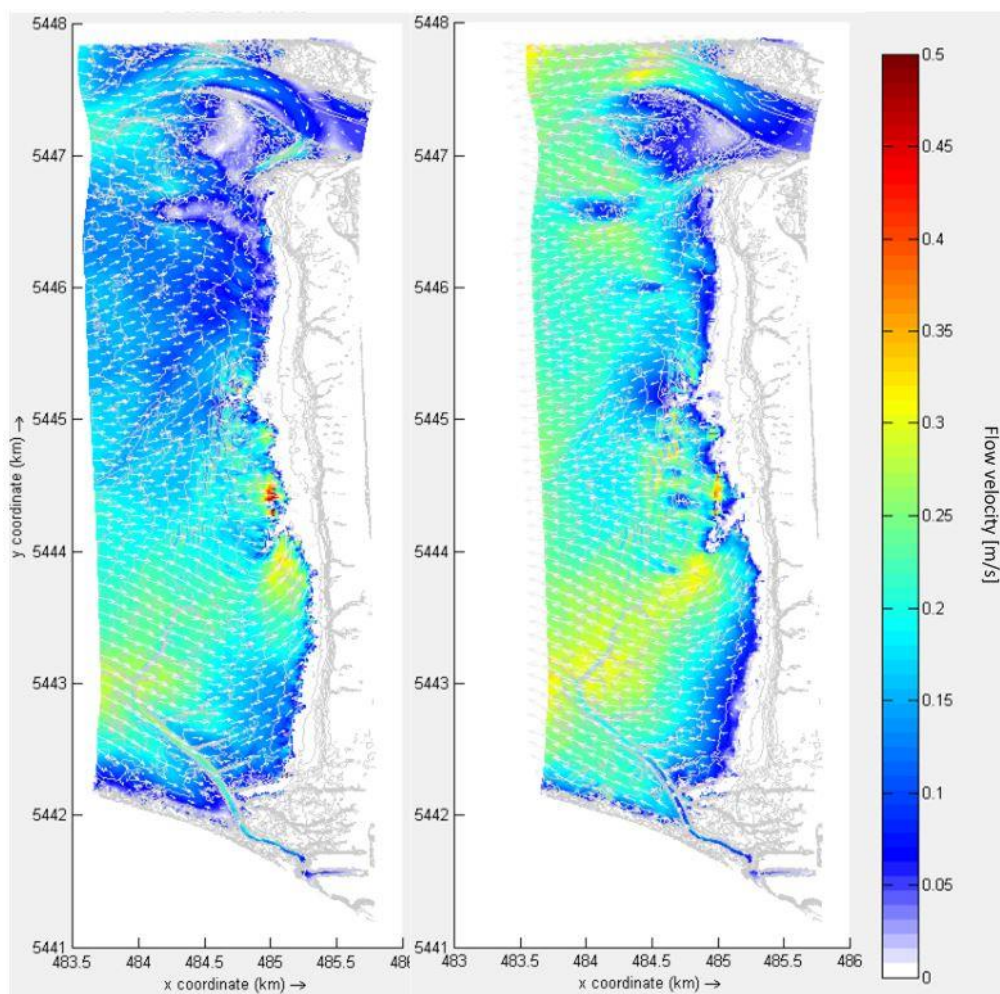


Figure 30 Predicted tidal flows from the Delft-3D model. Left: flood, Right: ebb

Most of the water behind the sand swells flows in and out either from the tidal network in the south or by flowing around the sand swells in the north.

Apart from general conclusions about the flow patterns during ebb flood, no other conclusions could be drawn from the model. Further refinement is needed (e.g. by strongly reducing the time step to a few seconds) in order to capture the dynamics of drainage during low tide.

7.2 Wave model

From the literature review it was found that waves could be an important factor for the marsh retreat. A model was made to simulate the progression of waves over the tidal flats.

7.2.1 Method

The calculation is based on the wave energy from the incoming waves. In linear wave theory wave height and energy are related as:

$$\text{Eq. 3} \quad E = \frac{1}{8} * \rho g * H^2$$

The waves are breaking due to the reduced water depth. The largest waves that can travel on the flats without breaking are calculated as:

$$\text{Eq. 4} \quad H_{max} = \gamma * h$$

H_{max}	=	Maximum wave height before breaking	[m]
γ	=	Breaking parameter	[-]

The calculation uses the model by Battjes and Janssen (1978) for dissipation of wave energy by wave breaking. The formula states:

$$\text{Eq. 5} \quad D_w = \frac{1}{4} Q_b \alpha \frac{\rho g}{T} H_{max}^2 \quad (\text{Battjes \& Janssen, 1978})$$

D_w	=	dissipated energy	$\left[\frac{J}{m^2 s} \right]$
Q_b	=	Fraction of breakers	[-]

α	=	Calibration factor	[-]
T	=	Wave period	[s]
H	=	Wave height	[m]

The fraction of breaking waves is calculated by the method proposed by Baldock, Holmes, Bunker, and van Weert (1998):

$$\text{Eq. 6} \quad Q_b = \exp\left(-\left(\frac{H_{max}}{H_{rms}}\right)^2\right) \quad (\text{Baldock et al., 1998})$$

The time averaged change of wave energy across the banks in the direction of travel follows from the energy balance in shallow water:

$$\text{Eq. 7} \quad \frac{dE c_g}{dx} = D_w$$

The bottom profile was derived from the 2013 Lidar data at FREMP transect J. The tide levels from the statistical tidal analysis were implemented as water levels and waves were selected from the wave analysis. A numerical scheme was used to solve the equations above for the wave height across the bank. The numerical scheme is presented in Appendix 9: Wave model.

7.2.2 Results

The sand swells do not affect the waves reaching the marsh at high water. The height of the sand swells compared to the water depth at high tide is too small for any significant effect in wave breaking.

A region where no wave breaking occurs is present directly behind the sand swells when the tide is at mean sea level or below. At mean high low water (MHLW) the sand swells shield the hinterland from waves almost completely.

The zone directly behind the sand swells

coincides with the region where isolated bulrush patches can still be found. Possibly the sand swells could support bulrush locally by wave breaking.

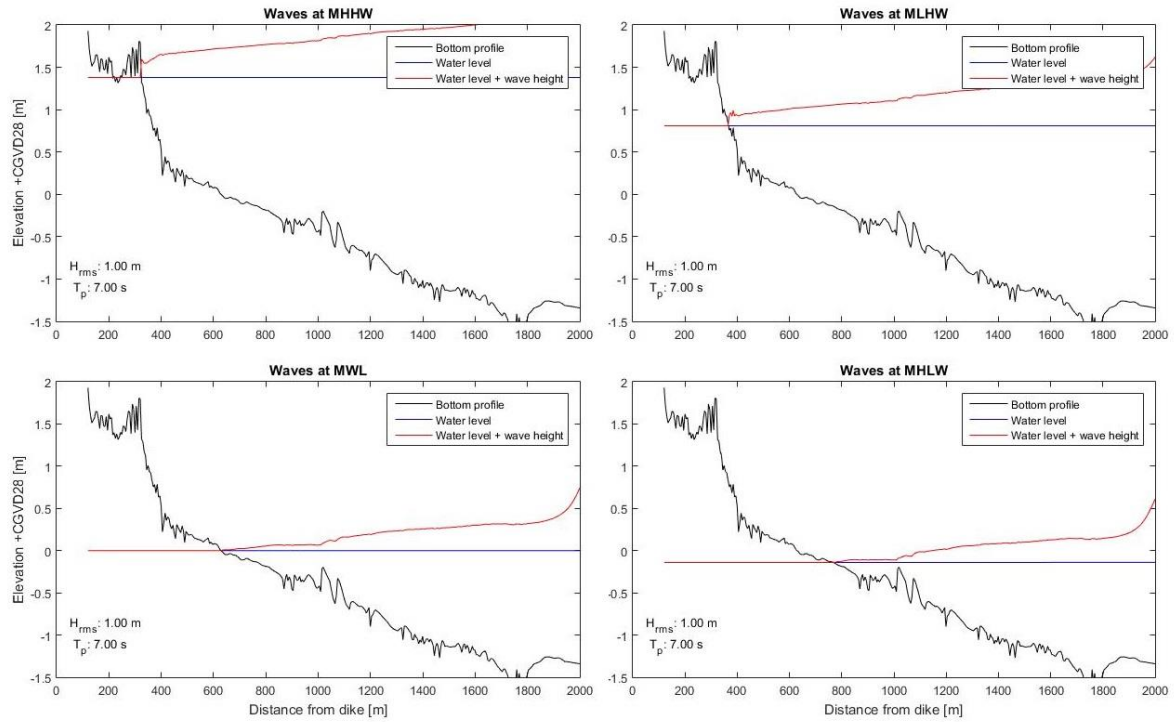


Figure 31 The progression of 1m waves over transect J

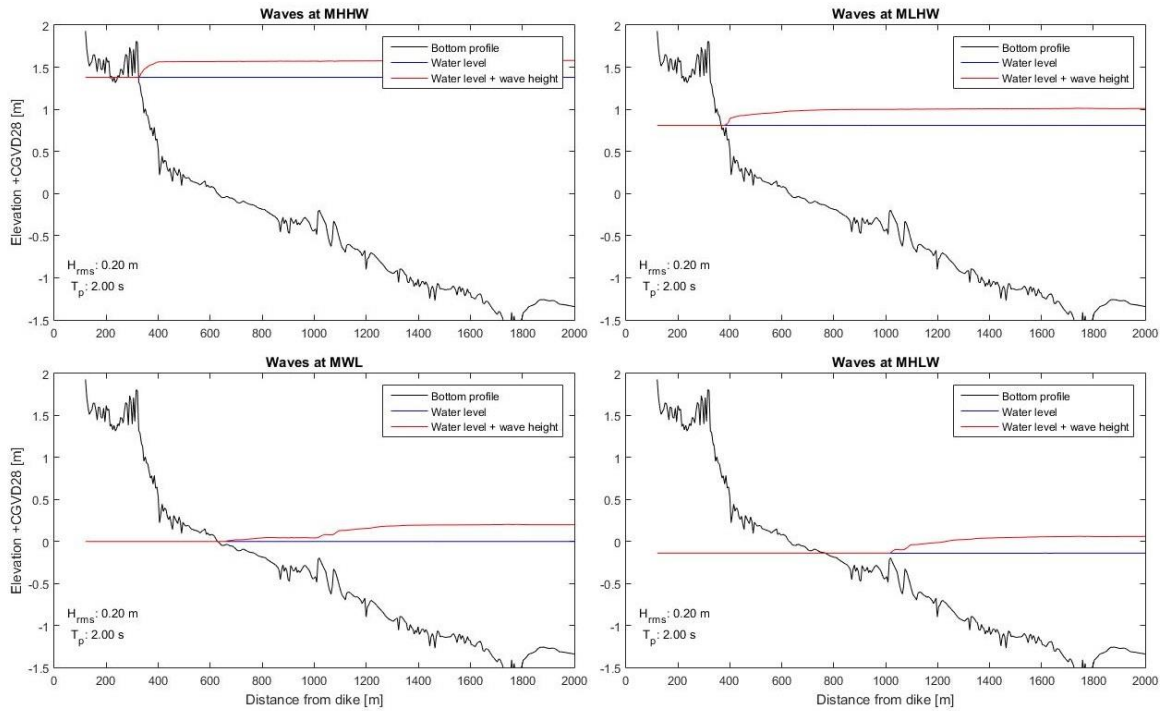


Figure 32 The progression of 0.2m waves over transects J

8 OVERVIEW OF CHANGES ON STURGEON BANK

The results from the literature and the analyses in this study are summarized and discussed in this chapter.

8.1 Before 1990

The tidal flats on Sturgeon Bank and the Fraser delta as a whole had been growing westward for the greater part of its history (Clague, Luternauer, & Hebda, 1983). Due to the tidal forcing and ample supply sediment had been steadily deposited on the banks.

The primary source of sediment is the Fraser river. The construction of jetties in the 1930's and dredging has most likely cut off the banks from any significant source of sediment (Atkins et al., 2016). Initially the construction of the Steveston jetty in particular could have allowed the marsh to expand as mud accumulated in the calmer environment (Hales, 2000). It was hypothesized that wave reflection off the jetty allowed sand swells to form which would have further encouraged the marsh growth (J. L. Luternauer, 1980; Medley & Luternauer, 1976).

From air photos and documentation (Medley & Luternauer, 1976) Sturgeon Bank had a growing system of tidal channels up until the 1980's. The growth of channels could be the result of the expanding marsh which makes the tidal currents flow in more concentrated streams while promoting further expansion (Temmerman et al., 2007).

Aerial imagery and satellite imagery shows that sometime between 1980 and 2001 this state shifted. A rapid recession of the marsh occurred while the majority of tidal channels disappeared.

8.2 Marsh recession

The moment the marsh started retreating was uncertain as different sources stated either growth of the marsh (M. Church & Hales, 2004; Hales, 2000) or retreat (Ilori, 2015; TRE Canada Inc., 2014) between 1985 and 2004. The current study found similar results as the latter. It concludes through satellite images and aerial pictures that marsh recession peaked in the 1990's and has been slowing down in recent years. Field measurements of the leading edge in 2011 and 2015 (Boyd & Mason, *pers. com.*) as well as observations the fieldwork and the satellite images in this study, all confirm the marsh is no longer severely receding and could even be stable.

Given these circumstances it is most probable the retreat was initiated sometime in the 1990's and has decelerated since. The retreat could be the result of a tipping point being reached in that period. The current marsh is approaching a new equilibrium.

8.3 Erosion and deposition

This study initially found elevation changes of 0.7 m based on bathymetries calculated from water levels on satellite images between 1990 and 2010 (Figure 14). The erosion is concentrated along a band in front of the current marsh. This area roughly coincides with the location of the marsh from before 1990. However longer inundation or a reduced drainage capacity can result in an over prediction of erosion with this method. Other methods were used to quantify erosion in recent years.

The Lidar elevations from 2013 were compared to measurements from 2015 and the GPS

elevations from the field work.

Between 2013 and 2016 no large-scale erosion has occurred at either transect I or J. To the contrary, transect I has experienced some deposition. The same was measured by environment Canada (Appendix 1: Maps: Sedimentation and erosion between 2011 and 2015). Erosion and deposition did occur locally but averaged across the whole area it remained constant. The changes that were measured were at most 1cm/year, given that there is some margin of error it is not possible to deduce any deposition or erosion trends.

The GPS elevations and in-situ measurements by environment Canada show that the flats in their current form are stable. The erosion that was found from the satellite studies is no longer present and there is no (longer) structural loss of sediment within the first kilometre between the current marsh edge and sand flats.

8.4 Soil composition

The sediment on Sturgeon Bank had been measured before in June 1992 (Feeney, 1995), February to April in 1993 and again in July of 2011 (McLaren & Ren, 1995; Wootton & Sarrazin, 2011). All studies used different methods to

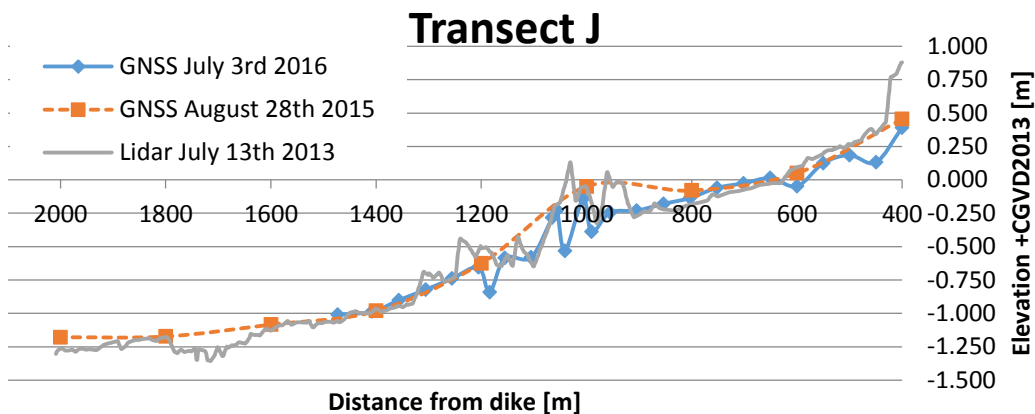


Figure 33 Elevations at transect J. Vertical datum of the Lidar was converted from CGVD28 to CGVD2013. Data sources: Lidar from Port Metro Vancouver, 2015 GNSS heights provided by Sean Boyd and Brad Mason

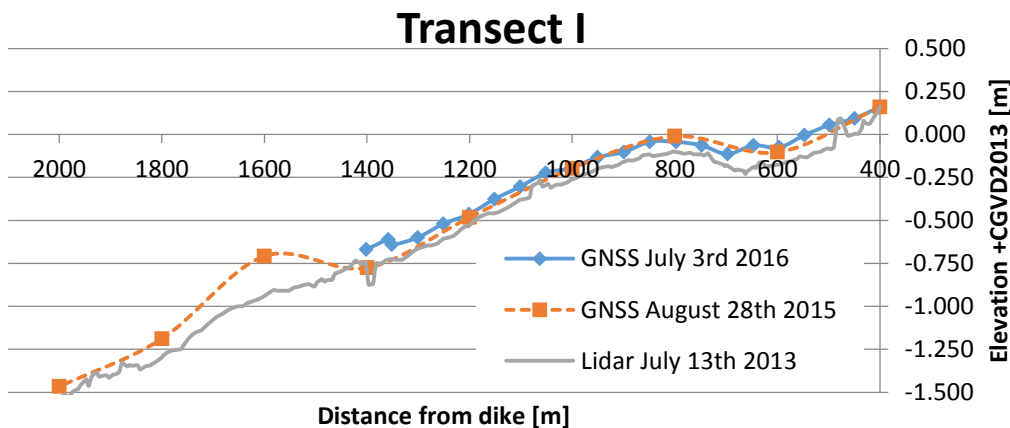


Figure 34 Elevations at transect J. Vertical datum of the Lidar was converted from CGVD28 to CGVD2013. Data sources: Lidar from Port Metro Vancouver, 2015 GNSS heights provided by Sean Boyd and Brad Mason

determine the grainsize distribution of the top 2, 10 and 16 cm of soil respectively.

The earliest samples from 1992 were taken mostly on the sand flats. All samples are sand except samples taken about 1.5 km from the dike. In the north end these samples are mud while in the middle silt or sand was observed.

The 1993 samples show again that the flats are predominantly sand. The samples closest to the marsh in the north and south were muddy and in the centre the samples were silty. Unfortunately, there were no samples taken close to the current marsh edge in the middle of Sturgeon Bank.

In 2011 samples were taken at the FREMP transects. The samples at the marsh edge were all composed of clay and silt (except for an anomaly at J1). As in 1993 the middle samples further from the edge become sandier in the middle than in the north and south.

Comparing the samples from 2016, 2011, 1993 and 1992 is difficult because the older studies took most samples on the flats and not within the marsh. Looking at the most shoreward of these samples there is a trend of increasing sand content in the north and middle of Sturgeon Bank while the south does not experience such change. The sand percentage of the soil behind the current bulrush islands was between 36 and 41% in 1993 and increased to 57-60% in 2011. One sample in 2016 shows a

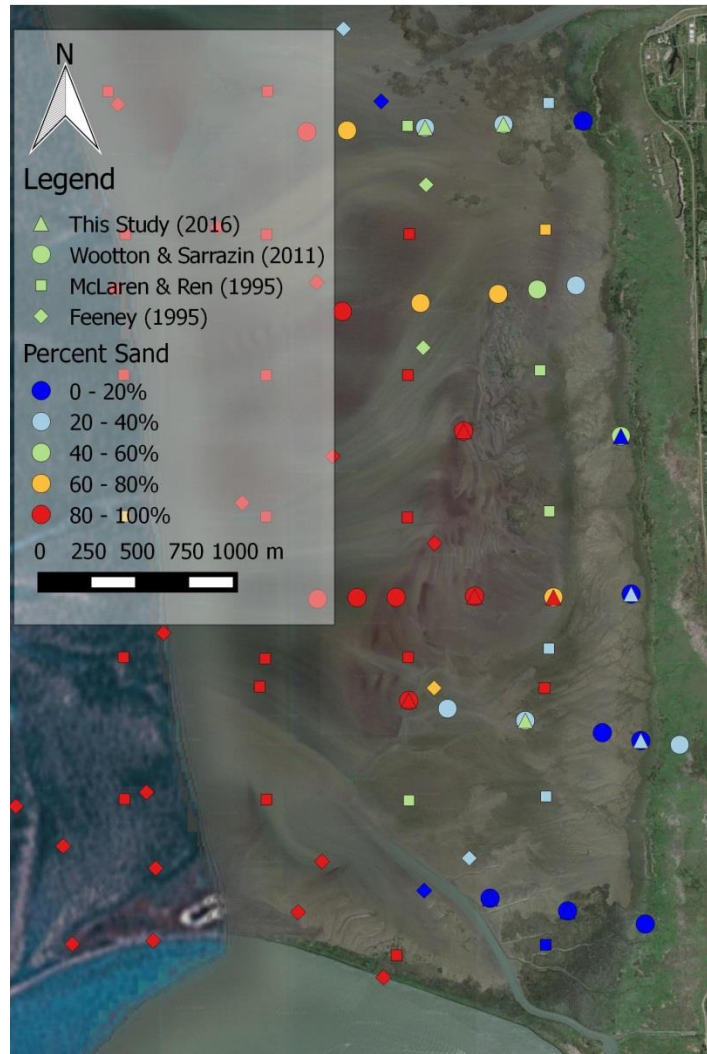


Figure 35 Comparison between samples of different studies. Background from Google maps

Table 6 Difference in sand particles measured in 2011 and 2016. Samples sorted from south to north. Source 2011 samples: Wootton and Sarrazin (2011)

Sample: FREMP site:	2011 % Sand ($>63 \mu\text{m}$)	2016 % Sand ($>63 \mu\text{m}$)	Difference % Sand
Z4	6.1%	13.3%	7.2%
Z6	9.4%	18.2%	8.8%
H2	11.4%	26.6%	15.2%
H5	27.4%	49.2%	21.8%
H8	86.0%	95.8%	9.8%
I2	14.0%	38.4%	24.4%
I4	60.3%	91.4%	31.1%
I6	93.1%	87.1%	-6.0%
J1	45.4%	4.9%	-40.5%
J5		95.5%	
L1	7.3%	6.1%	-1.2%
L3	22.6%	54.1%	31.5%
L5	27.6%	57.3%	29.7%

further increase of sand to 91%.

Because the 2011 and 2016 samples are from the same locations they can be compared directly. In the south (Z4 and Z6) the sand content hasn't changed much. Also at L1, located within north of the marsh, no large changes were found. Most of the changes were at the centre where all samples except for the ones that were already primarily sand, had a significant increase of sand of up to 31.5%. The only anomaly was found at J1 which was reported to have a very high sand content for its location at the marsh edge in 2011.

Each study analysed grainsizes with a different method which could have introduced biases in the results of each study. Feeney (1995) used wet sieving, settling tube and sedigraph. McLaren and Ren (1995) used a laser particle sizer, Wootton and Sarrazin (2011) used a combination of sieving and sedigraph while in this study a combination of sieving and a hydrometer was used.

Furthermore, the difference in season between the measurements in 1993 and 2011 could have played a part as well.

Nevertheless, the change in sand content measured within the last 23 years are beyond what can reasonably be expected from natural variation or difference in measuring techniques. It is therefore concluded sand is being transported towards the marsh and/or fines are being eroded.

The erosion of fines seems likely since the satellite study indicated erosion did occur there in the past. However, the recent bathymetry changes since 2013 do not show much erosion. At some areas (mainly transect I) there has been some deposition. The layer of sand visible in the cores at transect I (Figure 27) could indicate the

deposition of fine sand. Transport of sand towards the marsh is thus supported by other analyses though erosion of fines cannot be ruled out.

9 POTENTIAL RETREAT MECHANISMS

9.1 Framework

Salt marshes are complex ecosystems on the boundary between sea and land. As such they are governed by a myriad of processes. The tidal flats on which the marsh grows are formed by a combination of sediment supply, tides, and waves. Tidal flows and waves transport sediment onto or away from the flats altering the bathymetry. However, propagation of waves and the tidal flows are highly affected by the bathymetry as well. The bathymetry will thus approach an equilibrium between with these forces (Friedrichs, 2011).

The growth of vegetation affects the tidal flats as well by adding roughness to the bottom and capturing fine sediment in between stems. Furthermore the roots bind the soil making it

more resistant to erosion (Fagherazzi et al., 2013). Vegetation thus indirectly induces bathymetric through altering tidal flows, waves, and transport of sediment.

The growth of the marsh is limited by inundation (Gray, Marshall, & Raybould, 1991). Mud pools can form at low tide inhibiting further growth of the marsh (John L. Luternauer, Atkins, Moody, Williams, & Gibson, 1995). Other factors that contribute to the growth/loss of the marsh are environmental factors like nutrients and salinity, and biological factors like plant disease, fungi, or grazing geese.

The couplings mentioned are simplified to a framework in figure 36. This provides a direction to establish a hypothesis. Each hypothesis will be presented within this framework.

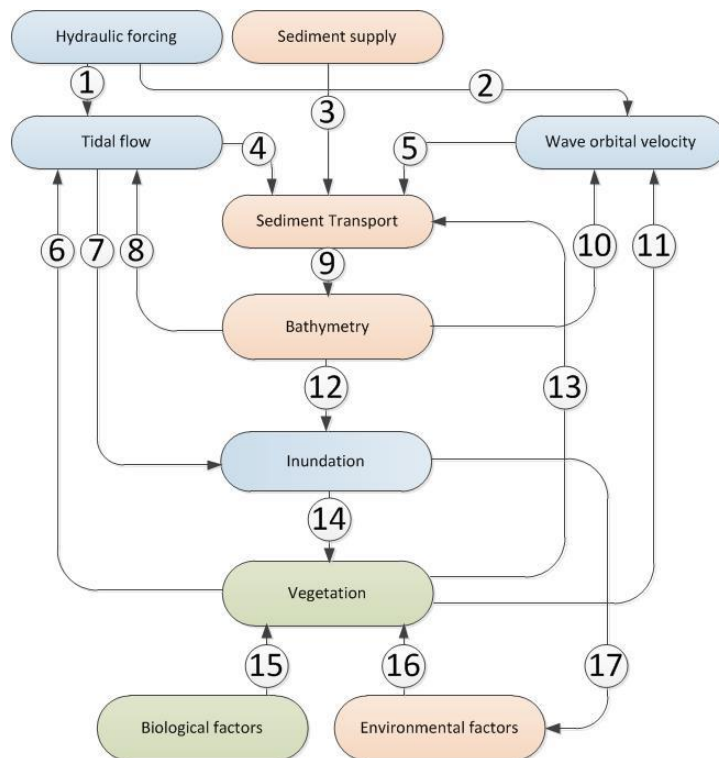


Figure 36 Interactions governing the tidal marsh

Several hypotheses are put forward based on the established framework. These do not encompass all possible mechanisms nor rule out the possibility other mechanisms could be present as well. They do need to be based to some degree on actual observed changes at or near Sturgeon Bank

9.2 Reduced sediment supply

Sediment is being dredged from the Fraser river to increasingly greater depths for shipping. As a consequence, the flow velocity in the river decreases as well as its capacity to transport heavier sediment. In theory, this could lead to a sediment deficit on Sturgeon Bank as less sand from the river is transported there.

The bathymetry of an estuary will approach a dynamic equilibrium with the tidal forcing, waves, and sediment supply such that the sediment transported away from the coast is compensated by the transport to the coast (relations 3, 4 and 5 in Figure 36). Since the tidal and wave forcing are initially the same, less sediment is being supplied than needed to maintain the coast. The result is an overall loss of sediment from the coast and a change in bathymetry (relation 9).

Sediment could be removed by wave action (relation 4), expansion/deepening of the tidal channels (relation 5) or a combination of the two. The loss of the flats increases the water depth, resulting in stronger wave action (relation 10) and an acceleration of erosion. The process would initially be very slow since the waves under normal conditions are quite small. However, when enough of the buffer has been eroded the erosion becomes more pronounced and can no longer be mitigated by other processes. A cliff forms where sediment is removed at the marsh

edge. Locally the elevation decreases which allows the tide to penetrate further inland and submerge the area below the cliff for longer (relations 12 and 7). The longer inundation prevents recolonization (relation 14) and the marsh retreats.

9.3 Relative sea-level rise

Sea-level rise is a threat to many marshes around the world. Some marshes like the one described by Schuerch et al. (2016) will easily accommodate the sea-level rise as there is enough supply of sediment. Other marshes that are unable to accrete fast enough will migrate landwards (Donnelly & Bertness, 2001). Many marshes are at risk of drowning when the vertical accretion on the marsh is out-paced by the accelerating rise in sea levels (FitzGerald, Fenster, Argow, & Buynevich, 2008). The retreat on Sturgeon Bank could be in this state.

Within the framework absolute sea-level rise can be considered a change in hydraulic forcing which results in higher tide levels (1). Subsidence should be considered as well as it lowers the bathymetry. Both will cause a longer inundation (7, 12) and drown the marsh vegetation (14). Normally the entire marsh would simply retreat landward and there would be no net loss of marsh. However, on Sturgeon Bank the dike prevents this retreat and so the marsh gets squeezed against it.

Only if enough sediment is being supplied to the marsh it can remain high enough to avoid longer inundation (9). When the sea-level rise outpaces accretion, the same mechanisms will be triggered as described in the reduced sediment supply hypothesis. Indeed, the lack of sediments to compensate the effect of sea-level rise can be

considered a sediment deficit like the one created by a reduced supply.

9.4 Sand swells

On Sturgeon Bank sand swells have been first documented in the 1970's (Medley & Luternauer, 1976). In aerial photos, they are visible even earlier in the 1950's. Based on the results of the aerial imagery analysis it was established that the sand swells are no longer at the same location as they were in 1986. The migration of sand swells landward could explain the transport of sand found from the soil investigation and the bathymetric surveys. It is hypothesized that the sand swells have migrated north east in this period resulting in marsh loss.

In the same period the sand swells were migrating most of the marsh recession was taking place as was found in both the satellite study the study by Illori (2015) and evidenced by the difference in marsh extend on the aerial pictures. A series of processes could have been initiated by the migration of the sand swells that has resulted in the marsh recession.

The sand swells are bathymetric features. As they migrate the bathymetry is changed. The changed bathymetry will affect the tidal flow (Figure 36 relations 8). The sand swells form a barrier for the incoming and outgoing tide when the water levels are low. This effect would be even stronger when the sand swell migrates over a tidal channel, a feature that is the main pathway for the in- and outgoing tide. When the sand swells are submerged they are influenced by the tidal current similar to dunes in a river where they impose a varying roughness on the flow (Fredsoe & Deigaard, 1992). In both cases the sand swells obstruct the free flow of water between the flats

and the marsh.

The obstruction of the flow by sand swells results in longer inundation when the tide is receding as it becomes exceedingly difficult for water to flow out of the area (Figure 36 relation 7). Locally the water can become trapped and areas remain continuously inundated during an entire tidal cycle. Because of the longer inundation, they are no longer suitable for marsh growth (Figure 36 relations 14).

A second effect the sand swells have relates to waves. At high tide waves can propagate over the shallow depths of the tidal flats. The slope of the flats is about 1×10^{-4} and can almost be seen as flat.

The sand swells are the only feature that limits the water depth before the waves can reach the marsh edge. By limiting the water depth, wave breaking is induced away from the marsh edge thus dissipating wave energy (Figure 36 relation 10).

In Möller and Spencer (2002) it was found that wave heights slightly increase at the marsh cliff by reflection. This prevents establishment of new vegetation as well lateral erosion of the marsh cliff (Van der Wal, Wielemaker-Van den Dool, & Herman, 2008) (Figure 36 relation 9 to 12 & 14). Thus, as sand swells migrate away from an area, former sheltered marsh is exposed to more wave energy leading to lateral erosion at the marsh cliff.

Finally, there is a direct relation to be found between the sand swells and the vegetation trough inundation (Figure 36 relation 12 & 14). The crests of the sand swells are higher in elevation than the surrounding flats thus reducing submergence time. Furthermore, the troughs will naturally collect any excess water leaving the top of the sand bars dry. Although the top of the front

sand swells might become more suitable for vegetation inundation wise, the breaking of waves would pose a problem. Hence the opportunity for marsh vegetation to establish is better at the most shoreward sand swells.

Summarized the hypothesis is as follows: migrating sand waves cause the marsh to retreat through obstruction of tidal flows resulting in longer inundation and exposing previously sheltered marsh to more wave energy. Simultaneously the area directly behind the first sand swells would be expected to remain suitable for vegetation due to its heightened elevation above the mud flat, explaining the presence of bulrush there as observed during the site visit.

9.5 Ponding

Ponds are depressions that remain filled with water once the tide has receded. At Sturgeon Bank, it is observed that just behind the retreating marsh edge small ponds have formed. Just in front of the marsh cliff pooling of water was observed as well (*pers. obs.*).

Various factors can cause the formation of ponds. The most obvious factor to be considered is the large amounts of algae observed during the fieldwork. Smothering of plants by debris and algae will lead to the decay of the plants. The depressions left behind are filled by water during high tide and are characterised by steep slopes (Harshberger, 1916).

The ponds form as a response to the death of the plants. The underlying peat is exposed and collapses. This severely decreases the elevation which in turn increases the likelihood of the pond being flooded in the future (DeLaune, Nyman, & W. H. Patrick, 1994). Once formed the ponds

expand by biochemical processes (van Huissteden & van de Plassche, 1998) or by surficial flooding of the adjacent marsh (Wilson et al., 2009). Ponds expand until eventually drained by a tidal channel (Wilson, Kelley, Tanner, & Belknap, 2010). At this point the pond has been converted into mud flat.

During the fieldwork two channels protruding into the marsh were measured about 160 m apart. The ponds were found only a few meters from the marsh edge. It is therefore more likely that as the ponds expand they will be drained once they have reached the edge, rather than by a tidal channel. This is a minor departure from the theory, but the mechanisms should still apply.

Following the conceptual model by Mariotti (2016) there are a few options for how the marsh will develop further. The first option is that the mud flat meets the hydraulic and environmental conditions for reestablishment. The second option is that initially these requirements aren't met but that through deposition they will be met eventually. In both cases there is a cycle of retreat and reestablishment.

A final option is that the mudflat will remain unsuitable for marsh growth. Mariotti (2016) suggests that under sea-level rise the marsh may receive sufficient deposition while the mud flats don't. In that case the marsh edge retreat by waves (see sea-level rise hypothesis) is amplified by the pond collapse regime. Any other mechanism that prevents mudflats from being recolonized suffices to induce a pond collapse regime in this conceptual model.

To summarize the mechanisms with the framework; a biological disturbance like repeated

smothering by algae results in local loss of marsh (Figure 36 relation 15). The exposed peat will collapse and be submerged by the tidal flow (relation 4, 9 and 13). Because the elevation has lowered locally it is more likely to be submerged repeatedly (relation 7 and 12). In the pond, biochemical conditions are altered (relation 17) such that bank erosion can take place (relation 16). This processes repeats until the pond is drained by tidal channels (relation 7) and the conditions for biochemical erosion are no longer present (relation 17).

9.6 Feedback mechanisms

Several mechanisms could accelerate an incidental die-off to a point where a small recession cascades into a large die-off.

Interactions between marsh vegetation and forcing were found in literature and can be applied to the recession on Sturgeon Bank. In this hypothesis no primary cause is defined, but states that any sort of significant die-off will inevitably lead to a collapse of the low marsh on Sturgeon Bank.

First, identical to the ponding hypothesis, when marsh dies the underlying sediment is exposed. This sediment is weak without the support of a living root system and collapses under wave action (DeLaune et al., 1994). In turn this leads to the area lowering in elevation and becoming waterlogged. This lowers the potential for recovery. When the area is continuously inundated the anaerobic bacteria produce toxic hydrogen sulphide. An accumulation of this compound turns the soil dark grey and less suitable for plant growth (van Huissteden & van de Plassche, 1998; Wilson et al., 2010). It could be possible algae survive and grow in the ponding water, turning the entire ponding hypothesis into

a feedback mechanism.

Marsh plants are an agent of the development of tidal channels within the marsh (Temmerman et al., 2007). A reduced plant cover would also reduce channelization. Bulrush used to grow primarily along the well-drained flats near the tidal channels (Hutchinson, 1982). The loss of the channels further reduces the habitat of bulrush.

Bulrush is effective at dampening wave heights (Blackmar, 2013) especially when a large extent is vegetated (van Loon-Steensma, Slim, Decuyper, & Hu, 2014). The continued loss of marsh vegetation thus allows bigger waves to reach the area. As a result, the marsh becomes susceptible to cliff erosion by waves.

In short, the death of vegetation would cause sediment to be exposed to wave action (13) and thus erosion of the bed (9) increasing inundation (12) and worsening the grow conditions of bulrush (14). The grow conditions are further decreased by accumulation of hydrogen sulphide (17) by bacteria. The death of the bulrush leads to less concentrated tidal flows (6). Channels decrease in drainage efficiency (7) and thus the area is less suitable for the establishment of bulrush (14). The last connection of bulrush in the framework is through wave action which increases when the bulrush dies (11). As a result, an erosional cliff forms within the marsh (5, 9).

The hypothesis could link the results from the aerial imagery (loss of channels), soil investigation (grey mud indicating hydrogen sulphide), satellite study (sudden erosion), wind analysis (storms at the time of erosion) and recent elevation measurements (minor cliff along the marsh edge in the middle).

10 EVALUATION OF POTENTIAL RETREAT MECHANISMS

10.1 Reduced sediment supply

The hypothesis states that due to the lower supply of sediment to Sturgeon Bank the amount of sediment transported away has become greater than the amount of that is sediment supplied as a result of dredging. The sediment is removed from the surface leading to lower elevations, increased inundation and eventually loss of the marsh.

For the data to support the hypothesis there must be proof of systemic loss of sediments. The satellite study and the report from TRE Canada Inc. (2014) indicated erosion in front of the current marsh edge. This study found a similar pattern of erosion close to the marsh edge. On the images that area was inundated at lower stages of the tide in recent years than it had been in the past.

Evidence of a reduced supply was found in cores by both Hales (2000) and Williams and Hamilton (1995). Both showed sedimentation rates had decreased by 50% since the 1950's. In this study it was found that near the marsh edge the amount of sand had increased when compared to the study by Wootton and Sarrazin (2011). Because lighter particles can be eroded more easily than sand there could be a loss of muddy sediments.

Elevation measurements in 2013, 2015 and 2016 as well as sedimentation measurements between 2011 and 2015 show no overall decrease in elevation. If erosion was structural the trend should continue as dredging has not decreased. A reduced sediment supply could have been created by other factors like the construction of jetties. Still these structures were constructed 30 to 50 years before the marsh retreated and did not

result in large degradation of the marsh in the decades after their construction (Hales, 2000).

Even more so, the fast retreat of the marsh between 1990 and 2000 was preceded by the placement of additional dredge spoil in 1980's at the bend of the Steveston Jetty (Levings, 2004). This sediment has been reworked landward suggesting that at least in the south there is transport of sediment towards rather than away from the marsh.

Finally there needs to be a mechanism in place capable of structurally eroding the tidal flats and marsh. Feeney (1995) measured that normal tidal flows are not capable of transporting sediment from the inner bank. Even if transport could be initiated by tidal flows the tidal signal is such that it favors deposition rather than erosion.

The only mechanism that has been identified to be capable of moving sediments is wave action during storms. However, such storm waves are episodic rather than structural.

There are no strong indications a reduced sediment supply is causing the retreat of the salt marsh. Although sedimentation rates on Sturgeon Bank have decreased (Williams & Hamilton, 1995), this decrease has not translated into the erosion implied by the hypothesis.

10.2 Relative sea-level rise

Crustal uplift is with only 0.25 mm/year insignificant for the Strait of Georgia (James, Hutchinson, Barrie, Conway, & Mathews, 2007). Subsidence on the hand is more significant with rates in Richmond of 1 mm/year (S Mazzotti, Lambert, Van der Kooij, & Mainville, 2009).

The absolute sea-level rise is the biggest contributor at a rate of about 1.7-1.8 mm/year (Stephane Mazzotti, Jones, & Thomson, 2008; S. Mazzotti, Lambert, Courtier, Nykolaishen, & Dragert, 2007). Combined the relative sea-level rise on Sturgeon Bank is 1.8-1.9 mm/year.

As a first approximation for the retreat it is assumed that Sturgeon Bank has a constant slope of 0.9×10^{-3} (average of the gradients measured on transects I and J during the fieldwork) and that there is no supply of sediment. Dividing the sea-level rise of 1.85mm/year by the slope a rate of 2.06m/year of retreat is calculated.

The Bruun rule is another method to estimate the retreat by sea-level rise. It assumes the same profile will be maintained and shifts landward by moving sediment from the upper slope down the lower slope. It can be calculated as:

$$\text{Eq. 8} \quad a = \frac{L * SLR}{h + d} \quad (\text{Bruun, 1988})$$

Where a is the landward retreat, L is the width of the active profile, h is the height of the dune or dike, d is the active depth and SLR is the rate of sea-level rise. The flat is about 7 km wide which is assumed to be the active length, the water depth at the edge of the flat is around 2.5 m at MSL and the dike is about 3.5 m above MSL. The landward retreat follows from the formula and is about 2.16 m/year.

A better way to calculate the retreat by sea-level rise with the Bruun rule is to assume the upper marsh is not part of the active profile as the plants will hold back the sediments. The marsh is about 500m wide and following from the fieldwork the scarp between the flats and the

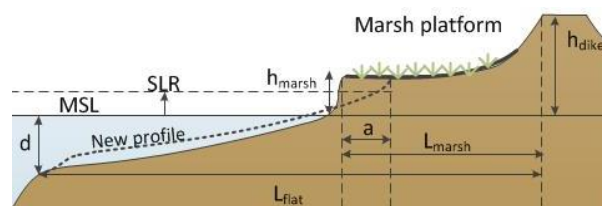


Figure 37 Bruun rule parameters applied to a schematised profile of Sturgeon Bank

marsh is around 0.5m high. The calculation with $L=6.5$ km, $d=2.5$ m, $h=0.5$ m and $SLR=1.85$ mm/year yields a retreat of 3.44 m/year.

If the sea-level rise would be the main driver of the marsh retreat, the expected rate of retreat would be in the order of 2- 3m/year. Between 1989 and 2011 a stretch of 500m of marsh has been observed to have disappeared near Steveston Road (Boyd et al., *Unpublished*). On average this recession amounts to 23m/year. The recession in the past decades is one order of magnitude greater than could be attributed to the sea-level rise alone.

Even though sea-level rise is unlikely to be the primary driver of the historic marsh recession, it can still have a contribution in the continued retreat of the marsh. Projections from the IPCC show an acceleration of the sea-level rise (J. A. Church et al., 2013). In the future sea-level rise, will have a bigger effect on the morphological development of Sturgeon Bank. A study on the effects of sea-level rise on the nearby Roberts Bank predicts that drastic changes would occur after 2050 when sea-level rise rates are considerably higher (Hill et al., 2013). Similarly, on Sturgeon Bank marsh retreat will become more drastic as sea-level rise increases.

Sea-level rise is a threat to the marsh on the long-term but the current sea-level rise rate is insufficient to cause the extensive marsh retreat

from the past 20 years. Sea-level rise is therefore a contributing factor to the marsh-retreat and not the primary driver. It does have the potential to become a primary driver in the future.

10.3 Sand swells

The hypothesis is that the movement of sand swells has resulted in a marsh recession by:

- Exposing previously sheltered marsh to more wave energy
- Blocking of tidal channels

The first part of the hypothesis can be evaluated with the results from the wave model. The current marsh scarp is around the 0.5 m+CGVD2013 (see section 6.2). The current marsh could therefore only be affected by waves at high tide. It is unlikely that the presence or absence of sand swells would directly affect the wave exposure of the marsh in its current state.

The marsh as observed on air photos from 1986 would have stretched to sand swells. It was observed that the sand swells on recent images look fainter than those on historic air photos. If that is the result of these features having reduced in height it is likely the area behind the sand swells has become more exposed. However, this cannot be validated without high resolution elevation data from that period.

The second part of the hypothesis involves the interaction between sand swells and channels. Movement of the sand swells has been observed on aerial imagery as well as rerouting of the channels and their disappearance. There is a clear interaction between the sand swells and the tidal flows. The flow model shows that water flows around the sand swells and only a portion is funnelled in between their troughs. The channels

from 1986 would have made flow through the sand swells more effective thus resulting in better drainage.

Both parts of the hypothesis are plausible.

However, the conditions required for the sand swells to move need to be more closely examined. The moment the sand swells were moved should coincide with the initiation of the marsh recession.

The sand swells are generated by wave action and can only be moved under extreme conditions (Appendix 10: Sand swells on Sturgeon Bank). The strongest storms were in 2000, 2001 and 2003 (section 3.3). The satellite analysis shows the marsh recession to have started before 2000 (section 5.6). The timeline thus suggests the marsh was already retreating before the storms hit Sturgeon Bank.

The hypothesis that the sand swells were the cause of the disappearance of the channels resulting in drowning of the marsh cannot be supported. It is still plausible the storms enabled the retreat to persist and prevented recolonization of the mud flats after the recession event.

10.4 Ponding

Marshes can retreat by a combination of ponds and algae. However, they will restore naturally if the mudflats retain their potential for marsh colonization. Examples of such cycles can be found around the world, e.g. in Maine, U.S.A. (Wilson et al., 2010) and the Rattekaai, the Netherlands (van Hulzen, van Soelen, Herman, & Bouma, 2006). The primary cause that prevents recolonization should be identified first. These possibilities include the other sand swell hypothesis and the sea-level rise hypothesis. Even

if on their own they would be insufficient to be treated as a primary cause the combination with this hypothesis could be sufficient to explain the retreat.

Wilson et al. (2010) deduced a footprint for salt pools in sediment cores. It was found that dark-grey layers of mud with 2- to 9% organic content and high water content were indicative of pools. From the cores taken at the marsh edge tested for organic content only cores from the middle and the north (J1 and L1) fit this description with organic content of 4%. Cores in the south (Z4 and Z6), though muddy, dark greyish and with high water content, only had 1% organic content. A core at the marsh edge in the center of Sturgeon Bank (I2) had a sandy top layer, black/grey mud under it followed by more brown-grey mud. This interpretation is highly subjective but could indicate ponding occurred before the deposition of sand. The cores might give some indication, but the small sample size is insufficient for any conclusion.

Though there are observations of ponds on Sturgeon Bank, it cannot result in marsh recession without a mechanism that keeps the mudflats from being recolonized. It is therefore better to assess a hypothesis that explains why no recolonization occurs before pursuing a detailed analysis of the ponding mechanisms.

10.5 Feedback mechanisms

Like the ponding hypothesis, the feedback mechanisms cannot explain the primary cause of the marsh recession. However, the combination of feedback mechanisms might be sufficient to prevent recolonization while the ponding mechanism is not.

Given that marsh had been present behind the sand swells since 1930 it is reasonable to assume this area was muddier due to the trapping of sediment by bulrush. The fine sediment could have filled in this area and form a terrace. This is plausible given the few sediment cores from earlier studies showed the mudflat contained more fines back then (Feeney, 1995; McLaren & Ren, 1995).

This would explain results from the satellite study. The bathymetry for 1990-1995 (Figure 13) shows a flat surface in the same area that was part of the marsh. The bathymetries for 2000-2005 and 2010-2015 subsequently show the loss of elevation in this area. The significant amount of erosion is expected from the hypothesis since the loose sediment would be eroded easily during wave action. The erosion was strongest near the boundary of the current marsh. This is in accordance with the wave model which predicts the waves at low water levels will not affect the hinterland because of the sand swells, but will affect the upper profile at high tide. The result is a depression between the middle marsh and the sand swells and the formation of a cliff in the profile. This change was found in the bathymetry for 2000-2005 (Figure 13). Indeed, the wind records from YVR show two strong storms hit in 2000 and 2001 further supporting the hypothesis.

The depression that formed after the storms becomes waterlogged. The wetter conditions would further decrease the potential for marsh recovery. Identical to the ponding mechanism, the sediment turns greyer by the accumulation of hydrogen sulphide in the soil, and the potential for recovery is decreased further.

Without recovery of the flats wave energy is no longer dissipated by plants and more wave energy is focussed at the marsh cliff. In response, the profile shifts towards a steeper marsh edge.

The feedback from marsh die-off and loss of tidal channels could not be established. These features are only visible on surveys or air photos, neither of which was available for the period between 1986 and 2001. It is plausible that the sand swells played a part in the disappearance of the channels as well (see sand swell hypothesis). This makes

establishing a cause and effect difficult as the disappearance of one will lead to the disappearance of the other.

There are good indications that feedback mechanisms have played a big part in the marsh recession of Sturgeon Bank. The hypothesis fits with results from the aerial and satellite studies. However, more conclusive evidence is needed to confirm the hypothesized mechanisms did occur and would produce the amount of retreat observed on Sturgeon Bank.

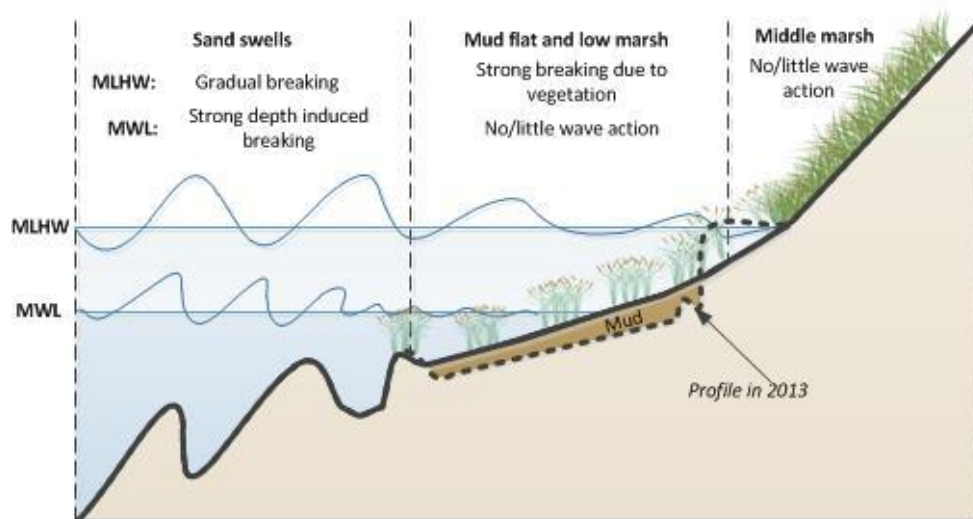


Figure 38 Conceptual schematisation of wave action in the marsh of 1986

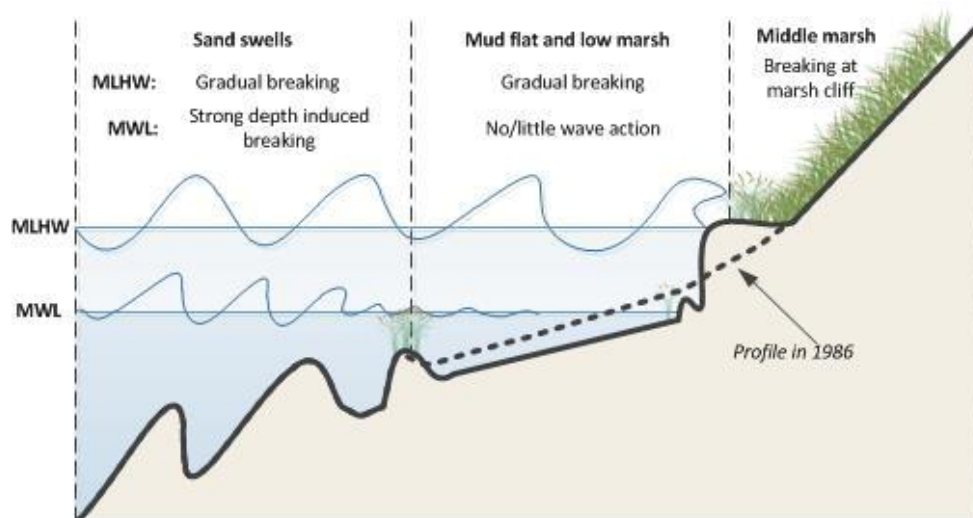


Figure 39 Conceptual schematisation of wave action in the marsh of 2013

11 SUMMARY OF POTENTIAL MECHANISMS

The goal of the study was:

- find potential mechanisms for the marsh retreat
- determine how these mechanisms would contribute to the marsh retreat

In Ch. 9 five hypotheses were put forward for the cause and mechanisms of the marsh recession.

None of the hypotheses put forward were sufficient to explain the start of the marsh recession on Sturgeon Bank, although a combination of several of the mechanisms may be the actual cause. The mutual interactions between marsh, hydraulic forcing and bathymetry make it so that one change would inevitably influence other mechanisms. Feedback mechanisms could explain most of the changes on Sturgeon Bank but this should be investigated further.

The supply of sediment to Sturgeon Bank has been reduced by the Fraser River jetties but Sturgeon Bank had been growing seaward before these interventions. The lack of supply has translated in a stabilization of the bank rather than active erosion. This is in accordance with the study of Hales (2000) who showed there was no shift towards erosion after the interventions, as well as the study by Feeney (1995) who showed that under normal conditions there is no to little erosion of sediments from the bed. Furthermore it can be concluded from the tidal signal that if sediment was eroded from the bed it is more likely to be deposited shoreward than be lost to the sea.

Sea-level rise could also be a contributor to the current recession given the lack of sediment being supplied. Sea-level rise combined with subsidence rates would result in a decrease in elevation of

approximately 1.85 mm/year relative to mean sea level. Without any sedimentation the marsh would retreat only by 2-3 m/year. This rate is far too slow to be the cause of the 400 m recession observed between 1989 and 2011. Furthermore, this type of structural retreat does not fit the sudden recession event observed on air photos and satellite images.

The hypothesis of movement of the sand swells by a storm does fit better with the episodic character of the retreat. The marsh area would likely have become waterlogged following the blockage of channels by the sand swells. A sudden die-off of marsh is likely if inundation increased beyond the tolerance of the bulrush.

Analysis of air photos shows the sand swells are a rather stable feature. They did only move twice since 1930: sometime between 1952 and 1979, and sometime between 1989 and 2001. Large waves generated by storm winds are required for this movement. Wind records at YVR airport show the largest storms from 1985 onward were in the years 2000, 2001 and 2003. Movement of sand swells is thus possible. However satellite images show the recession commenced in the 1990's which is before any storms hit the bank. This could thereby not be the only / initial mechanism that induced the retreat. It does remain plausible that the storms pushed the system further into recession by eroding parts of the already dying marsh.

Although ponding was initially conceived as a primary cause originating from a disturbance by grazing or algae, it could not be fully supported. Examples from literature like

van Hulzen et al. (2006) show that this mechanism does not cause permanent loss of marsh unless other mechanisms prevent recovery.

A primary cause was not identified and the proposed hypotheses could not be substantiated. Even if the primary cause is not identified, the feedback mechanisms that accelerated the retreat once it started were explored still.

Several feedback mechanisms were considered as a result of initial marsh loss: sediment becomes more vulnerable for erosion, tidal channels are less effective, and wave energy is dissipated less. Secondary feedback follows in the form of erosion, waterlogging, and biochemical degradation of the soil all of which further decrease the odds of bulrush to re-establish. These hypothesized feedbacks could explain results from the satellite study, aerial imagery, sediment samples and storm analysis. However, more research is needed to determine whether these mechanisms did occur and what magnitude of recession these mechanisms would produce. Furthermore, it does not resolve the initial cause of the marsh recession.

During the study more mechanisms were proposed for the recession. These were discarded either because of time constraints or feasibility considerations. Natural variability, sorting of sediments, salinity change and the discharge of precipitation on Sturgeon Bank from Richmond at the pumping stations were briefly looked at as mechanisms but not investigated.

12 RECOMMENDATIONS

The study could not conclude which processes were the ultimate cause of the recession because of the complex interactions between them. These interactions are still not fully understood. More insight into the retreat and growth of marsh can be gained by collection more data, studying the morphology and ecology, and testing the mechanisms in the field with a pilot. The recommended studies will aid in the development of a more successful marsh restoration strategy by exploring how these mechanisms could contribute to or inhibit new marsh growth.

12.1 Data collection

It is recommended to continue collecting baseline data of Sturgeon Bank such as the bathymetry, wave heights, water levels, soil composition and marsh edge. Bathymetries provide valuable insight in erosion/deposition patterns over time. The last wave data was measured in 1976 while the latest continuous flow and water level measurements were from 1995. Actual wave heights and flows on Sturgeon Bank in its current state remain unknown and can only be approximated by formulas and models at the moment. Soil samples should continue to be taken to see if the bed continues to become coarser as was observed in this study. The marsh edge should continue to be monitored. Much remains unclear about how the marsh recedes. By continuously monitoring a specific marsh section the stages of recession can easily be observed.

From air photos the exact position has been found of tidal channels that have disappeared since the marsh recession. Cores should be taken at these locations to find out whether these channels disappeared by filling in with fine

sediment or because of erosion of the surrounding flats. This information can tell a great deal about how and why the channels disappeared.

During the study a number of reference levels were used to track the elevation. It is recommended that an official conversion between chart datum (CD), CGVD28 and CGVD2013 is made and validated in the field. This allows for a consistent conversion between reference levels. Because of the shallow slope of Sturgeon Bank errors of a few centimeters can lead to large errors in assessing the hydrology and topography.

12.2 Morphological studies

Sand swells were found to be an important feature of Sturgeon Bank. The sand swells appear to have influenced the position of the historic marsh and affected the tidal channels in that area. Still, very little is known about how they formed, how they move and how they affected the channels and vegetation exactly. A study of these features would provide a valuable insight into the marsh system of Sturgeon Bank and might provide further indications for why the marsh receded.

The tidal channels on Sturgeon Bank have also undergone significant changes that need to be explored further. Especially the interaction between the channels and the presence of bulrush is of high importance for future restoration strategies. The mechanisms that resulted in the loss of tidal channels should be identified to determine whether there is a link with marsh recession and thus if they can be prevented in the future, while mechanisms that make the channels expand could be encouraged.

12.3 Ecological studies

An interesting approach to analyse the marsh dynamics on Sturgeon Bank is to identify windows of opportunity for marsh growth. The combined stress on the plants from processes such as submergence and wave forces should remain low enough for a certain period of time in order for the marsh to grow. A study using this approach could identify how and when the marsh shifted from a state with a large marsh to a state with a small marsh.

The tolerance of bulrush to salinity should be investigated further. There are indications that salinity is an important parameter for the growth of bulrush. The difference in salinity between Westham Island and Sturgeon Bank could explain partially the difference in marsh extent.

During the Sturgeon Bank Marsh Recession Program Update meeting (16th of June, 2016) it was suggested that the yearly freshet in spring could be a factor in the marsh recession on Sturgeon Bank. In spring during the freshet a large amount of fresh water is discharged into the Strait of Georgia. The freshet coincides with the early grow season of bulrush. Possibly a (series of) year(s) with weak freshet(s) created a more saline environment in which bulrush could not reemerge.

12.4 Pilot study

The current study has analysed a large quantity of historic data like water levels, winds, satellite images and aerial imagery over large time scales. There is however a gap of knowledge in the interactions between the bulrush and the physical environment.

The hypothesized mechanisms that are believed

to prevent recolonization of marsh on the mud flats are:

- Loss of tidal channels
- Extended inundation
- Increased wave action

It would be interesting to organize a pilot to study these mechanisms and especially their interaction in more detail. In theory, by mitigating these effects it could be expected that the marsh can be re-established. The results from such a small scale pilot would therefore provide useful insights for [1] the historic marsh recession by confirming the hypothesized feedback processes as well as [2] provide valuable lessons for a marsh recovery strategy in the future. It is therefore highly recommended to conduct such a study. In the literature review a number of restoration projects have been discussed. Similar concepts can be tested for the restoration of Sturgeon Bank.

A few examples of how these measures can be tested are provided below:

1. One or more drainage channel(s) can be dug through the sand swells (approx. 250 m) to aid drainage of the near shore area in a specific location. Secondary ditches could be connected to the channel as well. The intervention aims to recreate part of the drainage system that had been lost between 1986 and 2001. With the drainage restored other measures can further be tested for marsh restoration.
2. Bulrush can be reintroduced in the drained environment. Replanting should mirror the growth pattern of real bulrush. As discussed, bulrush growing in high densities is more resilient to scouring and disturbances. Small plots with a high stem densities are therefore preferred over

large plots with a smaller stem density.

The submergence can be reduced by elevating the surface above the current mud flat. This can be accomplished by using material dredged from the channel and ditches to create local mounds, similar to the bulrush elevated on the landward crests of the sand swells. Sediment from the maintenance dredging could be tested as well to see if it is suitable for restoration projects in the future.

3. To limit erosion by waves and smothering by algae before any plants have colonized the mound a temporary protection can be placed in front of the mounds. This could be a simple structure like groynes or a mound of coarse sand. Rocks or large structures are not expected to be required since big waves are already dissipated along the shallow foreshore.

In theory these measures should provide the window of opportunity required for a series of positive feedback mechanisms when the bulrush recolonises:

- Increased resistance to erosion by higher root and stem densities
- Reduction of wave action by vegetation
- Promoting further sedimentation of fines by trapping between the stems
- Creating / Reinforcing water drainage patterns due to the local flow resistance exerted by the bulrush.

The regrowth of marsh may act as a catalyst and create conditions for marsh growth at the current edge of the marsh assisted by the improvement of the drainage by the channels, reduced wave action and sediment that is transported from the mounds to the marsh development.

The pilot should monitor the growth as well as flow patterns / drainage and sediment deposition near the marsh edge as well.

A pilot study provides insight into the hypothesized mechanisms and their interactions and provide data needed to quantify these effects. Furthermore it provides an opportunity to test a restoration strategy.

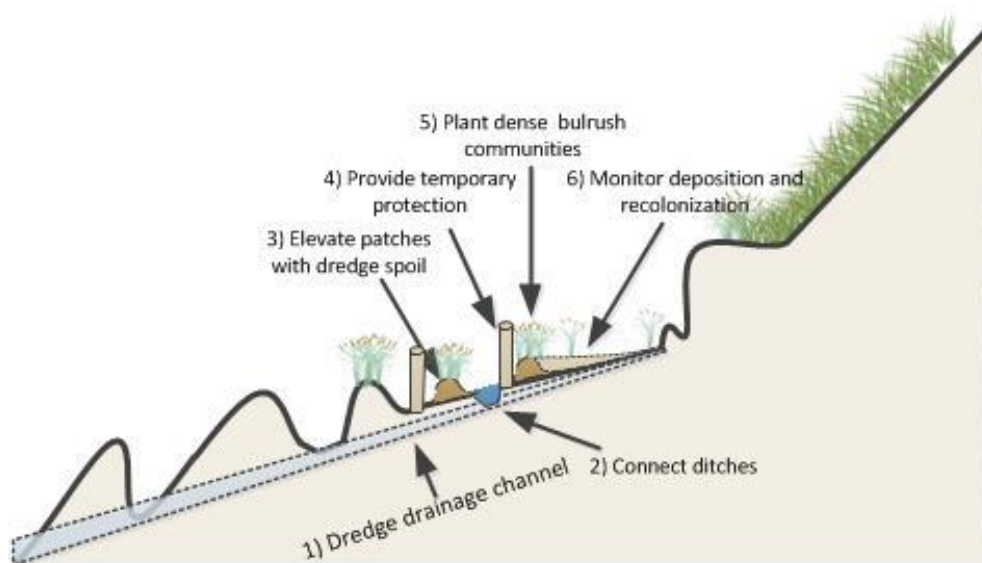


Figure 40 Measures that can be undertaken for a pilot

13 REFERENCES

- Adams, D. A. (1963). Factors Influencing Vascular Plant Zonation in North Carolina Salt Marshes. *Ecology*, 44(3), 445-456. doi:10.2307/1932523
- Adams, M. A., & Williams, G. L. (2004). Tidal marshes of the Fraser River estuary: composition, structure, and a history of marsh creation efforts to 1997. *Fraser River Delta, British Columbia: Issues of an Urban Estuary, Geol. Surv. Can. Bull*, 567, 147-172.
- Alber, M., Swenson, E. M., Adamowicz, S. C., & Mendelssohn, I. A. (2008). Salt Marsh Dieback: An overview of recent events in the US. *Estuarine, Coastal and Shelf Science*, 80(1), 1-11. doi:<http://dx.doi.org/10.1016/j.ecss.2008.08.009>
- Albert, D. A., Cox, D. T., Lemein, T., & Yoon, H.-D. (2013). Characterization of *Schoenoplectus pungens* in a Great Lakes Coastal Wetland and a Pacific Northwestern Estuary. *Wetlands*, 33(3), 445-458. doi:10.1007/s13157-013-0402-4
- Amos, C. L., Feeney, T., Sutherland, T. F., & Luternauer, J. L. (1997). The Stability of Fine-grained Sediments from the Fraser River Delta. *Estuarine, Coastal and Shelf Science*, 45(4), 507-524. doi:10.1006/ecss.1996.0193
- Atkins, R. J., Tidd, M., & Ruffo, G. (2016). Sturgeon Bank, Fraser River Delta, BC, Canada: 150 Years of Human Influences on Salt Marsh Sedimentation. *Journal of Coastal Research*, 75(sp1), 790-794. doi:10.2112/SI75-159.1
- Attard, M. E., Venditti, J. G., & Church, M. (2014). Suspended sediment transport in Fraser River at Mission, British Columbia: New observations and comparison to historical records. *Canadian Water Resources Journal / Revue canadienne des ressources hydriques*.
- Baldock, T. E., Holmes, P., Bunker, S., & van Weert, P. (1998). Cross-shore hydrodynamics within an unsaturated surf zone. *Coastal Engineering*(34), 173-196. doi:10.1016/S0378-3839(98)00017-9
- Balke, T., Herman, P. M. J., Bouma, T. J., & Nilsson, C. (2014). Critical transitions in disturbance-driven ecosystems: identifying Windows of Opportunity for recovery. *Journal of Ecology*, 102(3), 700-708.
- Balke, T., Stock, M., Jensen, K., Bouma, T. J., & Kleyer, M. (2016). A global analysis of the seaward salt marsh extent: The importance of tidal range. *Water Resources Research*, 52(5), 3775-3786. doi:10.1002/2015WR018318
- Barrie, J. V., & Currie, R. G. (2000). Human impact and sedimentary regime of the Fraser River delta, Canada. *Journal of Coastal Research*, 16(3), 747-755.
- Battjes, J. A., & Janssen, J. P. F. M. (1978). *Energy loss and set-up due to breaking random waves*. Paper presented at the Proceedings of 16th Conference on Coastal Engineering, Hamburg, Germany. <http://repository.tudelft.nl/islandora/object/uuid%3A2fba43fe-f8bd-42ac-85ee-848312d2e27e>
- Blackmar, P. J. (2013). *Experimental and Numerical Modeling of Wave Height Attenuation by Emergent Coastal Vegetation*. (Master of Science), Oregon State University. Retrieved from <https://ir.library.oregonstate.edu/xmlui/bitstream/handle/1957/40002/BlackmarPhilipJ2013.pdf?sequence=1>

- Bouma, T. J., Friedrichs, M., Van Wesenbeeck, B. K., Temmerman, S., Graf, G., & Herman, P. M. J. (2009). Density-dependent linkage of scale-dependent feedbacks: a flume study on the intertidal macrophyte *Spartina anglica*. *Oikos*, 118(2), 260-268.
- Boyd, S., McKibbin, R., & Moore, K. (Unpublished). *The bulrush marshes of the Fraser River Delta have undergone significant changes between 1989 & 2011 (DRAFT)*.
- Bruun, P. (1988). The Bruun Rule of Erosion by Sea-Level Rise: A Discussion on Large-Scale Two- and Three-Dimensional Usages. *Journal of Coastal Research*, 4(4), 627-648. Retrieved from <http://www.jstor.org/stable/4297466>
- Canadian Hydrographic Service. (2016). Tide table, vol. 5.
- Church, J. A., Clark, P. U., Cazenave, A., Gregory, J. M., Jevrejeva, S., Levermann, A., . . . Unnikrishna, A. S. (2013). *Sea Level Change. In: Climate Change 2013: The Physical Science Basis. Contribution of Working Group I to the Fifth Assessment Report of the Intergovernmental Panel on Climate Change*. Retrieved from Cambridge, United Kingdom and New York, NY, USA.: https://www.ipcc.ch/pdf/assessment-report/ar5/wg1/WG1AR5_Chapter13_FINAL.pdf
- Church, M., & Hales, W. (2004). The Tidal Marshes of Fraser Delta: 75 years of Growth and Change. *Discovery*, 36, 28-33.
- Church, M., & Krishnappan, B. G. (1998). Sediment Sources, Transport Processes, and Modeling Approaches for the Fraser River. *HEALTH OF THE FRASER RIVER AQUATIC ECOSYSTEM*, 1, 63-80.
- Clague, J. J., Luternauer, J. L., & Hebda, R. J. (1983). Sedimentary environments and postglacial history of the Fraser Delta and lower Fraser Valley, British Columbia. *Canadian Journal of Earth Sciences*, 20(8), 1314-1326. doi:10.1139/e83-116
- Corenblit, D., Tabacchi, E., Steiger, J., & Gurnell, A. M. (2007). Reciprocal interactions and adjustments between fluvial landforms and vegetation dynamics in river corridors: A review of complementary approaches. *Earth-Science Reviews*, 84(1-2), 56-86. doi:<http://dx.doi.org/10.1016/j.earscirev.2007.05.004>
- Costanza, R., d'Arge, R., de Groot, R., Farber, S., Grasso, M., Hannon, B., . . . van den Belt, M. (1998). The value of the world's ecosystem services and natural capital. *Ecological Economics*, 25(1), 3-15. doi:[http://dx.doi.org/10.1016/S0921-8009\(98\)00020-2](http://dx.doi.org/10.1016/S0921-8009(98)00020-2)
- DeLaune, R. D., Nyman, J. A., & W. H. Patrick, J. (1994). Peat Collapse, Ponding and Wetland Loss in a Rapidly Submerging Coastal Marsh. *Journal of Coastal Research*, 10(4), 1021-1030. Retrieved from <http://www.jstor.org/stable/4298293>
- Deltares. (2014). *Delft3D-FLOW: Simulation of multi-dimensional hydrodynamic flows and transport phenomena, including sediments. User Manual* (3.15.34158 ed.). Delft: Deltares.
- Donnelly, J. P., & Bertness, M. D. (2001). Rapid shoreward encroachment of salt marsh cordgrass in response to accelerated sea-level rise. *Proceedings of the National Academy of Sciences*, 98(25), 14218-14223. doi:10.1073/pnas.251209298
- Fagherazzi, S., FitzGerald, D. M., Fulweiler, R. W., Hughes, Z., Wiberg, P. L., McGlathery, K. J., . . . Johnson, D. S. (2013). 12.12 Ecogeomorphology of Salt Marshes A2 - Shroder, John F

- Treatise on Geomorphology* (pp. 182-200). San Diego: Academic Press.
- Feeney, T. (1995). *Physical control on the distribution of contaminants on Sturgeon Bank, Fraser River Delta, British Columbia*. (MSc.), The University of British Columbia, Vancouver.
- Fisheries and Oceans Canada. (2013). *MEDS102: Sturgeon Bank February 1974*. Retrieved from: <http://www.meds-sdmm.dfo-mpo.gc.ca/isdm-gdsi/waves-vagues/plot-trace/result-eng.asp?medsid=MEDS102&s1=1974-02&s2=1976-04>
- FitzGerald, D. M., Fenster, M. S., Argow, B. A., & Buynevich, I. V. (2008). Coastal Impacts Due to Sea-Level Rise. *Annual Review of Earth and Planetary Sciences*, 36(1), 601-647. doi:10.1146/annurev.earth.35.031306.140139
- Foreman, M. G. G., Sutherland, G., & Cummins, P. F. (2014). M2 tidal dissipation around Vancouver Island: an inverse approach. *Continental Shelf Research*, 24, 2167-2185.
- Fredsøe, J., & Deigaard, R. (1992). Chapter 9. Current-generated bed waves *Mechanics of Coastal Sediment Transport* (pp. 261-289): World Scientific Publishing Co. Pte. Ltd.
- Friedman, J. (2015). Earth Engine (EE) Morphology. Retrieved from <https://svn.oss.deltares.nl/repos/openearthtools/trunk/python/applications/e-coast/eeMorphology.py>
- Friedrichs, C. T. (2011). 3.06 - Tidal Flat Morphodynamics: A Synthesis *Treatise on Estuarine and Coastal Science* (pp. 137-170). Waltham: Academic Press.
- Gray, A. J., Marshall, D. F., & Raybould, A. F. (1991). A century of evolution in *Spartina anglica*. *Adv. Ecol. Res.*(21), 1-62.
- Hales, W. J. (2000). *The Impact of Human Activity on Deltaic Sedimentation, Marshes of the Fraser River Delta, British Columbia*. (Doctor of Philosophy), the university of British Columbia, Vancouver.
- Harrison, P. J., Yin, K., Ross, L., Arvai, J., Gordon, K., Bendell-Young, L., . . . Shepherd, P. (1999). The delta foreshore ecosystem: past present status of geochemistry, benthic community production and shorebird utilization after sewage diversion. *HEALTH OF THE FRASER RIVER AQUATIC ECOSYSTEM*, 189-210.
- Harshberger, J. W. (1916). The Origin and Vegetation of Salt Marsh Pools. *Proceedings of the American Philosophical Society*, 55(6), 481-484. Retrieved from <http://www.jstor.org/stable/983982>
- Hill, P. R., Butler, R. W., Elner, R. W., Houser, C., Kirwan, M. L., Lambert, A., . . . Solomon, S. (2013). Impacts of Sea Level Rise on Roberts Bank (Fraser Delta, British Columbia). *Geological Survey of Canada, Open File 7259*. doi:10.495/292672
- Hill, P. R., Conway, K., Lintern, D. G., Meulé, S., Picard, K., & Barrie, J. V. (2008). Sedimentary processes and sediment dispersal in the southern Strait of Georgia, BC, Canada. *Marine Environmental Research*, 66, S39-S48. doi:10.1016/j.marenvres.2008.09.003
- Holdredge, C., Bertness, M. D., & Altieri, A. H. (2009). Role of Crab Herbivory in Die-Off of New England Salt Marshes
- Papel de la Herbivoría de Cangrejos en la Declinación de Marismas de Nueva Inglaterra. *Conservation Biology*, 23(3), 672-679. doi:10.1111/j.1523-1739.2008.01137.x
- Houser, C., & Hill, P. (2010). Wave attenuation across an intertidal sand flat:

- implications for mudflat development. *Journal of Coastal Research*, 403-411.
- Hu, Z., van Belzen, J., van der Wal, D., Balke, T., Wang, Z. B., Stive, M., & Bouma, T. J. (2015). Windows of opportunity for salt marsh vegetation establishment on bare tidal flats: The importance of temporal and spatial variability in hydrodynamic forcing. *Journal of Geophysical Research: Biogeosciences*, 120(7), 1450-1469. doi:10.1002/2014JG002870
- Hutchinson, I. (1982). Vegetation–environment relations in a brackish marsh, Lulu Island, Richmond, B.C. *Canadian Journal of Botany*, 60(4), 452-462. doi:10.1139/b82-061
- Ilori, C. (2015). *Twenty nine years of recession on Sturgeon and Roberts Banks*.
- Isachsen, P. E., & Pond, S. (2000). The Influence of the Spring-neap Tidal Cycle on Currents and Density in Burrard Inlet, British Columbia, Canada. *Estuarine, Coastal and Shelf Science*, 51, 317-330.
- James, T. S., Hutchinson, I., Barrie, J. V., Conway, K. W., & Mathews, D. (2007). Relative Sea-Level Change in the Northern Strait of Georgia, British Columbia. *Géographie Physique et Quaternaire*, 59(2-3), 113-127. doi:10.7202/014750ar
- Kirwan, M. L., Walters, D. C., Reay, W. G., & Carr, J. A. (2016). Sea level driven marsh expansion in a coupled model of marsh erosion and migration. *Geophysical Research Letters*, 43(9), 4366-4373. doi:10.1002/2016GL068507
- Kostachuk, R. A., & Luternauer, J. L. (2004). Sedimentary processes and their environmental significance: lower main channel, Fraser River Estuary. *Fraser River Delta, British Columbia: Issues of an Urban Estuary, Geological Survey of Canada, Bulletin no. 567*, 81-92.
- Kostaschuk, R. A., Stephan, B. A., & Luternauer, J. L. (1993). Suspended sediment concentration in a buoyant plume: Fraser River, Canada. *Geo-Marine Letters*, 13, 165-171.
- Levine, J. M., Brewer, J. S., & Bertness, M. D. (1998). Nutrients, Competition and Plant Zonation in a New England Salt Marsh. *Journal of Ecology*, 86(2), 285-292. Retrieved from <http://www.jstor.org.tudelft.idm.oclc.org/stable/2648552>
- Levings, C. D. (1980). CONSEQUENCES OF TRAINING WALLS AND JETTIES FOR AQUATIC HABITATS AT TWO BRITISH COLUMBIA ESTUARIES. *Coastal Engineering*, 4, 111-136. doi:10.1016/0378-3839(80)90010-1
- Levings, C. D. (2004). *Two decades of fish habitat restoration and bioengineering on the Fraser River estuary, British Columbia, Canada*. Paper presented at the OCEANS'04. MTTs/IEEE TECHNO-OCEAN'04.
- Luternauer, J. L. (1976). Fraser Delta sedimentation, Vancouver, British Columbia. *Geological Survey of Canada*(Report of activities Part A). Retrieved from ftp://ftp2.cits.rncan.gc.ca/pub/geott/ess_pubs/119/119844/pa_76_1a.pdf
- Luternauer, J. L. (1980). Genesis of morphological features on the western delta front of the Fraser River, British Columbia – status report of knowledge. In S. B. McCann (Ed.), *The Coastline of Canada* (pp. 381-396): Geological Survey of Canada.
- Luternauer, J. L., Atkins, R. J., Moody, A. I., Williams, H. E., & Gibson, J. W. (1995). Chapter 11 Salt Marshes. In G. M. E. Perillo (Ed.), *Developments in Sedimentology* (Vol. Volume 53, pp. 307-332): Elsevier.
- Luternauer, J. L., Duggan, D., & Hendry, M. (1984). Development-induced tidal flat erosion, Fraser River Delta. *Current*

- Research, Part A, Geological Survey of Canada*, 75-80.
- Marani, M., D'Alpaos, A., Lanzoni, S., & Santalucia, M. (2011). Understanding and predicting wave erosion of marsh edges. *Geophysical Research Letters*, 38(21), n/a-n/a. doi:10.1029/2011GL048995
- Marinonea, S. G., Pond, S., & Fyfe, J. (1996). A Three-dimensional Model of Tide and Wind-induced Residual Currents in the Central Strait of Georgia, Canada. *Estuarine, Coastal and Shelf Science*, 43, 157-182.
- Mariotti, G. (2016). Revisiting salt marsh resilience to sea level rise: Are ponds responsible for permanent land loss? *J. Geophys. Res. Earth Surf.*(121). doi:10.1002/2016JF003900.
- Mariotti, G., & Fagherazzi, S. (2010). A numerical model for the coupled long-term evolution of salt marshes and tidal flats. *Journal of Geophysical Research: Earth Surface*, 115(F1), n/a-n/a. doi:10.1029/2009JF001326
- Marsh, A. C. (2007). *EFFECTS ON A SALT MARSH ECOSYSTEM FOLLOWING A BROWN MARSH EVENT* (Master of Science in Biology), East Carolina University.
- Mazzotti, S., Jones, C., & Thomson, R. E. (2008). Relative and absolute sea level rise in western Canada and northwestern United States from a combined tide gauge-GPS analysis. *Journal of Geophysical Research: Oceans*, 113(C11), n/a-n/a. doi:10.1029/2008JC004835
- Mazzotti, S., Lambert, A., Courtier, N., Nykolaishen, L., & Dragert, H. (2007). Crustal uplift and sea level rise in northern Cascadia from GPS, absolute gravity, and tide gauge data. *Geophysical Research Letters*, 34(15), n/a-n/a. doi:10.1029/2007GL030283
- Mazzotti, S., Lambert, A., Van der Kooij, M., & Mainville, A. (2009). Impact of anthropogenic subsidence on relative sea-level rise in the Fraser River delta. *Geology*, 37(9), 771-774.
- McKee, K. L., Mendelssohn, I. A., & D. Materne, M. (2004). Acute salt marsh dieback in the Mississippi River deltaic plain: a drought-induced phenomenon? *Global Ecology and Biogeography*, 13(1), 65-73. doi:10.1111/j.1466-882X.2004.00075.x
- McKee, K. L., & Patrick, W. H. (1988). The Relationship of Smooth Cordgrass (*Spartina alterniflora*) to Tidal Datums: A Review. *Estuaries*, 11(3), 143-151. doi:10.2307/1351966
- McLaren, P., & Ren, P. (1995). *SEDIMENT TRANSPORT AND ITS ENVIRONMENTAL IMPLICATIONS IN THE LOWER FRASER RIVER AND FRASER DELTA*. #6-2810 Fulford-Ganges Road, Salt Spring Island, B.C., V8K 1Z2: GeoSea Consulting (Canada) Ltd.,.
- McLoughlin, S. M., Wiberg, P. L., Safak, I., & McGlathery, K. J. (2015). Rates and Forcing of Marsh Edge Erosion in a Shallow Coastal Bay. *Estuaries and Coasts*, 38(2), 620-638. doi:10.1007/s12237-014-9841-2
- McPherson, R., Blackmar, P., & Heilman, D. (2015). Restoring Estuarine Habitat in Galveston West Bay Through Placement of Dredged Sediments: Monitoring and Lessons Learned *The Proceedings of the Coastal Sediments 2015*: World Scientific.
- Medley, E. (1978). *Dendritic Drainage Channels and Tidal Flat Erosion, West of Steveston, Fraser River Delta, British Columbia*. (Bachelor of Science), The University of British Columbia.
- Medley, E., & Luternauer, J. L. (1976). *Use of aerial photographs to map sediment distribution and to identify historical changes on a tidal flat* Retrieved from <http://edmedley.com/blog/wp->

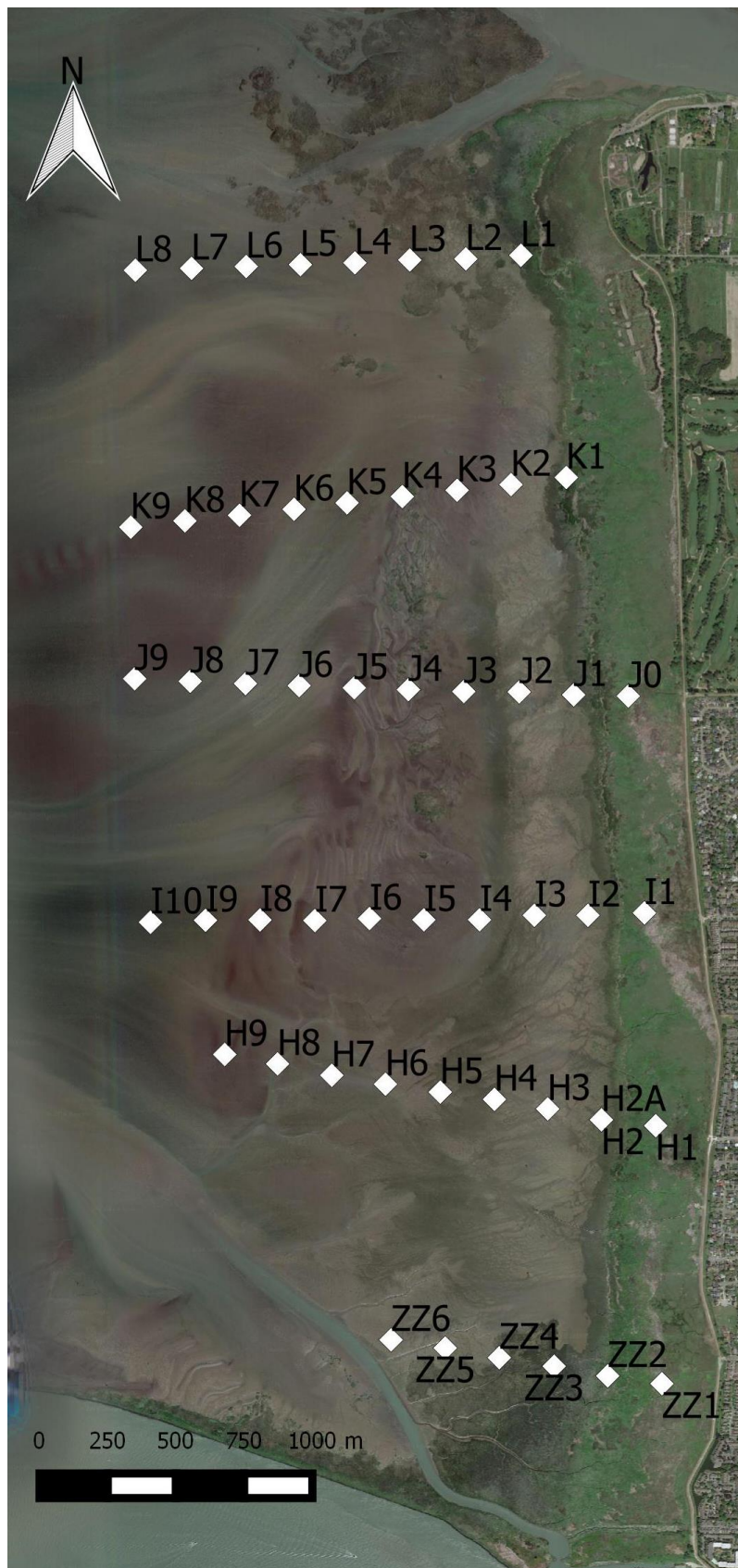
- [content/uploads/2008/06/medley-and-luternauer-1976.pdf](#)
- Mikhailov, V. N., Mikhailova, M. V., & Rets, E. P. (2007). River and Sea Water Interaction and Delta Formation in Tidal Mouth Area of the Fraser River (Canada). *Water Resources*, 34(5), 571–586.
- Milliman, J. D. (1980). Sedimentation in the Fraser River and its estuary, southwestern British Columbia (Canada). *Estuarine and Coastal Marine Science*, 10(6), 609-633. doi:[http://dx.doi.org/10.1016/S0302-3524\(80\)80092-2](http://dx.doi.org/10.1016/S0302-3524(80)80092-2)
- Ministry of Forests, Lands and Natural Resource Operations. (2015). Sturgeon Bank Wildlife Management Area. Retrieved from http://www.env.gov.bc.ca/fw/habitat/conservation-lands/wma/sturgeon_bank/
- Möller, I., & Spencer, T. (2002). Wave dissipation over macro-tidal saltmarshes: Effects of marsh edge typology and vegetation change. *Journal of Coastal Research*, SI 36, 506-521.
- Morris, J. T., Sundareshwar, P. V., Nietch, C. T., Kjerfve, B., & Cahoon, D. R. (2002). RESPONSES OF COASTAL WETLANDS TO RISING SEA LEVEL. *Ecology*, 83(10), 2869-2877. doi:10.1890/0012-9658(2002)083[2869:ROCWTR]2.0.CO;2
- Natural Resources Canada. (2016, 05-07-2016). Passive Control Networks. Retrieved from <http://webapp.geod.nrcan.gc.ca/geod/ata-donnees/passive-passif.php?locale=en>
- Nelson, R. C. (1987). Design wave heights on very mild slopes—an experimental study. *Transactions of the Institution of Engineers, Australia. Civil engineering*, 29(3), 157-161.
- Nidzieko, N. J. (2010). Tidal asymmetry in estuaries with mixed semidiurnal/diurnal tides. *Journal of Geophysical Research: Oceans*, 115(C8), n/a-n/a. doi:10.1029/2009JC005864
- Northwest Hydraulic Consultants. (2002). *Review of Lower Fraser River Sediment Budget, Final Report*. Retrieved from <http://www.dfo-mpo.gc.ca/Library/349131.pdf>
- Northwest Hydraulic Consultants Ltd. (2014). *Proposed Roberts Bank Terminal 2 Technical Report Coastal Geomorphology Study* Retrieved from <http://www.ceaa-acee.gc.ca/050/documents/p80054/101370E.pdf>
- Nyman, J. A., DeLaunel, R. D., Roberts, H. H., & Patrick, W. H. (1993). Relationship between vegetation and soil formation in a rapidly submerging coastal marsh. *Mar. Ecol. Prog. Ser.*, 96, 269-279.
- Parente, C. (2013). *TOA reflectance and NDVI calculation for Landsat 7 ETM+ images of Sicily*. Paper presented at the Electronic International Interdisciplinary Conference. September, 2. - 6. 2013
- Pawłowicz, R., Beardsley, B., & Lentz, S. (2002). Classical tidal harmonic analysis including error estimates in MATLAB using T_TIDE. *Computers & Geosciences*, 28(8), 929-937. doi:[http://dx.doi.org/10.1016/S0098-3004\(02\)00013-4](http://dx.doi.org/10.1016/S0098-3004(02)00013-4)
- Reed, A. S. (2001). Rates and Processes of Marsh Shoreline Erosion in Rehoboth Bay, Delaware, U.S.A. *Journal of Coastal Research*, 17(3), 672-683. Retrieved from <http://www.jstor.org/stable/4300218>
- Richmond. (2005). *Heritage Inventory*. Retrieved from <http://www.richmond.ca/plandev/planning2/heritage/HeritageInv/HeritageInventory.pdf>

- Schrift, A. M., Mendelssohn, I. A., & Materne, M. D. (2008). Salt marsh restoration with sediment-slurry amendments following a drought-induced large-scale disturbance. *Wetlands*, 28(4), 1071-1085. doi:10.1672/07-78.1
- Schuerch, M., Scholten, J., Carretero, S., García-Rodríguez, F., Kumbier, K., Baechtiger, M., & Liebetrau, V. (2016). The effect of long-term and decadal climate and hydrology variations on estuarine marsh dynamics: An identifying case study from the Río de la Plata. *Geomorphology*, 269, 122-132. doi:<http://dx.doi.org/10.1016/j.geomorph.2016.06.029>
- Silinski, A., Fransen, E., Bouma, T. J., Meire, P., & Temmerman, S. (2016). Unravelling the controls of lateral expansion and elevation change of pioneer tidal marshes. *Geomorphology*, 274, 106-115. doi:<http://dx.doi.org/10.1016/j.geomorph.2016.09.006>
- Silliman, B. R., van de Koppel, J., Bertness, M. D., Stanton, L. E., & Mendelssohn, I. A. (2005). Drought, Snails, and Large-Scale Die-Off of Southern U.S. Salt Marshes. *Science*, 310(5755), 1803. Retrieved from <http://science.sciencemag.org/content/310/5755/1803.abstract>
- <http://science.sciencemag.org/content/310/5755/1803.long>
- Sutherland, G., Garrett, C., & Foreman, M. (2005). Tidal Resonance in Juan de Fuca Strait and the Strait of Georgia. *J. Phys. Oceanogr.*, 35, 1279-1286.
- Teal, J. M., & Weishar, L. (2005). Ecological engineering, adaptive management, and restoration management in Delaware Bay salt marsh restoration. *Ecological Engineering*, 25(3), 304-314. doi:<http://dx.doi.org/10.1016/j.ecoleng.2005.04.009>
- Temmerman, S., Bouma, T. J., Koppel, J. V. d., Wal, D. V. d., Vries, M. B. D., & Herman, P. M. J. (2007). Vegetation causes channel erosion in a tidal landscape. *Geology*, 35(7), 631.
- Thomson, R. E. (1981). *Oceanography of the British Columbia Coast*. Ottawa: Department of Fisheries and Oceans.
- TRE Canada Inc. (2014). *Erosion Study over Sturgeon Bank, West of Lulu Island using Historical Geo-referenced Spaceborne Radar imagery*. Report prepared by TRE Canada Inc. for Port Metro Vancouver. Doc Ref.:JO14-3021-Rep1.1. Report authored by Vicky Chun-yi Hsiao and Jean Pascal Iannacone, approved by Giacomo Falorni., Vancouver BC.
- U.S. Geological Survey. (2015). *Landsat—Earth observation satellites*. Retrieved from www.usgs.com
- Underwood, S. G., Steyer, G. D., Good, B., & Chambers, D. (1991). *Bay bottom terracing and vegetative planting: an innovative approach for habitat and water quality enhancement*. Paper presented at the Annual Conference on Wetlands Restoration and Creation, Hillsborough Community College, Tampa, FL, USA.
- van de Koppel, J., van der Wal, D., Bakker, J. P., & Herman, P. M. (2005). Self-organization and vegetation collapse in salt marsh ecosystems. *The American Naturalist*, 165(1), E1-E12.
- Van der Wal, D., Wielemaker-Van den Dool, A., & Herman, P. M. J. (2008). Spatial patterns, rates and mechanisms of saltmarsh cycles (Westerschelde, The Netherlands). *Estuarine, Coastal and Shelf Science*(76), 357-368. doi:10.1016/j.ecss.2007.07.017
- van Eekelen, E., Baptist, M. J., Dankers, P., Grasmeijer, B. T., van Kessel, T., & van Maren, D. S. (2016). Muddy waters and the Wadden Sea harbours.

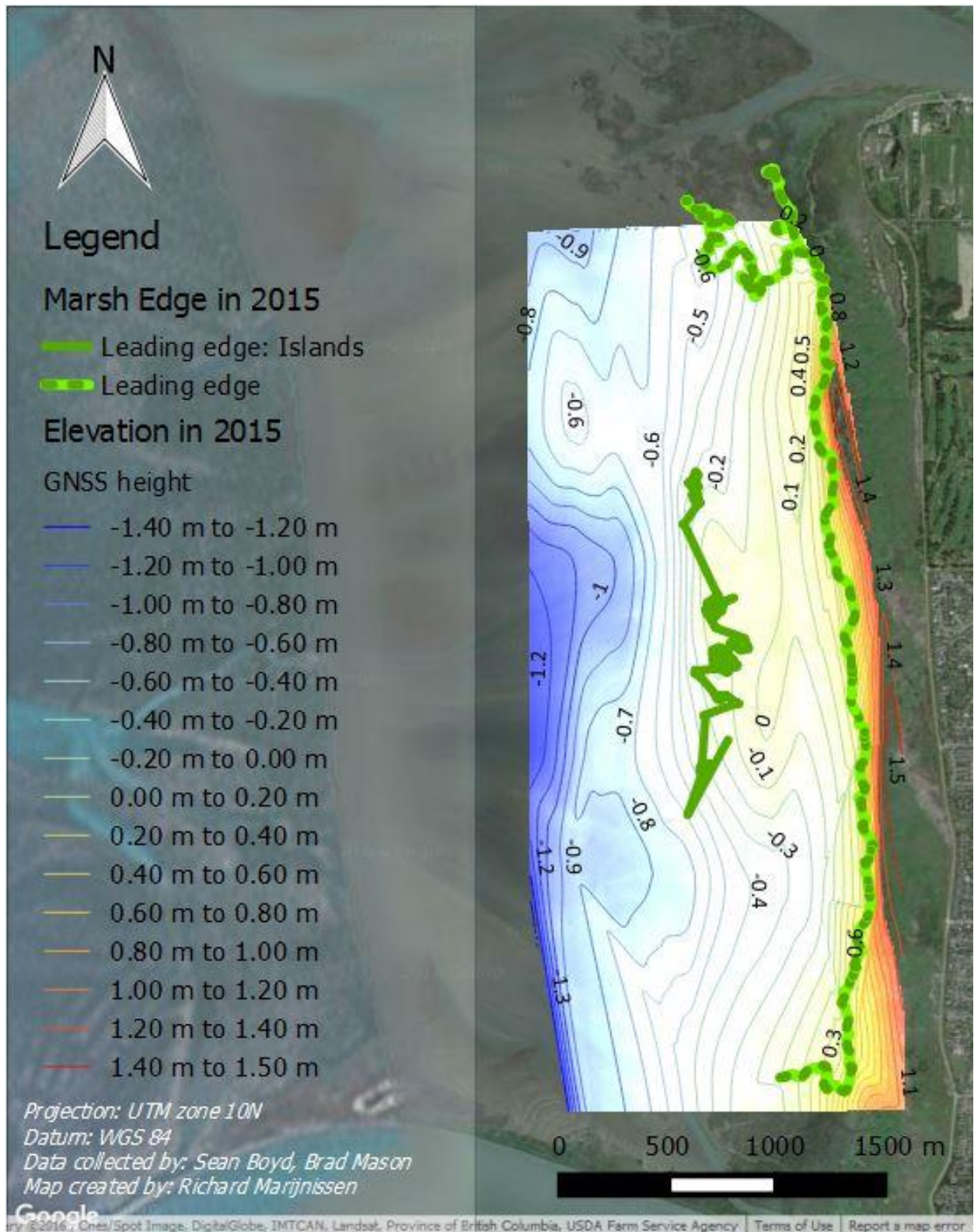
- van Huissteden, J., & van de Plassche, O. (1998). Sulphate reduction as a geomorphological agent in tidal marshes ('Great Marshes' at Barnstable, Cape Cod, USA). *Earth Surface Processes and Landforms*, 23(3), 223-236. doi:10.1002/(SICI)1096-9837(199803)23:3<223::AID-ESP843>3.0.CO;2-I
- van Hulzen, J. B., van Soelen, J., Herman, P. M. J., & Bouma, T. J. (2006). The significance of spatial and temporal patterns of algal mat deposition in structuring salt marsh vegetation. *Journal of Vegetation Science*, 17(3), 291-298. doi:10.1111/j.1654-1103.2006.tb02448.x
- Van Loon-Steensma, J. M., & Slim, P. A. (2012). The impact of erosion protection by stone dams on salt-marsh vegetation on two Wadden Sea barrier islands. *Journal of Coastal Research*, 29(4), 783-796.
- van Loon-Steensma, J. M., Slim, P. A., Decuyper, M., & Hu, Z. (2014). Salt-marsh erosion and restoration in relation to flood protection on the Wadden Sea barrier island Terschelling. *Journal of Coastal Conservation*, 18(4), 415-430. doi:10.1007/s11852-014-0326-z
- Van Rijn, L. C. (1993). *Principles of sediment transport in rivers, estuaries and coastal seas* (Vol. 1006): Aqua publications Amsterdam.
- Weinstein, M. P., Teal, J. M., Balletto, J. H., & Strait, K. A. (2001). Restoration principles emerging from one of the world's largest tidal marsh restoration projects. *Wetlands Ecology and Management*, 9(5), 387-407. doi:10.1023/A:1012058713910
- Williams, H. F. L., & Hamilton, T. S. (1995). Sedimentary Dynamics of an Eroding Tidal Marsh Derived from Stratigraphic Records of 137CS Fallout, Fraser Delta, British Columbia, Canada. *Journal of Coastal Research*, 11(4), 1145-1156.
- Williams, H. F. L., & Roberts, M. C. (1989). Holocene sea-level change and delta growth: Fraser River delta, British Columbia. *Canadian Journal of Earth Sciences*, 26(9), 1657-1666.
- Wilson, K. R., Kelley, J. T., Croitoru, A., Dionne, M., Belknap, D. F., & Steneck, R. (2009). Stratigraphic and Ecophysical Characterizations of Salt Pools: Dynamic Landforms of the Webhannet Salt Marsh, Wells, ME, USA. *Estuaries and Coasts*, 32(5), 855-870. doi:10.1007/s12237-009-9203-7
- Wilson, K. R., Kelley, J. T., Tanner, B. R., & Belknap, D. F. (2010). Probing the Origins and Stratigraphic Signature of Salt Pools from North-Temperate Marshes in Maine, U.S.A. *Journal of Coastal Research*, 1007-1026. doi:10.2112/JCOASTRES-D-10-00007.1
- Wood, G. (Producer). (2014). Richmond's Sturgeon Banks eroding at an alarming rate. *Richmond News*. Retrieved from <http://www.richmond-news.com/news/richmond-s-sturgeon-banks-eroding-at-an-alarming-rate-1.1271973>
- Wootton, A., & Sarrazin, R. (2011). *Roberts and Sturgeon Banks 2011 Habitat Inventory*. Retrieved from <http://www.cmNBC.ca/sites/default/files/RSB%20Habitat%20Inventory%20Final%20Report%20Aug%2030%202011.pdf>

A. APPENDIX 1: MAPS AND FIGURES

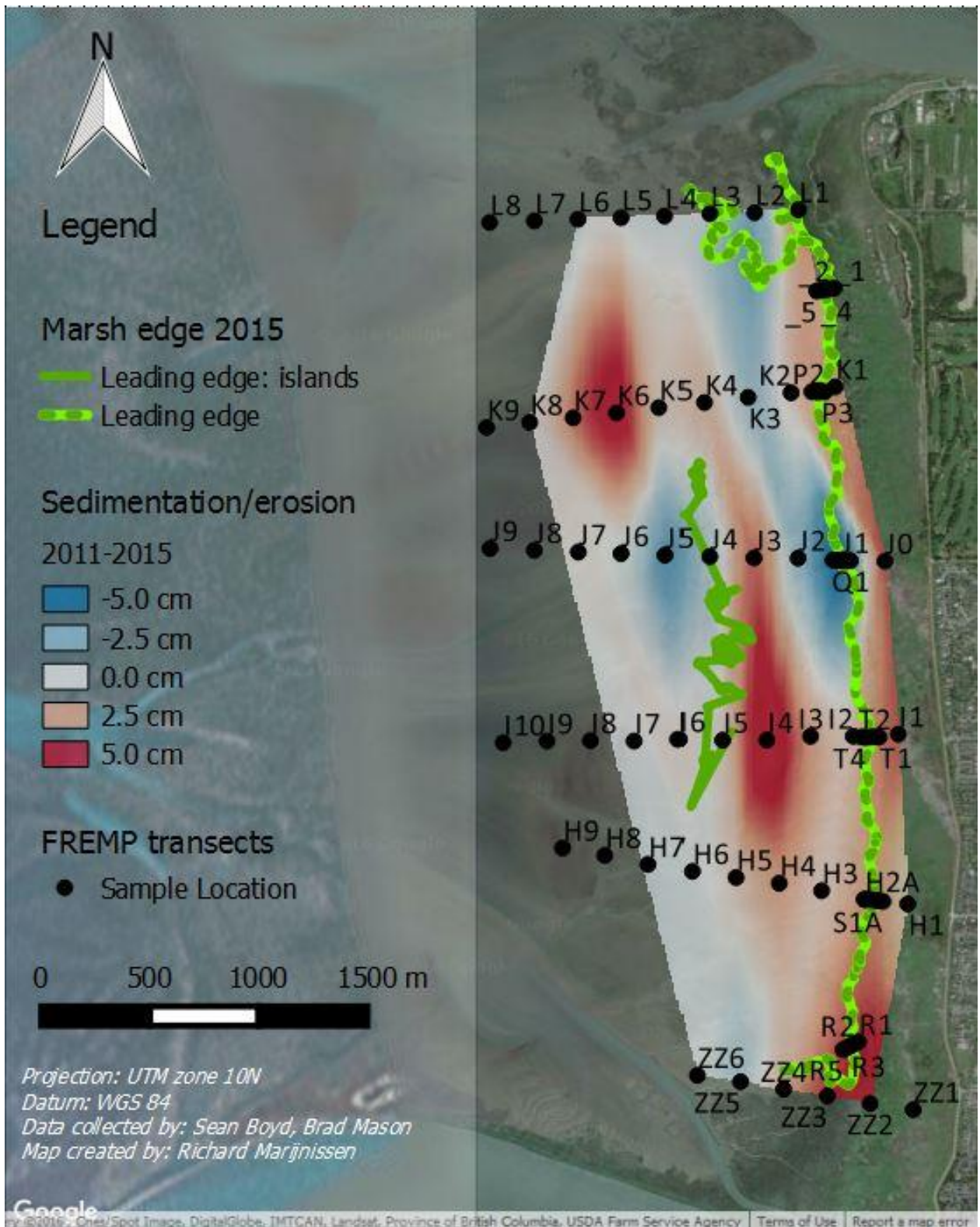
FREMP Locations



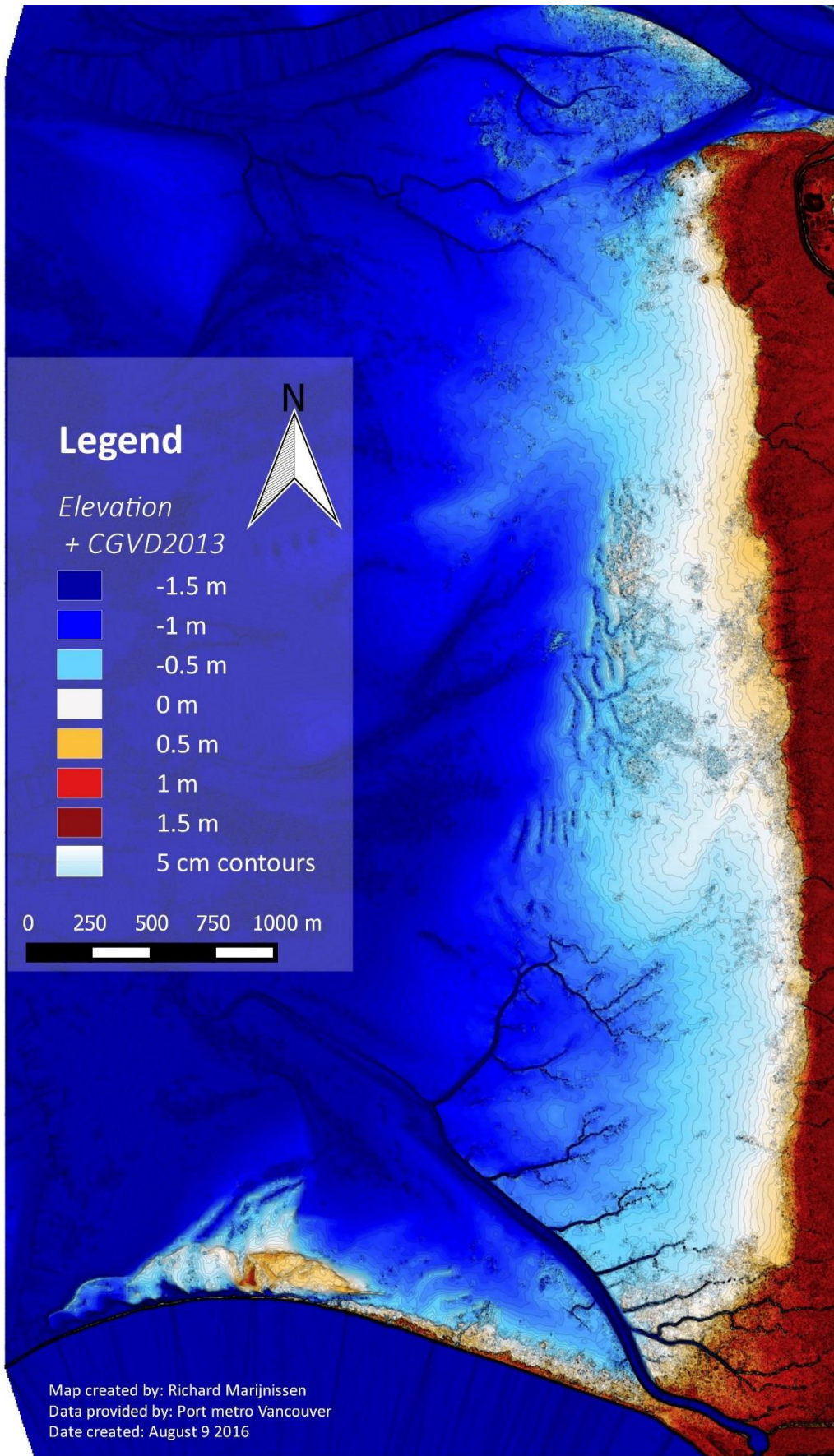
Elevation in 2015



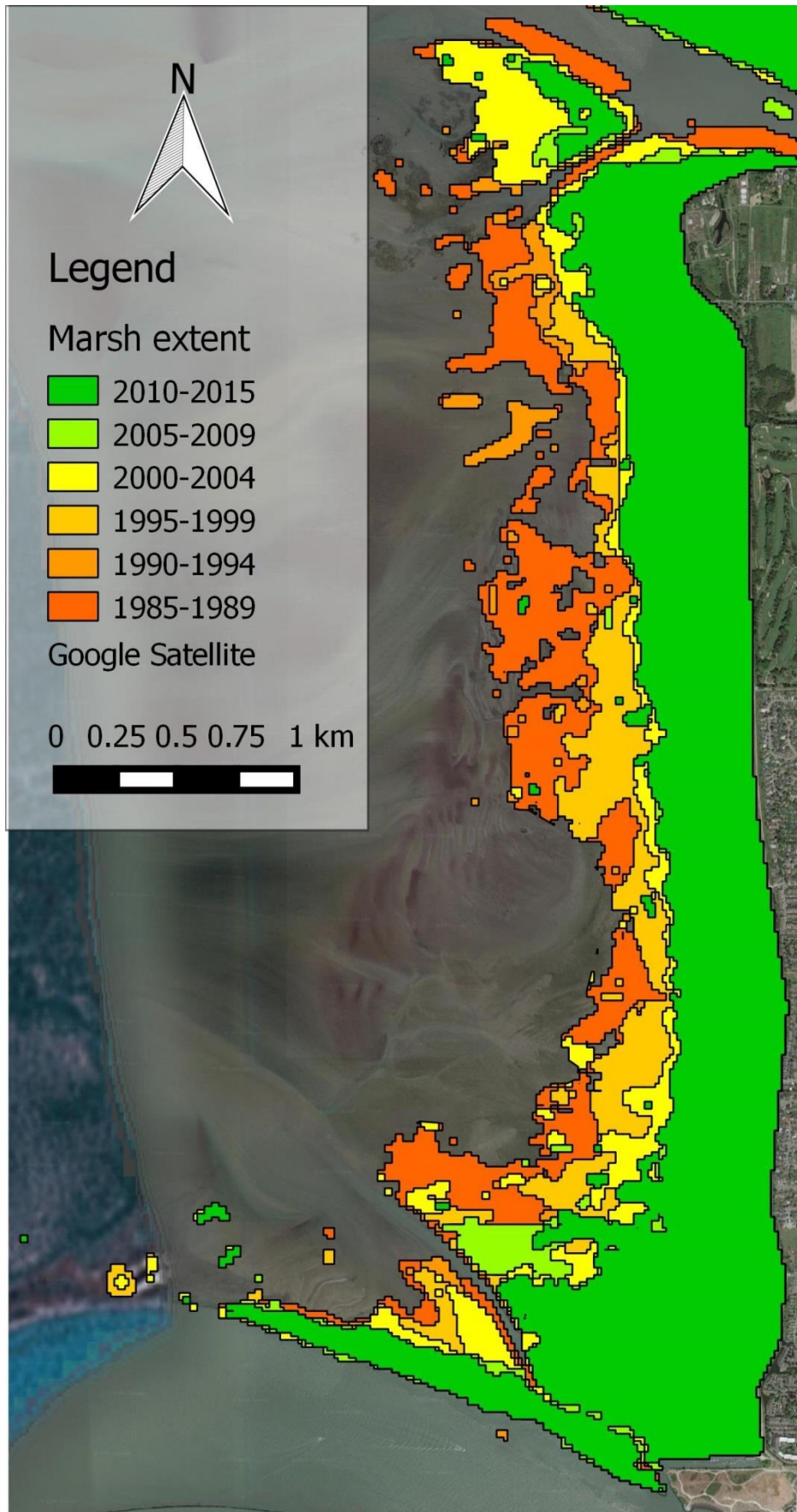
Sedimentation and erosion between 2011 and 2015



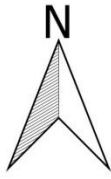
Elevation measured by Lidar in 2013




Satellite study: Elevation Changes



Satellite study: Bathymetry change

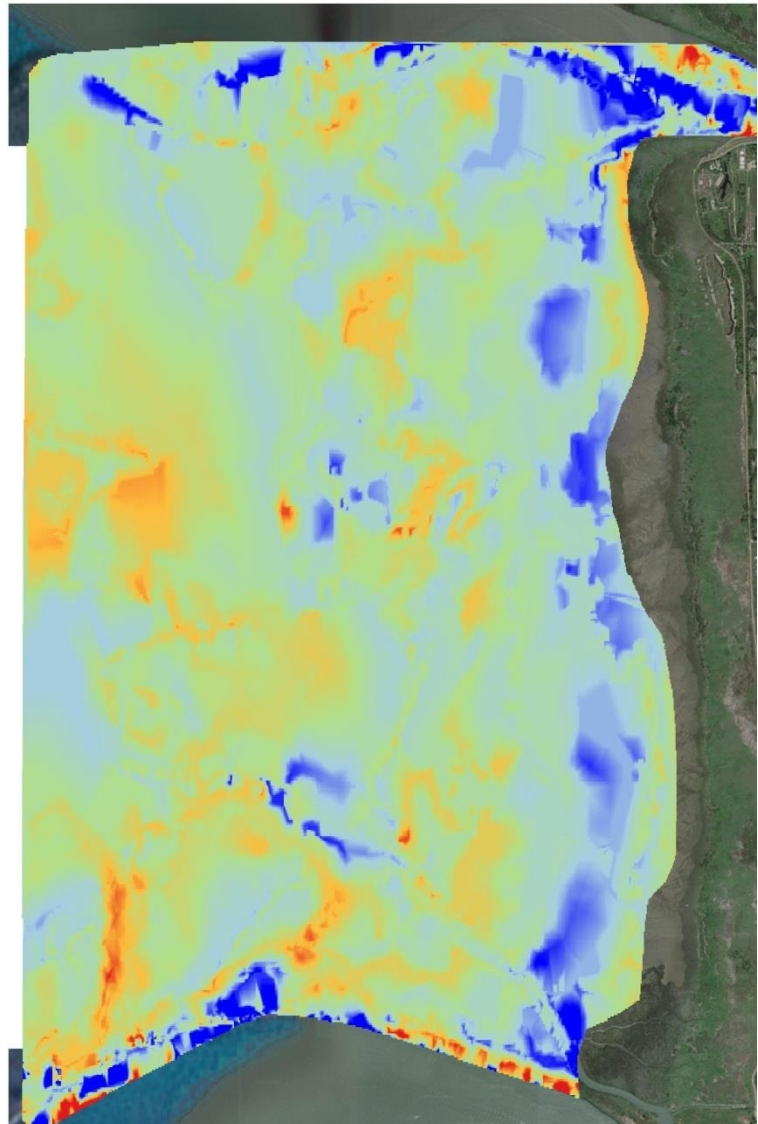



Bathymetry change
1990-2010 [m]

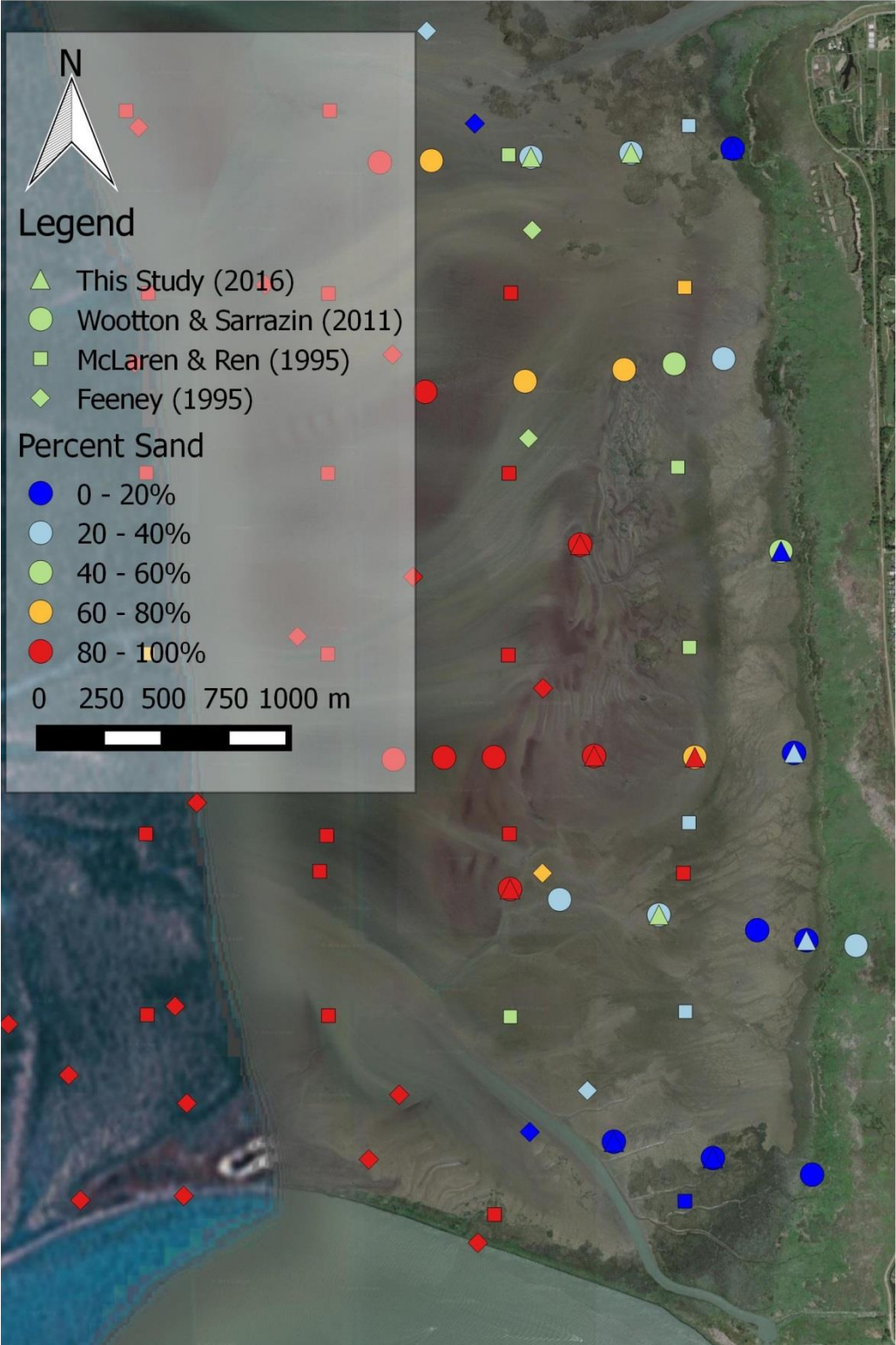
-  -1
-  -0.5
-  0
-  0.5
-  1

Google Satellite

0 0.5 1 1.5 km



Sediment sample locations of various studies



B. APPENDIX 2: TIDE ANALYSIS, METHOD & ASSUMPTIONS

Method

Water levels have been measured at Point Atkinson for a long period of time. It is one of the closest tide gauges near Sturgeon Bank and therefore used to analyze the tides that would be found at Sturgeon Bank.

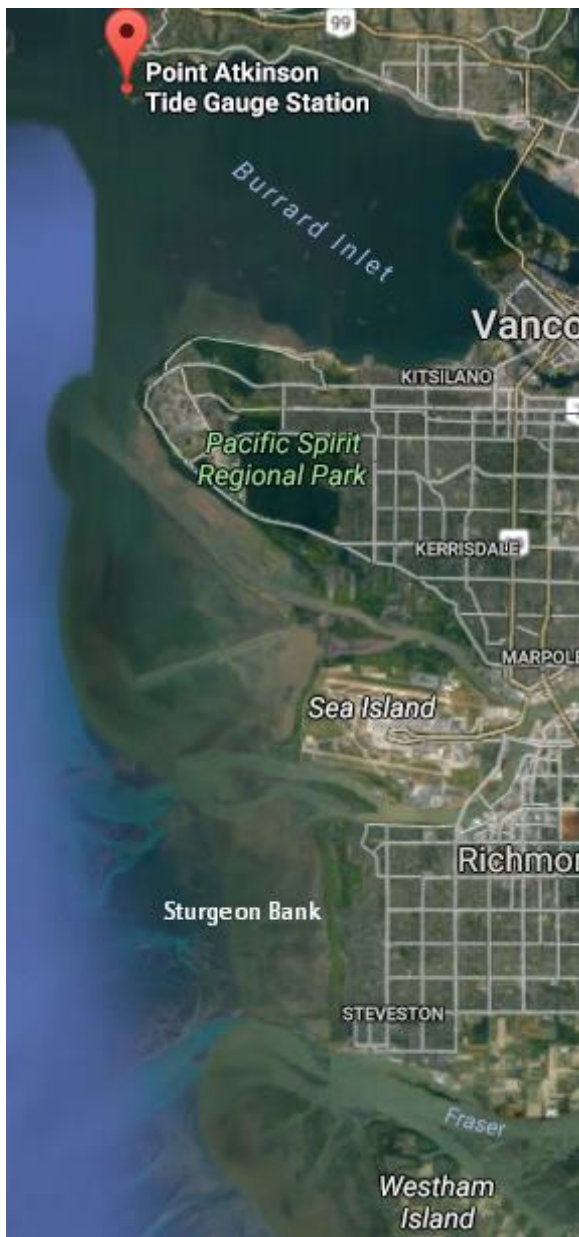


Figure B- 1 Location of Point Atkinson

Table B- 1 Information on Point Atkinson tide station

Station Information	
Station Name:	Point Atkinson, B.C.
Station Number:	7795
Latitude Decimal Degrees:	49.337° N
Longitude Decimal Degrees:	123.253° W
Datum:	CD
Time Zone:	PST
Status:	PERMANENT
Alternate Station Name:	Caulfeild Cove, Sandy Cove
Established:	1897
Province:	BC
Ownership:	PAC
Tide Table Volume:	5
Reference Station:	7795
Geo Location:	STRAIT OF GEORGIA http://isdm-gdsi.gc.ca/isdm-gdsi/twl-mne/inventory-inventaire/sd-ds-eng.asp?no=7795&user=isdm-gdsi&region=PAC
URL	

From the site of Fisheries and Oceans Canada (see Table B- 1) the hourly water levels were retrieved for the period 1984 to 2016. The downloaded files were imported and analysed with the `t_tide` algorithm from Pawlowicz et al. (2002). The algorithm calculates the tidal constituents from the time series.

The tide is semi-diurnal which means there are two high and two low waters a day. These were analysed with a script in the computational program matlab. The script collects the high and low waters by finding the daily minima and maxima.

```

%% Import hourly water levels
WL=csvread('Data/1984-2016.csv');
%% Find mean water
MWL=mean(WL);
%% Calculate MHHW and MLHW
[HHW, lcHHW]=findpeaks(WL, 'MinPeakDistance',20);
[HW, lcHW]=findpeaks(WL);
A=[lcHW;lcHHW];
B=[HW; HHW];
ind=sum(bsxfun(@eq, A(:), A(:).'))==1;
LHW=B(ind);
lcLHW=A(ind);
MHHW=mean(HHW)
MLHW=mean(LHW)

%% Calculate MLLW and MLHW
[LLW, lcLLW]=findpeaks(-WL, 'MinPeakDistance',20);
[LW, lcLW]=findpeaks(-WL);
LLW=-LLW; LW=-LW;
A=[lcLW;lcLLW];
B=[LW; LLW];
ind=sum(bsxfun(@eq, A(:), A(:).'))==1;
HLW= B(ind);
lcHLW=A(ind);
MLLW=mean(LLW)
MHLW=mean(HLW)

```

Figure B- 2 Script used to calculate mean high and low waters

Finally the skewness of the signal was determined with the formula:

Eq. B- 1

$$\gamma_1 = \frac{\frac{1}{n-1} \sum_{i=1}^n (\zeta'_i - \bar{\zeta}')^3}{\left[\frac{1}{n-1} \sum_{i=1}^n (\zeta'_i - \bar{\zeta}')^2 \right]^{\frac{3}{2}}}$$

ζ' = Time derivative of the water level

n = Number of records

Source: (Nidzieko, 2010)

It was implemented in the script with a few additional lines of code.

```

%% Calculate skewness
dt= 60*60; %1 hour between points
n=length(WL);
hmean=mean(WL);
dhdt=(WL(2:end)-WL(1:end-1))./dt;
dhdtmean=mean(dhdt);

mu3=1/(n-1)*sum((dhdt-
dhdtmean).^3);
sigma3=(1/(n-1)*sum((dhdt-
dhdtmean).^2)).^(3/2);

gamma=mu3/sigma3

```

Figure B- 3 Script calculating the skewness of the signal

Assumptions

The tidal signal is complicated by a strong spring-neap variation. Averaging the results over a long period of time (1984 to 2016) ensured that such variability was not affecting the results. A drawback of this approach is that, while representative, the results do not necessarily

reflect the tide on a given day. The skewness varies with the spring-neap cycle and it is at some stages ebb-dominant, even though the tide is flood dominant throughout most of the signal. The lowest water level on a day can be anything from 0 m+CD to 2 m+CD. It is emphasized that any transport of sediments by the tide is highly variable and thus the timing with other types of forcing is crucial on shorter time scales. For this study only the long-term “net” tide is considered.

Another factor that needs to be considered is the difference in environment between Point Atkinson and Sturgeon Bank. Point Atkinson lies at the end of the Burrard inlet which is located within mountainous terrain. Also, this inlet is affected by the different mountain streams that drain into the inlet. Sturgeon Bank on the other hand is located at the edge of the delta with only one major river.

Tide tables are published for a location called Sand Heads which is at the end of the Steveston Jetty at the south east corner of Sturgeon Bank (Canadian Hydrographic Service, 2016). The tide table of Point Atkinson mostly shows the same water levels as the chart for the Sand Heads. Only the high and low waters are more extreme at Point Atkinson than at the Sand Heads (0.1-0.2 m). Because of the high similarity between the two locations it can be assumed that results from analysing the tidal signal at Point Atkinson apply for Sturgeon Bank.

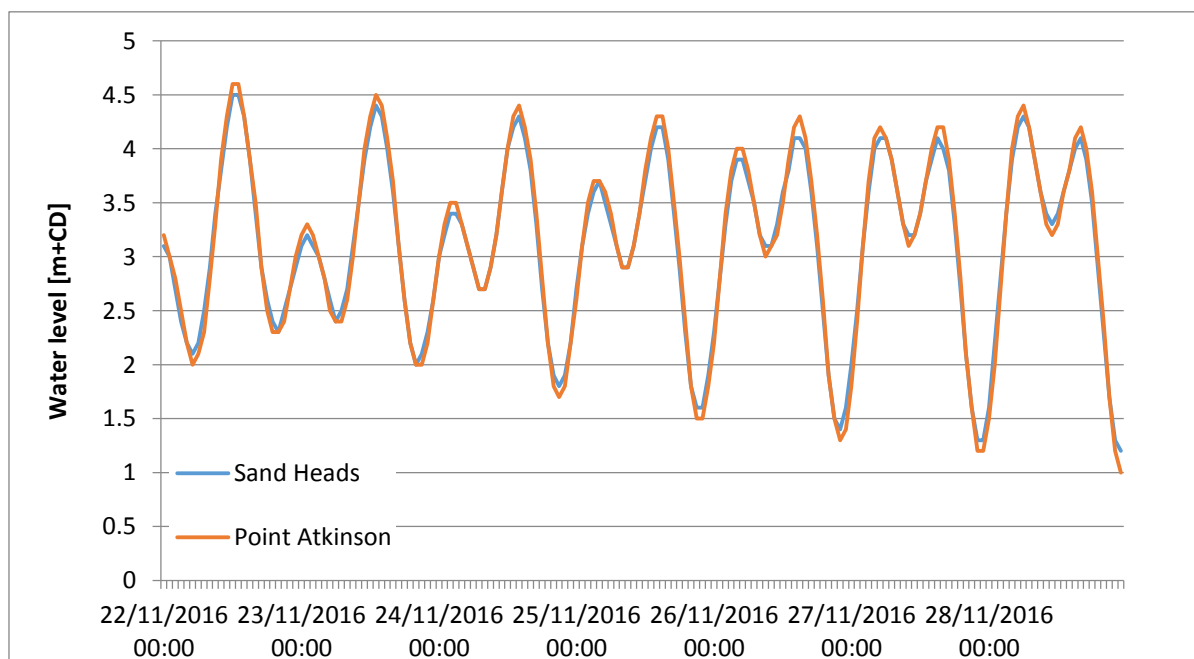


Figure B- 4 The tide at Sand Heads and Point Atkinson predicted by the tide tables(Canadian Hydrographic Service, 2016)

C. APPENDIX 3: INUNDATION BY THE TIDE

Method

The inundation by the tide was analysed by combining the data from the tidal analysis with the Lidar bathymetry. For each part of the bathymetry it was calculated how often the elevation was below the water level from the time series. An inundation frequency of 100% means the area was continuously submerged, 0% means that the area has never been flooded. An inundation frequency of 50% is obtained when the area is at mean sea level. The map below was produced by this calculation.

Results and discussion

The inundation by the tide mostly reflects the elevations. However, some interesting observations can be made. The bulk of the marsh is submerged infrequently. A very sharp transition takes place within 50 to 100 m from regular (40% or more) to no submergence (less than 1%). This transition is at the same position as the marsh edge along most of Sturgeon Bank, except for the far north and far south. At the sand swells the relatively small elevation change has a large influence on submergence time. The most landward crests of the sand swells are submerged 50-55% of the time while the troughs are submerged for 10% longer. This explains the local presence of bulrush islands. However, inundation alone does not explain the presence or absence of bulrush on the entirety of the bank, In the centre no bulrush grows at 50-60% submergence time while in the north and south it does.

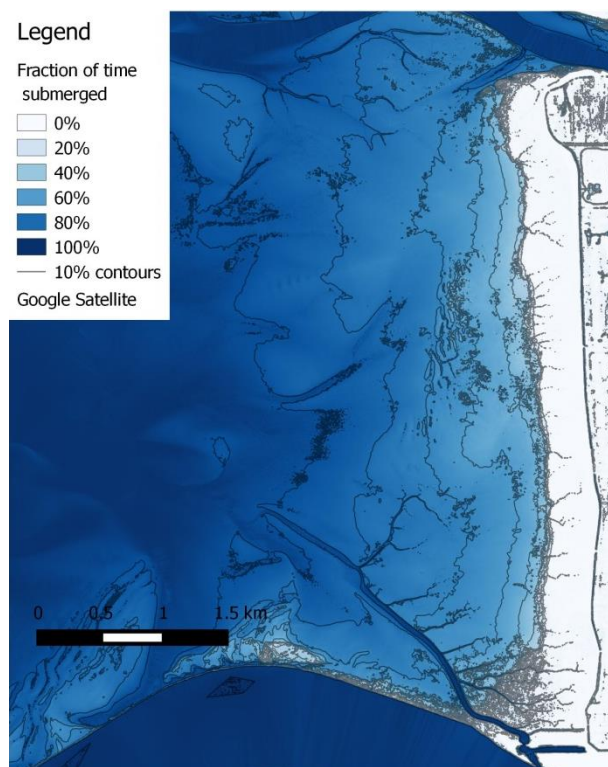


Figure C-1 Inundation map from Lidar and tide signal

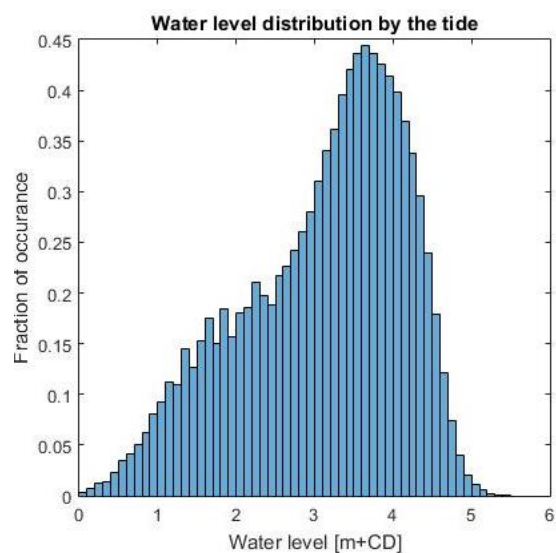


Figure C-2 Water level distribution of the tide

D. APPENDIX 4: STORM ANALYSIS, METHOD AND SCRIPTS

The wind data from 1985 to 2013 was imported from the climate website of the Government of Canada (Table D- 1). The data is an hourly time-series of dates, wind speed and wind direction along with other weather information irrelevant for the analysis.

The analysis was conducted to find the historic storm events and to determine how exceptional these storm events were. To do so first all wind speeds below 18 m/s were discarded. The script then cycles through all hours and stores the date, wind direction at that time, the average of the wind speeds recorded within 24 hours of the measurement and the average direction within those 24 hours. Furthermore, the minimum and maximum water level within 24 hours of the recorded wind speed was stored to give the tidal range at that day (Figure D- 2). Finally, the stored results were sorted by maximum wind speed and presented in a table (Table 4 in section 3.3 of the report).

The frequency of storm events was calculated by fitting an extreme value distribution to the data. At first the maximum wind speed was calculated for each year. However, the 30 data points proved insufficient to reliably fit a distribution. When the maximum recorded wind speed of each month was plotted, there were enough points. Calmer summer months could skew the results but it is assumed these will not significantly affect the interpretation of the results. From the fitted extreme value distribution, the wind speeds for different return periods are extrapolated. The results are found in table 3 in section 3.3.

Station Name	VANCOUVER INT'L A
Province	BRITISH COLUMBIA
Latitude	49.2
Longitude	-123.18
Elevation	4.3
Climate Identifier	1108447
URL	http://climate.weather.gc.ca/historical_data/search_historic_data_e.html

Table D- 1 The source of the wind data

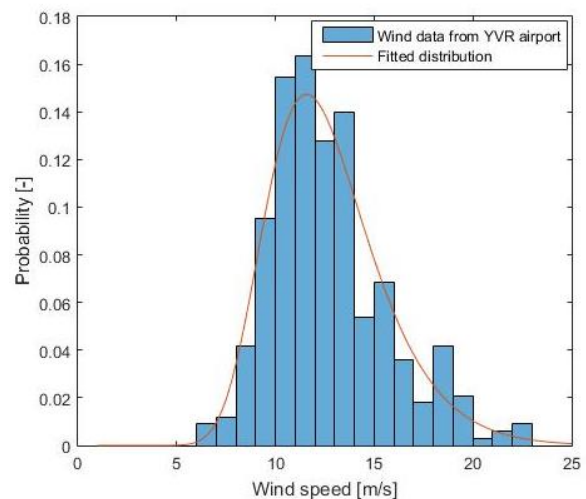


Figure D- 1 Extreme value distribution fitted to the maximum hourly averaged monthly wind speed

```

%% Import wind data and tides
...
%% Return storm dates, storm wind speed, wind direction and tidal range during storms
istorm=find(WindSpeed>18); %Find exact time of storm winds ws>18 m/s
nnn=length(istorm);
aa=1;
    for iii=1:nnn
        DateIII=DatesWind(istorm(iii)); %store the date of the ith storm in the loop for
easier coding
            %find the indices of all hours from the day with the storm
            iiistormday=istorm(iii)-12:istorm(iii)+12;
            pDates=DatesWind(iiistormday);
            if ~isnan(pDates(1))
                pWindSpeed=WindSpeed(iiistormday);
                pWindDir=WindDir(iiistormday);
                pWindDir(pWindDir<180)=pWindDir(pWindDir<180)+360;
                for kkk=1:length(pDates)
                    test=TideWL(pDates(kkk))==TideDatesNum;
                    if ~isempty(test)
                        pTide(kkk,1)=test;
                    end
                end
                %Store output
                Storms.Date(aa) = datestr(DateIII);
                Storms.MaxWind(aa)=WindSpeed(istorm(iii));
                Storms.MeanWind(aa)=mean(pWindSpeed);
                Storms.WindDir(aa)=WindDir(istorm(iii));
                Storms.MeanWindDir(aa)=mean(pWindDir);
                if Storms.MeanWindDir(aa)>360
                    Storms.MeanWindDir(aa)=Storms.MeanWindDir(aa)-360;
                end
                if ~isempty(pTide)
                    Storms.TideRange(aa)=max(pTide)-min(pTide);
                end
                aa=aa+1;
            end
    end
end

```

Figure D- 2 Script to analyse storms from the wind time series

```

%% Compute return period of storms
%fit maximum measured hourly wind speeds of all months to extreme value distribution
sfit=fitdist(maxWindSpeed,'gev');

%Compute pdf for speeds between 0 and 25 m/s
u=1:0.1:25;
y=pdf(sfit,u);

% plot histogram of distribution
...
%Calculate windspeed with a given return period
ReturnPeriod=[1, 2, 5, 10, 20, 50].*12; %years (*12 to convert to months)
p=1./ReturnPeriod;
ReturnPeriodWindSpeed=icdf(sfit,1-p);

%Show results in table
...

```

Figure D- 3 Script to compute the return period of storm winds

E. APPENDIX 5: SATTELITE STUDY, SCRIPTS

A large amount of coding was required to execute the approach outlined in section 5.4. The scripts are presented in this appendix. Credit for the Earth Engine script goes to Josh Friedman who was kind enough to lend his script from the Earth Engine morphology application he developed (Friedman, 2015).

Code made in the Google Earth Engine. The script can be accessed and executed via this link:

<https://code.earthengine.google.com/11f1c41c06919b25fe605af99cecf3c2>

```
//concept for MSc EE analysis
//J. Friedman
//Apr 19 2016

//temporal extents
//var startTime = '1980-01-01'
//var endTime = '2016-03-01'
  //day of the year to limit seasonal effects
  var startDoY = 122;
  var endDoY = 245;

//define spatial extents
var geometry = ee.Geometry.Polygon( ... );
//var aoi = Map.getBounds(true)
var aoi = geometry;

//define cutoff threshold for ndvi
var thresh = -0.25; //0.2 for water line, -0.25 for middle marsh

//load L8 image collection
var L8 = ee.ImageCollection('LANDSAT/LC8_L1T_TOA')
  //.filterDate(startTime, endTime)
  .filterBounds(aoi)
  .filterMetadata('CLOUD_COVER','less_than',5)
  .filter(ee.Filter.dayOfYear(startDoY, endDoY))
  .select(['B4','B5'],['R','NIR']);

//ADD MORE COLLECTIONS
var L7 = ee.ImageCollection('LANDSAT/LE7_L1T_TOA')
  //.filterDate(1999-01-01, 2003-02-02)
  .filterBounds(aoi)
  .filterMetadata('CLOUD_COVER','less_than',5)
  .filter(ee.Filter.dayOfYear(startDoY, endDoY))
  .select(['B3','B4'],['R','NIR']);

var L5 = ee.ImageCollection('LANDSAT/LT5_L1T_TOA')
  //.filterDate(startTime, endTime)
  .filterBounds(aoi)
  .filterMetadata('CLOUD_COVER','less_than',5)
  .filter(ee.Filter.dayOfYear(startDoY, endDoY))
  .select(['B3','B4'],['R','NIR']);

//MERGE COLLECTIONS TOGETHER
var IMAGES=L8.merge(L7).merge(L5).sort('system:time_start', false);
```

```

//go through the images
var num = IMAGES.size().getInfo();
print(num) //NUMBER OF IMAGES IN COLLECTION

for (var ii = 0; ii < num; ii++) { //REPEAT EQUAL TO NUMBER OF IMAGES IN COLLECTION

  //get an image (based on index)
  var im = ee.Image(IMAGES.toList(1,ii).get(0)).clip(aoi);

  //calculate NDVI
  var ndvi = im.normalizedDifference(['R','NIR']).focal_median(2);

  //get date
  var imdate =
ee.Algorithms.Date(im.get('system:time_start')).format('yyyyMMddHHmm').getInfo();
  var year = ee.Algorithms.Date(im.get('system:time_start')).format('yyyy').getInfo();

  //add to map
  Map.addLayer(ndvi,{min:-1,max:1},'ndvi '+imdate,false);

  //clip to specific threshold level
  var clipped = ndvi.mask(ndvi.lte(thresh));
  Map.addLayer(clipped,{min:-1,max:1},'clipped '+imdate,false);

  // determine edge -> build vector from raster
  var clipped = clipped.cast({'nd':'int'});
  var coastline = clipped.reduceToVectors(null, aoi, 15);
  var cl = ee.Image(0).mask(0).toByte();
  cl = cl.paint(coastline, 0, 0.25);

  //LOOK FOR ADDITIONAL EDGES

  //add to map
  if(year >=1985 ){var color='ff0000';} //red
  if(year >=1990 ){var color='ff7f00';} //orange
  if(year >=1995 ){var color='00ff00';} //green
  if(year >=2000 ){var color='00ff7f';} //cyan
  if(year >=2005 ){var color='0000ff';} //blue
  if(year >=2010 ){var color='7f00ff';} //purple
  if(year >=2016 ){var color='000000';} //black

  Map.addLayer(cl,{palette: color },'edge '+imdate,false);
  Map.setCenter(-123.19596290588379, 49.151510076469755, 13);

  //export to kml
  Export.table.toDrive({
    collection: coastline,
    description: imdate,
    fileFormat: 'KML'});

  //POST-PROCESS IN MATLAB
}

```

Figure E- 1 Script to extract marsh and water lines from LandSat satellite imagery

Matlab script which does the following:

- 1) Import the water/coast lines from the KML files
- 2) Filter the lines based on date, water level at the time and noise
- 3) Export the cleaned water/marsh lines into a new file called Coast.mat

```

%% Setup filters
Filter.WL=0; %1=filer on, 0=filter off
Filter.Dates=0;%1=filer on, 0=filter off
threshWLHigh=3;
threshWLLow=-1;
startDate='01-01-1985';
endDate='01-01-2016';
%% Import Tide table
...

%% Import KML files
...
%% Collect all data in structure Coast

```



```

index=1;
i3=1;
fprintf('3. Process Coastlines \n');
for i=1:length(files)
    if(files(i).isdir==0)
        name=files(i).name;
        Coast(index).date=datetime(name(1:end-4), 'InputFormat', 'yyyyMMddHHmm'); %format
Coast: yyyyMMddHHmm; format Marsh:ddMMyyyyHHmm
        %round time to nearest hour
        datemin=minute(Coast(index).date);
        if(datemin>=30)
            Coast(index).date=Coast(index).date-minutes(datemin)+hours(1);
        else
            Coast(index).date=Coast(index).date-minutes(datemin);
        end
        Coast(index).kml= kml2struct([Folder, name]);
        Coast(index).Tide=transpose(TideTableWL(Coast(index).date==TideTableDates));
        KML= Coast(index).kml;
        Coast(index).longitude=KML(1).Lon;
        Coast(index).latitude=KML(1).Lat;
        %Check if there is too much noise (more than 50 polygons)
        if(length(Coast(index).kml)>50)
            Noisy=1;
        else
            Noisy=0;
        end
        %Check whether water level was found in table table
        if isempty(Coast(index).Tide)==1
            WLMissing=1;
        else
            WLMissing=0;
        end
        %Filter dates
        if(Filter.Dates==0 || ( datenum(Coast(index).date)>=datenum(startDate) &&
datenum(Coast(index).date)<=datenum(endDate)))
            metDates=1;
        else
            metDates=0;
        end
        %Filter water level
        if(Filter.WL==0 || ( Coast(index).Tide>=threshWLLow &&
Coast(index).Tide<=threshWLHigh))
            MetWL=1;
        else
            MetWL=0;
        end
        %Process data if filter conditions are met
        if(metDates==1 && MetWL==1 && WLMissing==0 && Noisy==0)
            for ii=2:length(KML)
                Coast(index).longitude=[Coast(index).longitude; KML(ii).Lon;];
                Coast(index).latitude=[Coast(index).latitude; KML(ii).Lat;];
                [Coast(index).X, Coast(index).Y]=
LatLon2XY(Coast(index).latitude,Coast(index).longitude,49.126906, -123.194153);
            end
            Coast(index).Z=transpose(ones(length(Coast(index).longitude),1).*(Coast(index).Tide));
            end
            index=index+1;
        else
            Coast=Coast(1:max(end-1,1));
        end
        fprintf('%f percent of coastlines processed \n', i/length(files)*100);
    end
end
%% Export Coast and create XYZ matlab file
...

```

Figure E-2 Script to import KML files and clean them for further processing

Matlab script to interpolate the bathymetries from 1985 to 2015 from the water lines in the Coast.mat file

```

%% Import coast.mat
...
%% Merge all X,Y and Z data into a arrays per period
startDate={'01-Jan-1985','01-Jan-1990','01-Jan-1995','01-Jan-2000','01-Jan-2005','01-Jan-2010'};
endDate={'31-Dec-1989','31-Dec-1994','31-Dec-1999','31-Dec-2004','31-Dec-2009','31-Dec-2015'};

%Area for fitting
FitArea=[[-123.25,-123.195]; [49.12, 49.18]];
RasterWidth=750;

Ycrosssection=[[1000,1029]; [3000,3029]; [5000,5029]];

X1985=[]; X1990=[]; X1995=[]; X2000=[]; X2005=[]; X2010=[];
Y1985=[]; Y1990=[]; Y1995=[]; Y2000=[]; Y2005=[]; Y2010=[];
Z1985=[]; Z1990=[]; Z1995=[]; Z2000=[]; Z2005=[]; Z2010=[];

if( (Coast(1).date)>= (startDate{1}) && (Coast(1).date)<= (endDate{1}))
    X1985=transpose(Coast(1).longitude);
    Y1985=transpose(Coast(1).latitude);
    Z1985=Coast(1).Z;
end
for i=2:length(Coast)
    if (~isempty(Coast(i).Z))
        if (Coast(i).date>=startDate{1} && Coast(i).date<= endDate{1})
            X1985=[X1985, transpose(Coast(i).longitude)];
            Y1985=[Y1985, transpose(Coast(i).latitude)];
            Z1985=[Z1985, Coast(i).Z];
        elseif( Coast(i).date>=startDate{2} && Coast(i).date<=endDate{2})
            X1990=[X1990, transpose(Coast(i).longitude)];
            Y1990=[Y1990, transpose(Coast(i).latitude)];
            Z1990=[Z1990, Coast(i).Z];
        elseif( (Coast(i).date)>= (startDate{3}) && (Coast(i).date)<= (endDate{3}))
            X1995=[X1995, transpose(Coast(i).longitude)];
            Y1995=[Y1995, transpose(Coast(i).latitude)];
            Z1995=[Z1995, Coast(i).Z];
        elseif( (Coast(i).date)>= (startDate{4}) && (Coast(i).date)<= (endDate{4}))
            X2000=[X2000, transpose(Coast(i).longitude)];
            Y2000=[Y2000, transpose(Coast(i).latitude)];
            Z2000=[Z2000, Coast(i).Z];
        elseif( (Coast(i).date)>= (startDate{5}) && (Coast(i).date)<= (endDate{5}))
            X2005=[X2005, transpose(Coast(i).longitude)];
            Y2005=[Y2005, transpose(Coast(i).latitude)];
            Z2005=[Z2005, Coast(i).Z];
        elseif( (Coast(i).date)>= (startDate{6}) && (Coast(i).date)<= (endDate{6}))
            X2010=[X2010, transpose(Coast(i).longitude)];
            Y2010=[Y2010, transpose(Coast(i).latitude)];
            Z2010=[Z2010, Coast(i).Z];
        end
    end
end

%Find indices within the fit area
i1985=find(X1985>=FitArea(1,1) & X1985<=FitArea(1,2) & Y1985>=FitArea(2,1) & Y1985<=FitArea(2,2));
i1990=find(X1990>=FitArea(1,1) & X1990<=FitArea(1,2) & Y1990>=FitArea(2,1) & Y1990<=FitArea(2,2));
i1995=find(X1995>=FitArea(1,1) & X1995<=FitArea(1,2) & Y1995>=FitArea(2,1) & Y1995<=FitArea(2,2));
i2000=find(X2000>=FitArea(1,1) & X2000<=FitArea(1,2) & Y2000>=FitArea(2,1) & Y2000<=FitArea(2,2));
i2005=find(X2005>=FitArea(1,1) & X2005<=FitArea(1,2) & Y2005>=FitArea(2,1) & Y2005<=FitArea(2,2));
i2010=find(X2010>=FitArea(1,1) & X2010<=FitArea(1,2) & Y2010>=FitArea(2,1) & Y2010<=FitArea(2,2));

```

```

% Create a fit within the defined area for interpolating
Fit1985=fit ([transpose(X1985(i1985)), transpose(Y1985(i1985))], transpose(Z1985(i1985)), 'linea
r');
Fit1990=fit ([transpose(X1990(i1990)), transpose(Y1990(i1990))], transpose(Z1990(i1990)), 'linea
r');
Fit1995=fit ([transpose(X1995(i1995)), transpose(Y1995(i1995))], transpose(Z1995(i1995)), 'linea
r');
Fit2000=fit ([transpose(X2000(i2000)), transpose(Y2000(i2000))], transpose(Z2000(i2000)), 'linea
r');
Fit2005=fit ([transpose(X2005(i2005)), transpose(Y2005(i2005))], transpose(Z2005(i2005)), 'linea
r');
Fit2010=fit ([transpose(X2010(i2010)), transpose(Y2010(i2010))], transpose(Z2010(i2010)), 'linea
r');

%Define X and Y extend

X=transpose(linspace(FitArea(1,1),FitArea(1,2),RasterWidth));
Y=transpose(linspace(FitArea(2,1),FitArea(2,2),RasterWidth));

%Interpolate a the bathymetry in the defined X, Y raster
for m=1:length(X)
    for n=1:length(Y)
        Zfit1985(n,m)=feval(Fit1985,[X(m),Y(n)]);
        Zfit1990(n,m)=feval(Fit1990,[X(m),Y(n)]);
        Zfit1995(n,m)=feval(Fit1995,[X(m),Y(n)]);
        Zfit2000(n,m)=feval(Fit2000,[X(m),Y(n)]);
        Zfit2005(n,m)=feval(Fit2005,[X(m),Y(n)]);
        Zfit2010(n,m)=feval(Fit2010,[X(m),Y(n)]);
    end
end
%Export Geotiff image of the interpolated bathymetries for plotting in Q-gis
ExportGeotiff([folderOUT,'1985'],X,Y,Zfit1985);
ExportGeotiff([folderOUT,'1990'],X,Y,Zfit1990);
ExportGeotiff([folderOUT,'1995'],X,Y,Zfit1995);
ExportGeotiff([folderOUT,'2000'],X,Y,Zfit2000);
ExportGeotiff([folderOUT,'2005'],X,Y,Zfit2005);
ExportGeotiff([folderOUT,'2010'],X,Y,Zfit2010);

```

Figure E- 3 Script to sort the lines in the Coast file into periods, interpolate a bathymetry for each and export for each a Geotiff image

F. APPENDIX 6: REPORT OF THE FIELDWORK

Goal

From the Sturgeon Bank stakeholders meeting some interesting suggestions for fieldwork have been put forward. Summarized they are:

1. Understand the system by examining the area and taking notes / pictures of observations
2. Retrieve sediment data to determine changes in sediment distribution as well as for use in the model.
3. Find locations with *Schoenoplectus pungens* (bulrush) still present and determine the common features between the locations. Common features could include:
 - a. Salinity
 - b. Elevation
 - c. Sediment
 - d. Drainage (channels present)
4. Examine the extend of the sand bar/ islands and its bulrush

Research methods

Photographs and observations

During the fieldwork general observations are made of the area. At first the physical environment is documented to get a better understanding of location. This includes but is not limited to: the soil, the different vegetation types and landforms (gullies, ridges, etc.). Furthermore, special attention has been paid to features that could indicate erosion like scarps and uprooted vegetation.

Piston samples

At predetermined locations along the FREMP transects the soil is sampled. The cores are weighed and filtered to arrive at a grain size distribution of the material at each location. The soil is affected by the sediments supplied to Sturgeon Bank, the presence of the bulrush, the tides and possibly waves.

Since the Steveston North Jetty was constructed the amount of sediment that can reach the bank has decreased. The relative amount of sand compared to mud supplied to the bank could have increased as most mud is diverted off-shore by the jetty. In this case a gradual coarsening of the bed is expected and a steepening of the profile. This hypothesis can be tested.

The presence of bulrush at a specific soil can be the result of 2 processes. The bulrush could prefer one type of soil or is simply outcompeted by another plant in coarser/finer soils. Another process is that the vegetation will naturally trap finer sediment. The bulrush edge should therefore have a higher fraction of mud compared to the flats just beyond the edge. The presence/absence of bulrush at a certain mud content could be used to determine the habitat required for the bulrush as well as the overall effect of vegetation on the mud content of the soil.

Both the influence of tides and waves are expected to decrease with increased elevation. The flow speeds should decrease as the depth decreases on the shallow slope of Sturgeon Bank due to friction. This will naturally result in a gradation of coarser sediments down the slope and finer sediments further up the slope. Cores taken at different elevations are expected to follow this trend.

GPS

The location of the cores and observations will be recorded. Observation from photos taken with an iPhone will record the GPS position automatically. For more accurate positions a GPS receiver is required.

GPS can also be used to measure elevation. The elevation of the leading edge should be uniform. Large deviations would indicate another influence is present that affects the grow of bulrush on the leading edge. This could be important to determine the conditions (un)suitable for marsh growth.

On Sturgeon Bank part of the sand flat is lightly raised and has bulrush. This feature is likely to be a sand bar. Little is known about the sand bars on Sturgeon Bank. A detailed elevation profile at this location could give more insight in this feature. If the elevation profile can be compared with earlier measurements the speed and direction the bars travel can be determined. It is hypothesized that this feature is suitable for bulrush due to its higher elevation but also impedes the drainage of water behind it. Understanding this feature would thus improve the understanding of the system.

Observations

While doing the fieldwork, photos were taken of notable features and interesting phenomena. The leading edge shows different characteristics from the north to the south. Far beyond the leading patches of vegetation can still be found on small islands. The CBC radio tower was built on a pier that stretches out far into Sturgeon Bank and between the poles of the piers vegetation is still present beyond the edge of the marsh surrounding it. Algae were observed covering and flattening patches of vegetation throughout Sturgeon Bank. Further walking on the soil proved difficult near the leading edge and especially between the creeks there, whereas further offshore walking got a lot easier. A layer of water was observed up until hundreds of meters from the leading despite low tides. At transect J sand swells were observed as the tops of these were dry while several centimetres of water was still present in the troughs between them. Finally, several large tidal channels were observed in the south of Sturgeon Bank. These channels are not found in the north of Sturgeon Bank.

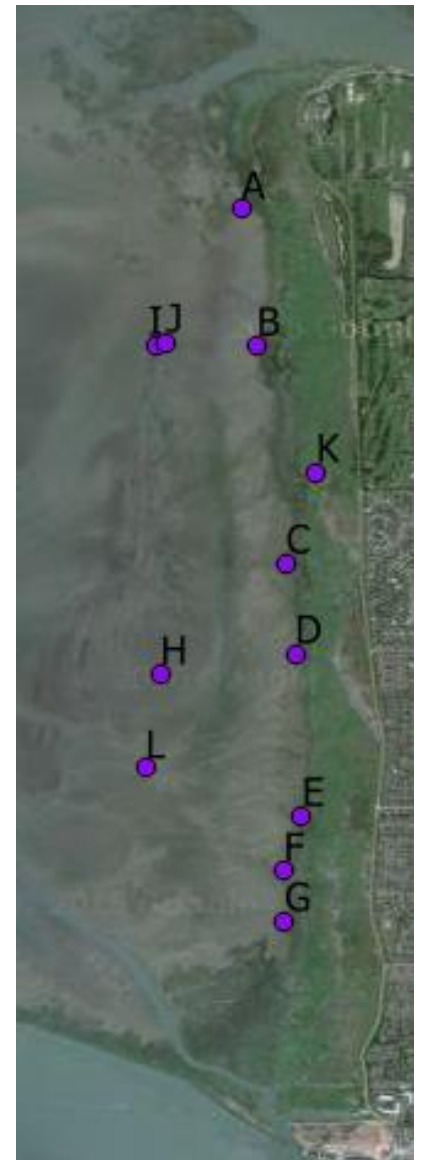


Figure F- 1 Location of the photos

Leading edge



Figure F- 2 Leading edge at A



Figure F- 3 Leading edge at B

Location A:

Date: 07-06-16 14:08:04

The leading edge is muddy. No scarps were observed nor any clumps. Also, there are no channels into the marsh. This photo was taken before the algae bloom. Later during the fieldwork algae was found between the stems.

Location B:

Date: 01-07-16 12:08:16

The edge is still muddy. No scarps are observed but dead roots can be found throughout the area. The roots are visible as black knobs sticking out of the mud (clearly visible on the left bottom corner of the image). Furthermore, large patches of algae can be found at the leading edge and between the stems of the vegetation.



Figure F- 4 Leading edge at C

Location C:

Date: 03-07-16 13:14:51

The area is characterized by the many clumps of mud in front of the leading edge. Many of the clumps contain the dead roots of *schoenoplectus pungens* and *bolboschoenus maritimus* which stick out of the clumps as black knobs. Some of the clumps still contain isolated patches of *pungens* and *maritimus*. In between the clumps small patches of *pungens* and *maritimus* can be found as well. Within the edge a similar pattern of clumps, small pools and creeks was observed as well. This suggests that the bare clumps used to be part of the marsh not too long ago. Furthermore, a large number of algae were found in between the creeks and between the stems of the vegetation.

The leading edge is wetter than the area further offshore. It is always covered with a small layer of water during low tide. In combination with wind from the west the water depth increases further.

Location D:

Date: 01-07-16 08:17:51

The same observations were made as at location C



Figure F- 5 Leading edge at D



Figure F- 6 Leading edge at E

Location E:

Date: 04-07-16 12: 39:23

The same observations were made as at location C

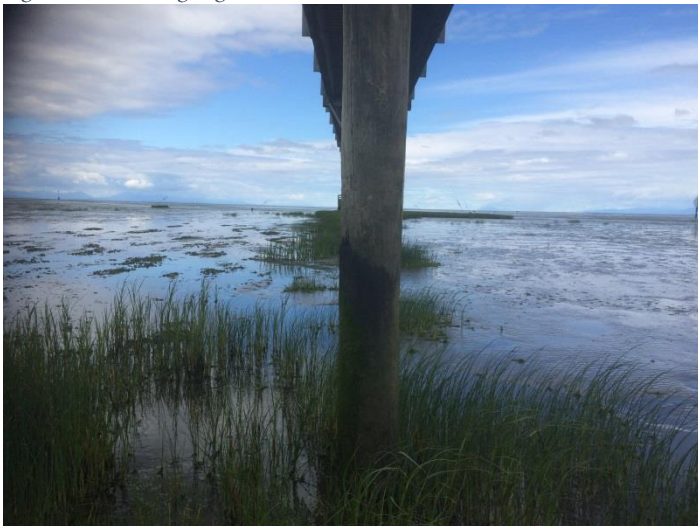


Figure F- 7 Leading edge at F

Location F:

Date: 04-07-16 11:02:58

This location is at the CBC radio tower pier. Between the poles of the pier large patches of vegetation still grow including *schoenoplectus pungens*, *bolboschoenus maritimus* and even some higher marsh species. They grow predominantly on the northern side of the pier where the elevation is slightly higher. Furthermore, the southern side was found to be muddier than the northern side and the south was covered by a deeper layer of water.



Figure F- 8 Leading edge at G

Location G:

Date: 04-07-16 11:49:00

The marsh in the south appears to be stable or growing. No clumps or scarps were found. A monoculture of *pungens* was found along the edge and some patches are growing in front of it. There are noticeably less algae in this area. The soil is more solid than along the edge north of the CBC radio tower pier.

Islands of vegetation



Figure F- 9 Bulrush islands at location H

Location H:

Date: 01-07-16 07:26:29

Islands of *schoenoplectus pungens* can be found within a band roughly 900 to 1200 m away from the dike (550 to 850 m from the leading edge) between FREMP transects I to K. The islands are higher than the surrounding flats. Unlike the marsh edge these islands are sandy and do not maintain a layer of water during low tide. Also, the *pungens* on the edge of the islands is denser and longer than on the leading edge of the marsh. Some islands were covered with algae whereas others were covered far less.

Sand swells



Figure F- 10 Sand swell at I

Location I:

Date: 01-07-16 11:48:32

The sand swells can be found between FREMP transects I, J, and K in a band 1000 to 1200m away from the dike. More could be present further off-shore but no observations were made there. The sand swells are roughly 100m wide and are completely dry during low tide. The troughs on the other hand are filled with water. The islands with *pungens* are growing on the most landward sand swells. It is unclear why some swells are vegetated while others are not.

Algae



Figure F- 11 Algae covering islands of bulrush at location J

Location J:

Date: 01-07-16 11:51:58

Algae (sea lettuce/*ulva*) is a big problem on Sturgeon Bank. It washes in with the tide and gets trapped in the stems of the vegetation on the islands. Some areas were flattened and completely covered by the algae during the fieldwork.



Figure F- 12 Algae covering the leading edge at location K

Location K:

Date: 03-07-16 12:54:58

The algae can cover a surprisingly large area along the leading edge as well. At this particular location, the algae had almost reached the middle marsh.

Tidal channels



Figure F- 13 Tidal channel at location L

Location L:

Date: 05-07-16 13 11 24

Tidal channels are only found in the south of Sturgeon Bank. They do not extend all the way to the marsh but branch off into smaller channels that become shallower closer to shore. The sides of the channels are covered with shells and the banks are quite muddy in contrast to the sand bars that are located in the north.

Drainage

On the 3rd of July when measuring the transects I and J with GPS a strong wind blew from the west with speeds up to 40 km/h. Despite the low tide, a large portion of Sturgeon Bank from the leading edge up to 1.4 km from the dike remained inundated. Most of the water was pooling about 100 to 200m from the leading edge. As we moved further offshore the water depth gradually decreased. Inundation is therefore not only related to elevation. Instead inundation is influenced by a combination of elevation, wind, and drainage patterns. (See figure F-17 and figure F-18 for the elevation of the transect and the locations where water was (not) observed).

This has further implications for measurements carried out during low tide, as there is no guarantee that all the water has drained from the area. When methods like LIDAR are employed a layer of water can result in an overestimation of the elevation at the leading edge. When satellite images are used to estimate the marsh edge an underestimation could be made as the water will reflect some of the light and distort the reflection of the vegetation.

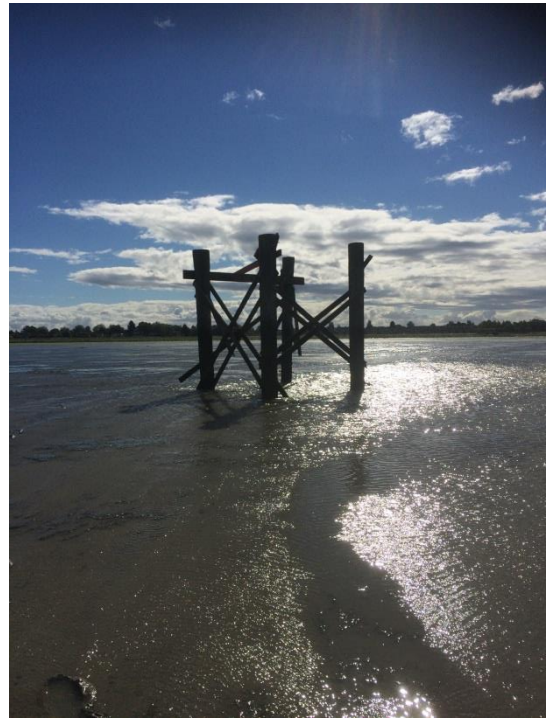


Figure F- 14 Looking landward 200m from the leading edge during a low tide and strong winds from the west

GPS measurements

Method

GPS measurements were carried on the 3rd and 4th of July in 2016. The instrument used is a GPS trimble that can record longitude, latitude, and elevation with an accuracy of 2 cm. Under the pole a small dish was attached to prevent the unit from sinking in the soft soil while recording the elevation.

FREMP transects I and J were surveyed at 50m intervals with additional points at locations of interest. The position of the FREMP sites had been established before and were clearly marked in the field by a set of stakes. The distance between the FREMP sites on the same transect is 200m so the additional points were determined beforehand by dividing the distance between the FREMP locations into 4. The original names of the FREMP sites were maintained and the new points were named as fractions (e.g. I2.25, I2.5, I2.75 for the points between FREMP sites I2 and I3).

Additional measurements of features of interest were determined on the spot. It was observed that a layer of water was maintained near the shore despite the low tide. The position where the layer of water was no longer observed was marked on each transect. Furthermore, sand bars and troughs were observed on transect J. If no predetermined location was close to the feature an additional point was measured.

Along Sturgeon Bank other features were measured as well. Three islands with vegetation located between transects I and J were measured for their location and elevation. Large islands were measured at multiple points to capture the location and elevation of the seaward edge, centre of the island and the landward edge.

The leading edge was measured at a handful of locations spanning both the north and south of Sturgeon Bank. The leading edge consist of several features including scarps, small channels, and clumps. Edges were measured at or near the edge of the marsh that extends continuously towards the dike. Small patches of vegetation were thus not counted as edge. If a scarp or clump was present, then the edge was measured at the lower elevation between them. The scarp was then measured separately. Clumps were present in front of the leading edge at a few locations. A number of clumps were measured near and further away from the edge.



Figure F- 15 A section of the leading edge with scarps



Figure F- 16 A clump in front of the leading edge

Results

Transects:

	Northing	Easting	GNSS Height [m]		Northing	Easting	GNSS Height [m]
12	5443970,311	485352,333	0,160	J1	5444778,948	485299,930	0,390
12.25	5443970,372	485302,988	0,093	J1.25	5444781,573	485250,207	0,131
12.5	5443970,432	485253,870	0,055	J1.5	5444784,336	485200,217	0,185
12.75	5443970,554	485204,920	-0,005	J1.75	5444787,005	485150,159	0,124
13	5443970,495	485155,720	-0,076	J.2	5444789,679	485100,202	-0,048
13.25	5443966,268	485105,442	-0,064	J.2.25	5444789,931	485049,476	0,013
13.5	5443962,129	485055,192	-0,114	J.2.5	5444790,407	484998,743	-0,026
13.75	5443958,073	485004,906	-0,064	J2.75	5444790,637	484947,889	-0,060
14	5443953,898	484954,712	-0,043	J3	5444791,139	484897,013	-0,136
14.25	5443953,951	484903,683	-0,043	J3.25	5444792,826	484846,243	-0,180
14.5	5443953,876	484852,777	-0,103	J3.5	5444794,553	484795,378	-0,230
14.75	5443953,754	484801,613	-0,133	J3.75	5444796,174	484744,826	-0,245
15	5443953,697	484750,501	-0,196	<i>Jdip</i>	5444796,062	484709,827	-0,390
15.25	5443954,898	484700,774	-0,224	J4	5444798,045	484693,738	-0,143
15.5	5443956,189	484650,852	-0,304	<i>Jdeep2</i>	5444798,125	484659,306	-0,532
15.75	5443957,359	484600,967	-0,376	J4.25	5444799,652	484644,243	-0,228
16	5443958,446	484551,072	-0,464	<i>Jtop</i>	5444801,242	484635,085	-0,284
16.25	5443956,585	484501,102	-0,520	J4.5	5444801,362	484594,692	-0,582
16.5	5443954,745	484450,895	-0,600	J4.75	5444803,022	484544,895	-0,586
16.75	5443952,868	484400,724	-0,642	<i>Jdeep</i>	5444804,918	484516,229	-0,842
<i>Idry</i>	5443952,184	484393,895	-0,612	J5	5444804,772	484495,242	-0,655
17	5443950,953	484350,623	-0,669	J5.25	5444806,775	484444,624	-0,740
				J5.5	5444808,608	484394,364	-0,823
				J5.75	5444810,773	484343,820	-0,901
				J6	5444812,829	484293,156	-0,987
				<i>Jdry</i>	5444816,822	484227,382	-1,009

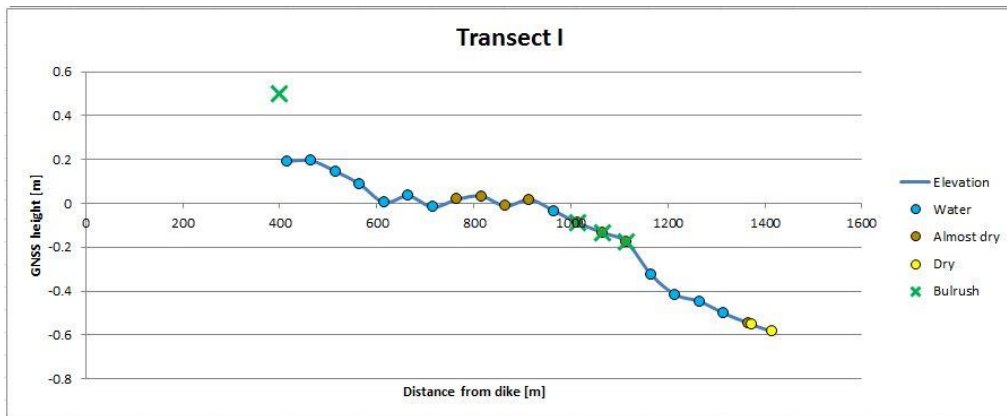


Figure F- 17 Elevation profile of transect I



Figure F- 18 Elevation profile transect J

Features

	Northing	Easting	GNSS Height [m]
Island 1:			
Seaward edge	5443855,392	484659,424	-0,302
Bare stretch	5443854,624	484666,189	-0,279
Middle	5443854,334	484676,193	-0,188
Pond	5443857,224	484683,088	-0,243
Behind pond	5443856,337	484689,168	-0,163
Landward edge	5443861,670	484705,746	-0,196
Island 2:			
Seaward edge	5443995,793	484788,883	-0,133
Middle	5443995,965	484790,640	-0,090
Landward edge	5443997,279	484794,306	-0,127
Island 3:			
Seaward edge	5444161,049	484834,346	-0,116
Middle	5444162,257	484839,905	-0,043
Landward edge	5444165,594	484845,465	-0,097

Patch 1:			
Middle	5442627.323	485263.081	0.29
Patch 2:			
Middle	5442657.277	485233.902	0.333
Leading edge 1:			
Edge	5444722,123	485344,562	0,414
Leading edge 2:			
Edge	5444657,633	485364,080	0,433
Scarp	5444657,677	485364,637	0,757
Leading edge 3:			
Edge	5444215,180	485370,955	0,354
Scarp	5444215,611	485371,336	0,571
Leading edge 4:			
Edge	5442565.916	485331.724	0.431
Leading edge 5:			
Edge	5442443.541	485345.846	0.549
Leading edge 6:			
Edge	5442454.156	485234.384	0.302
Leading edge 7:			
Edge	5442463.857	485243.898	0.319
Leading edge 8			
Edge	5443133.727	485416.691	0.381
Scarp	5443134.172	485416.83	0.719
Clump 1:	5443101.006	485395.492	0.543
Clump 2:	5443105.139	485385.057	0.535
Clump 3:	5443110.062	485384.383	0.515
Clump 4:	5443120.403	485382.867	0.5
Clump 5:	5443141.785	485377.294	0.452
Channel 1:			
Right bank	5443099.093	485409.04	0.44
Right bottom	5443098.652	485408.748	0.357
Middle	5443096.39	485409.662	0.392
Middle 'solid'	5443096.784	485409.204	0.164
Left bottom	5443095.684	485412.161	0.39
Left bank	5443095.426	485412.414	0.517
Channel 2:			
Right bank	5442948.679	485387.638	0.581

Right bottom	5442948.103	485387.949	0.439
Middle	5442947.177	485388.313	0.447
Middle 'solid'	5442947.169	485387.973	0.247
Left bottom	5442946.485	485389.105	0.465
Left bank	5442946.09	485389.873	0.505
CBC radio tower pier			
At leading edge	5442830.949	485309.15	0.37
Middle of the pier, north side	5442852.036	485268.809	0.309
Middle of the pier, south side	5442837.091	485262.775	0.183
Tip of the pier, north side on clump 1	5442862.377	485236.504	0.344
Tip of the pier, north side on clump 2	5442875.106	485220.191	0.248
Tip of the pier, north side between clumps	5442875.358	485213.6	0.102
Southwest of the pier at cable anchor	5442829.556	485143.197	-0.018

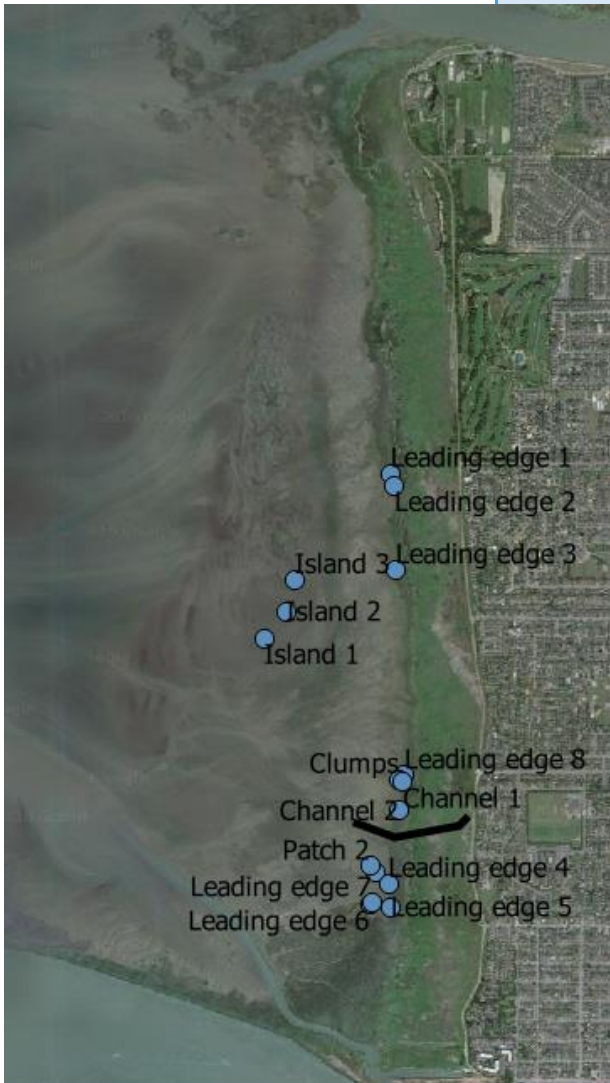


Figure F- 19 Locations of measured features

Sediment retrieval

A piston sampler was used to collect cores from the surface up to a depth of 16 cm. The cores were then placed on a plastic tube to inspect and document the retrieved sample. Finally, the samples were sealed in a plastic container and sent for transport to the lab a few days later.

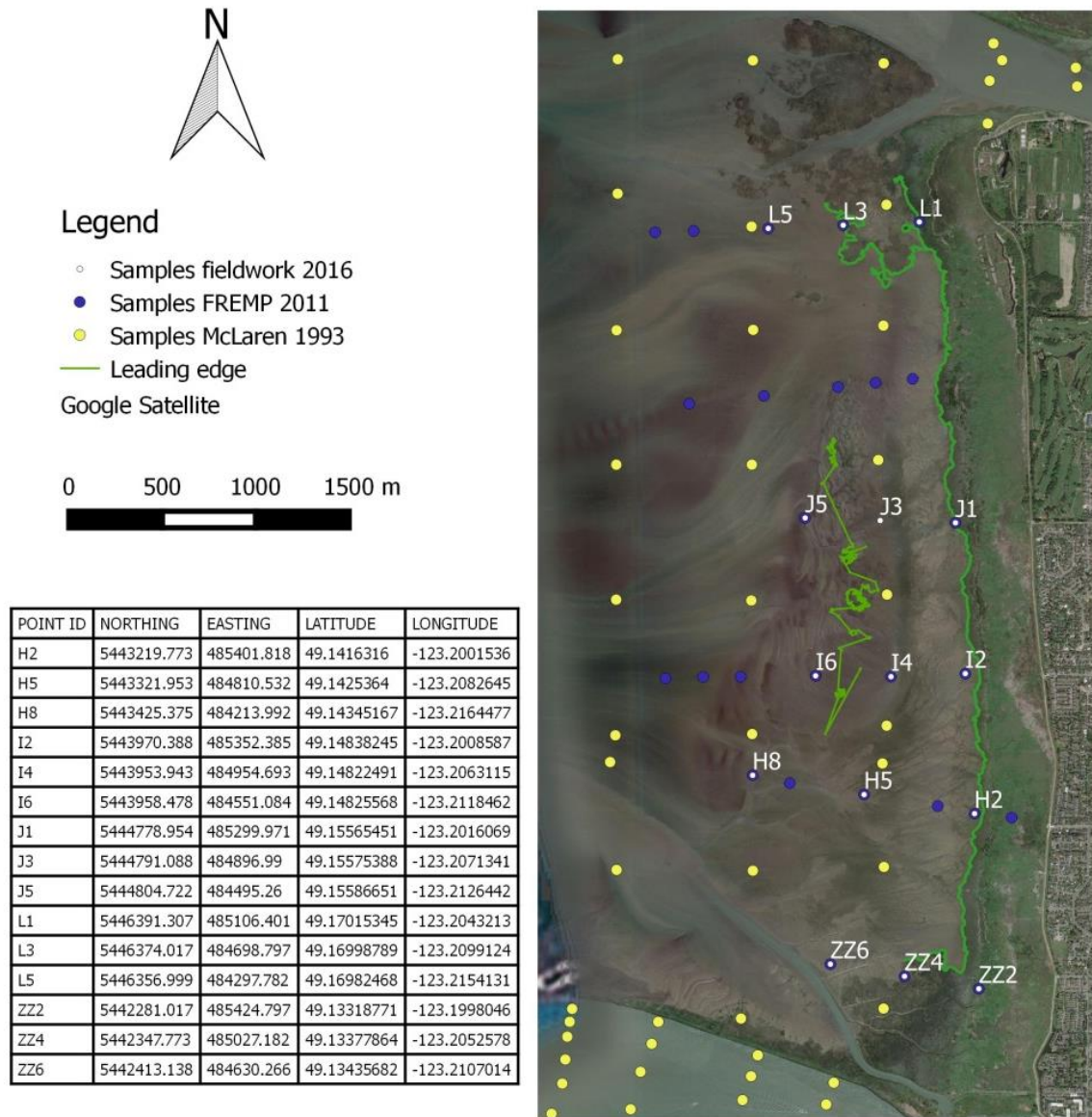


Figure F- 20 Sediment sample locations



Figure F- 21 Sample L1

The actual FREMP stakes could not be found within the marsh vegetation. Instead the sample was taken near the radar tower on the L transect which is quite close to the reported FREMP L1 site.

This sample was taken within the marsh. The core is brown on the surface and black further down. Most of it is fine mud.



Figure F- 22 Sample L3

L3 was at the marsh edge and shows a similar profile as L1. It is brown near the surface and black further down



Figure F- 23 Sample L5

L5 is browner overall and the top is siltier than on L1 and L3.



Figure F- 24 Sample J1

J1 was taken just within the leading edge between the marsh vegetation. The core was very soft and fragile. It is most like composed of very fine mud.



Figure F- 25 Sample J5

Sample J5 was taken on one of the sand bars. It shows a large contrast with J1 as it is composed of coarse sand and even contains some shells.



Figure F- 26 Sample I2

Sample I2 was taken just in front of the leading edge. Like J1 it was very fragile and soft. The top is slightly brownish.



Figure F- 27 Sample I4

Sample I4 was taken in between the sand bars and the leading edge. The top is much siltier than at I2.



Figure F- 28 Sample I6

Sample I6 was taken just beyond the islands with pungens and is more solid than I2 and I4. The top is definitely sandier.



Figure F- 29 Sample H2

Sample H2 was taken at the leading edge of the H transect very close to a clump that contains dead roots. The sample is soft and is most likely composed of fine mud.



Figure F- 30 Sample H5

For its location, it was muddier than expected. H5 almost had a rubbery feel to it. It is likely to be a combination of mud and silt.



Figure F- 31 Sample H8

H8 was just beyond one of the tidal channels. Landward of the channel the soil had been muddy whereas on this side of the channel it felt sandier. The core shows a sandy top soil with a muddier layer underneath it.



Figure F- 32 Sample Z4

Z4 was at the leading edge in the south of Sturgeon Bank. Several smaller branches of the tidal channel had to be crossed to reach this location from Z6. The soil was quite muddy but didn't feel as soft as the leading edges of J and I.



Figure F- 33 Sample Z6

The location of Z6 was located between 2 branches of the tidal channel. The sample was quite muddy. The top is brownish and gradually becomes more black further down.

G. APPENDIX 7: SEDIMENT ANALYSIS

Procedure

The sediment samples were transported to the lab in the Netherlands where they were analysed. The transport took several days so first the samples were inspected for any damage or loss during transport. After inspection, the samples were separated into pure mud samples and courser samples. Sample H5 was added to the mud samples as a reference.

The sand/silt samples were analysed by sieving. First the samples were dried. Then the fines were removed from the sample by wet sieving over a 40 μm sieve. After drying the samples were sieved and weighed to arrive at the grain size distribution.

The mud from the mud samples is too fine for a sieve analysis. A different procedure was used to

measure the grainsizes. A sedimentation test with hydrometer was used for these samples. Samples needed to be treated before the test could be performed. Organic material was removed with hydrogen peroxide and sand particles were removed by sieving. The fines left were mixed with water and brought in suspension within a glass cylinder. The density of the mixture was measured at different intervals with a hydrometer. The method determines the grain sizes with Stokes' law which relates the particle settling velocity to the grain size.

Finally, an analysis was performed with laser diffraction. The sample is mixed with water and pumped through a tube. A set of lasers positioned along the tube measure the light

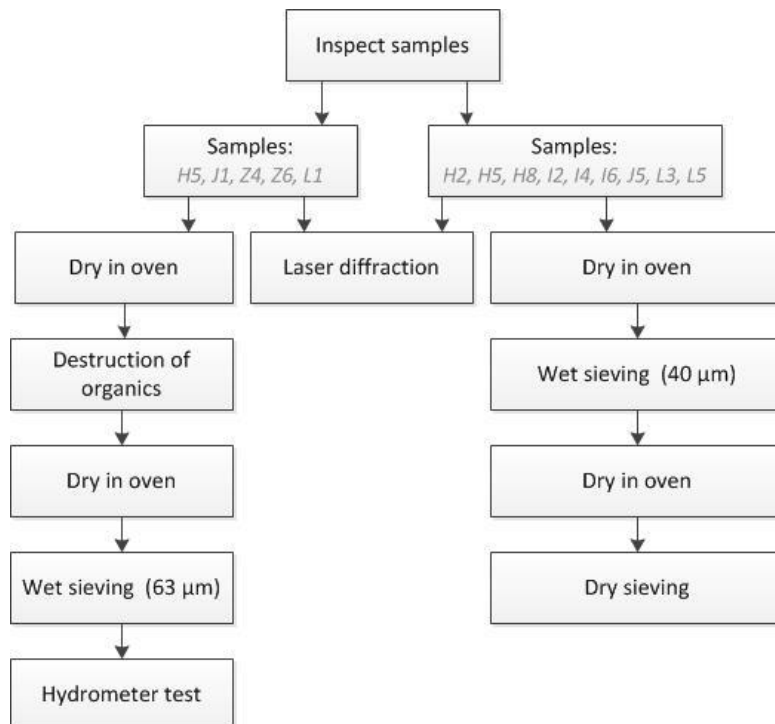


Figure G- 1 Setup of the experiments

obstruction by the particles. From the obstruction, the grain size is calculated.

Each of the procedures described is explained more detail in the sections below.

Treatment

Only drying and destruction of organic material was necessary for the procedure. Drying of the samples was done by leaving the samples in an oven at 107 °C overnight.

Destruction of organic material was done by putting the soil with 200 ml of demineralized water in a glass cylinder. The cylinders were placed in a water bath with a constant temperature. At regular 1 hour intervals, the H₂O₂ solution was added to the soil until no reaction was taking place. The solution of water and H₂O₂ was drained and the rest of the sample was put back in the oven to dry.

Sieving

Sieving was carried out in two stages. First the fines were removed from the sample by putting the sample onto the sieve with the smallest mesh (40 µm) and wash out the fines with tap water. Afterwards the sample are dried for the second stage.

After wet sieving the samples are placed onto a sieve tower with the sieves of sizes 710 µm, 500 µm, 355 µm, 250 µm, 180 µm, 150 µm, 125 µm, 106 µm, 90 µm, 75 µm, 63 µm, 53 µm and 40 µm. The sieve tower was shaken for 15 minutes and the soil on each sieve was weighed.

Hydrometer

After the required treatment, the soil was wet sieved on a 63 µm sieve. The fines with sizes smaller than 63 µm were placed in a glass cylinder

filled with demineralised water. The cylinder was shaken to suspend the fines in the water and then placed in a water bath to maintain a constant temperature. A calibrated hydrometer was placed at the water surface to measure the density of the suspension after 30 s, 1 min, 2.5 min, 4 min, 8 min, 30 min, 2 hours, 8 hours, and 24 hours.

Laser diffraction

From the sample about 2 grams of soil was brought in suspension in a small beaker. The suspension was pumped through the particle sizer (type Mastersizer Hydro 2000E). From each sample 2 tests were carried out. After each test the tubes were rinsed with demineralised water.

The particle sizer could not be calibrated to the specifications. It was suspected that either dirt or a scratched lens in the sizer affected the readings. The laser diffraction was carried out for only four samples and compared to the results from the sieve analysis to check the reliability.

The initial results showed strong deviations from the results of the sieve analysis. Also, the variation within the measurements was quite high. The insufficient calibration, the limited size of the sample as well roots within the sample all negatively affected the results. It was decided to discontinue tests with laser diffraction.

Results

Water content

Table G- 1 Water content of the received samples

Sample	Weighed wet [g]	Weighed dry [g]	Mass of water [g]	Water content [%]
H2	119.28	85	34.28	29%
H5	124.67	95.99	28.68	23%
H8	119.28	95.62	23.66	20%
I2	77.74	57.78	19.96	26%
I4	71.88	57.8	14.08	20%
I6	115.35	92.05	23.3	20%
J1	75.75	47.25	28.5	38%
J5	94.46	76.21	18.25	19%
Z4	114.82	81.17	33.65	29%
Z6	115.82	82.29	33.53	29%
L1	78.45	48.8	29.65	38%
L3	107.92	83.35	24.57	23%
L5	115.18	91.06	24.12	21%

Organic material

Table G- 2 Organic content of received samples

Sample	Before treatment [g]	After treatment [g]	Organic material [g]	Organic content [%]
H5	53.02	52.47	0.55	1%
J1	33.16	31.99	1.17	4%
Z4	31.7	31.38	0.32	1%
Z6	30.92	30.48	0.44	1%
L1	31.12	29.75	1.37	4%

Particle size distribution

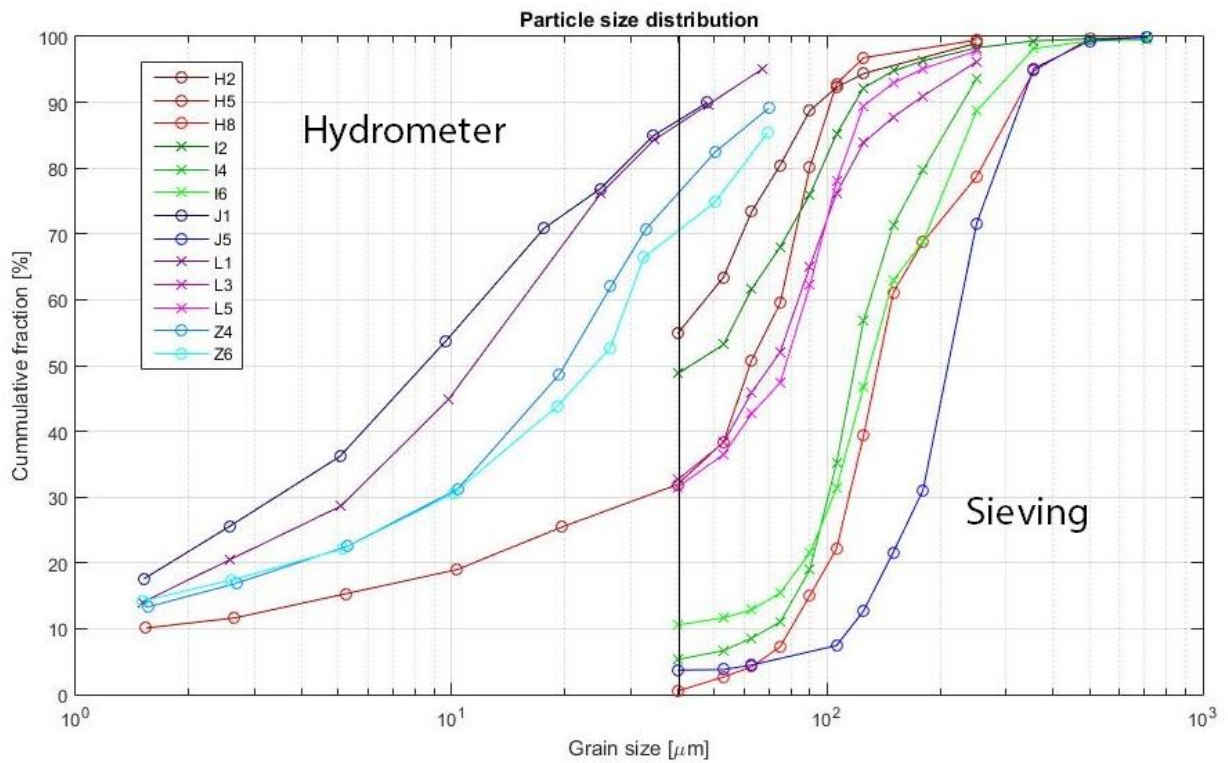


Figure G-2 Particle size distributions

Table G-3 Grain fractions of the samples in micrometres

	Nominal grain sizes in µm												
	H2	H5	H8	I2	I4	I6	J1	J5	L1	L3	L5	Z4	Z6
D₁₀			80		70			115					
D₂₀		12	101		91	86	2	145	2				4
D₃₀		34	115		101	104	4	177	5			10	10
D₄₀		54	126		110	117	6	195	8	55	59	15	17
D₅₀		62	137	44	119	130	9	213	12	71	78	20	24
D₆₀	48	75	149	61	131	145	13	230	17	84	88	26	30
D₇₀	60	83	189	79	148	184	17	247	22	97	98	32	40
D₈₀	74	90	258	97	181	219	29	287	30	115	109	47	60
D₉₀	96	102	324	119	232	264		332	49	171	129		

Laser diffraction distributions

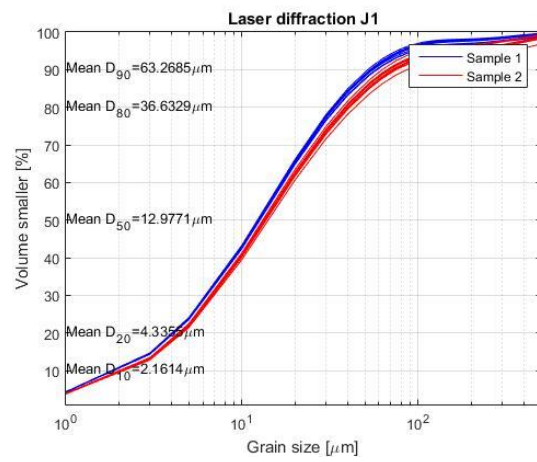
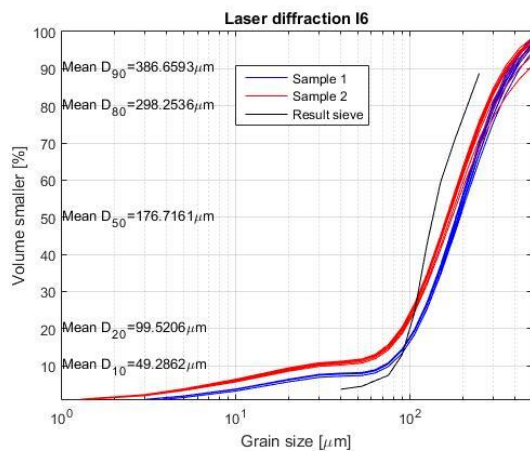
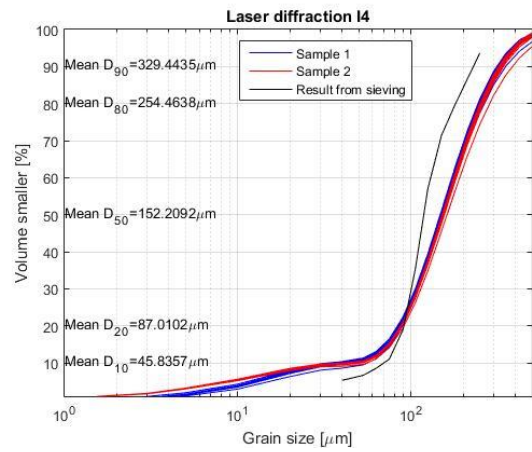
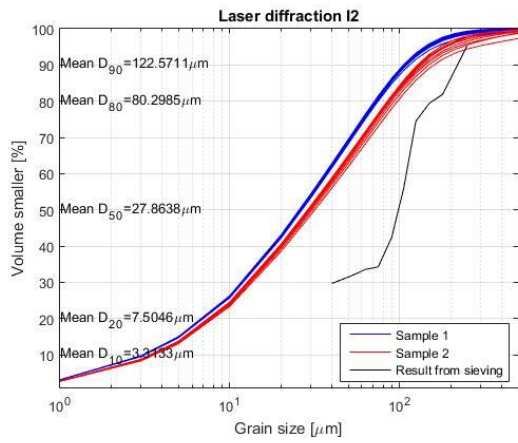


Figure G-3 Particle sizes measured by laser diffraction

H. APPENDIX 8: FLOW MODEL

Model description

In the previous chapter, it was concluded a flow model was needed to properly evaluate the hypotheses. Delft-3D is a numerical program that simulates the flow of water by solving the depth-averaged Navier-Stokes equations at different points in time. The rigid vegetation module in Delft-3D was used to simulate the roughness imposed by the marsh and bulrush islands. A detailed description of the software can be found in the user manual (Deltares, 2014).

Model domain

The model domain extends roughly three quarters of the tidal flats. In the east, the model is bounded by the dike, in the south by the Steveston jetty and in the north east partially by Swishwash island. The domain was chosen such that the flow over a long stretch of tidal flats leading up to the marsh is modelled and drainage to in middle arm of the Fraser would be included.

The model domain was decomposed into 2 sections. The first section is only used to model how the tide travels across the flats. The grid size in this section could be made quite coarse in the order 90x90m grid cells. To simplify the calculations a 2D depth averaged approach was adopted so the domain was not gridded in the vertical.

The second section models the flow over and around the sand swells and in and out of the channels. Because of this a very fine mesh had to be applied of 12x12 m, 7.5 times smaller than the first section. Like in the first section no vertical layers were implemented.

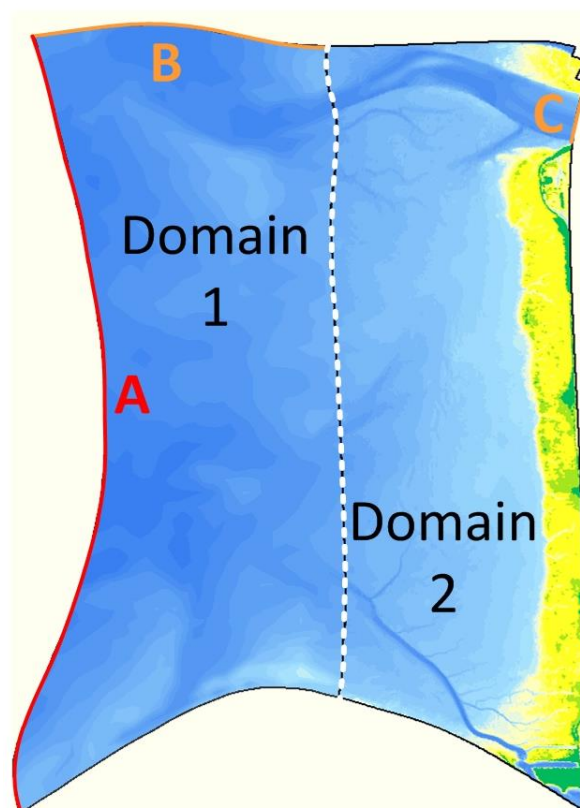


Figure H- 1 Model domains and boundaries. A is a water level boundary, B and C are Neumann boundaries. The dotted white dotted line shows the boundary between the 2 domains

The bathymetry from the 2013 Lidar measurements was imported onto the grid. For the coarse domain the points the depth in each grid cell was obtained by averaging while for the fine grid additional points needed to be generated through interpolation. The resulting bathymetry is shown in Figure H- 1.

Time frame

The time frame of each simulation is about 3 days. The first day is used for spin-up after which 2 full tidal cycles can be used for results. The time scale is short with only 1 minute which is enough to resolve the different stages of the tide.

Processes

The model resolves the water levels and flow velocities within the domain. On top of hydraulic forcing other factors were included as well. The wind was included in the model. Wind speed and direction were taken directly from measurements at the Sand Heads station.

Vegetation was included through the rigid vegetation model that was implemented. The location of the marsh edge and bulrush islands were taken from recent GPS field measurements (Mason, 2016, *pers. com.*). The stem densities assumed in the model were based on measurements by Boyd et al. (*Unpublished*). It is assumed that the bulrush islands have stem densities of on average 75 stems/m². The inner marsh is assumed to have densities of 150 stems/m². Channels and depressions within the marsh were made less dense by scaling the stem densities to the elevation. The average diameter and height of bulrush is assumed to be 40 cm with a diameter of 4mm that tapers off towards the end.

A number of processes were omitted to reduce the computational effort for the calculations. This was necessary in order to complete all the computations within the available time.

Morphology was not included. The current research shows very little morphological change is expected to occur unless extreme conditions are modeled (Feeney, 1995) or decadal time scales are modeled. Neither was carried out in order to keep the computational time manageable.

Waves were not included as the intention of the model is to calculate the flow patterns. A separate

simpler model for waves was already introduced which suffices for the current research questions.

Density differences were omitted since initial tests showed salinities across the domain simply become the salinity imposed at the western boundary. The discharge of the middle arm is neglected as well as discharges through gaps in the jetty and through Garry Slough and thus the western boundary is the only one with in/outflow of salinity concentration (see boundary conditions).

Initial and boundary conditions

Only one initial condition needs to be specified for the flow model which is water level. The initial water level within the entire domain is equal to the first water level specified at the tide boundary. This way instabilities during the spin-up of the model are avoided.

Three boundaries are defined within the model: a tide boundary in the west (A), a Neumann boundary in the north (B) and a Neumann boundary in the east (C) (Figure H- 1).

Boundary A represents the tide further out on the flats. The boundary was taken along the deep part of the flats which is where the tide is expected to arrive first. The water levels imposed are taken directly from measurements from the point Atkinson station. Because this station is about 20 km to the north there is a slight error in time lag and amplitude expected between the modelled tide and the actual tide.

Boundary B is set at the middle of the Middle Arm of the Fraser where it splits in a section that goes north around Swishwash island (not in the

model) and a section that goes south around the island. The boundary allows the part of the incoming tide that would curve north to leave the domain. If not included a concentrated flow would be generated along the boundary of the model. This boundary was only implemented in domain 1 since the island is included in domain 2. Only a very limited flow is expected perpendicular to the direction of the Middle Arm across the island so a closed boundary is justified.

Boundary C is at the eastern end of the domain where the Middle Arm flows south of Swishwash island. There are no measurements from this part of the river. Of the flow from the Fraser river 88% flows through the Main and only 12% through the North Arm (Milliman, 1980). The Middle Arm is a small offshoot from the North Arm. The North Arm is dredged for navigation and carries the majority of the discharge. The remaining discharge through half of the Middle Arm is expected to be so small that it will not have a significant effect on the propagation of the tide. When the tide is low the river will stay within the banks of the Middle Arm and thus not affect the flow on Sturgeon Bank. Because of these considerations, the boundary was set as a Neumann boundary where the tide can flow out of the domain but no discharge into the domain is modelled.

Additional boundaries were considered but not implemented. The jetty is a closed structure in the model. The gaps are so small that only a limited exchange of water is expected and will not affect the general flow patterns. For the same reason the end of the tidal channel at Garry Slough is closed as well.

Table H- 1 Physical and numerical parameters

Hydrodynamic:		
Gravity:	9.81	m/s ²
Water density	1025	kg/m ³
Air density	1	kg/m ³
Wind:		
Drag coefficient	0.00063	-
Wind speed	Time series	m/s
Wind direction	Time series	Degrees
Roughness (Chezy):		
Sand	65	m ^{1/2} /s
Mud	90	m ^{1/2} /s
Viscosity:		
Hor. eddy viscosity	1	m ² /s
Numerical:		
Threshold depth	0.075	m
Marginal depth	999	m
Smoothing time	30	min

Physical and numerical parameters

Most of the parameters were set at default values. Only the parameters adjusted for the model will be discussed. A complete overview of the parameters and values is given in Table H- 1.

Bottom roughness was adjusted within the domain to reflect the areas with mud and the areas with sand. Because the slope on Sturgeon is so shallow it is expected that a variation of roughness could cause water to pool slightly at edge with sand. The muddy and sandy areas were determined from sediment studies (see section 8.4). The area in between sand and mud was filled in by a gradient between the two roughness values for mud and sand.

The threshold depth is the depth below which a computational cell is considered dry. Dry cells are

not used in the next computational time step as to prevent water depths from becoming negative. If this occurs the computation will become unstable. In order to capture as much of the flooding and drying process on the bank the value was adjusted as far down as possible. Simulations with multiple threshold values showed that 7.5 cm was the minimum threshold that could be used without the computation becoming unstable.

The marginal depth was increased to 999 m. This changes the scheme to calculate the water depth at cell faces and not use the mean value in the cell centre. The reason is that small variations in water depth on a shallow slope could be important for the overall flow patterns.

Validation

Even though many measurements and observations have been carried out there was little data measured that could be used to validate the flow model. Two field observations were used to validate the model: the time at which the tide reached the FREMP stakes at 2 transects on the 18th of July (Balke, 2016, *pers. com.*) and my own observations of where water was (not) present on the 3rd of July of 2016.

Tide progression

First the time of the rising tide at the FREMP locations was tested. On the 18th of July, the wind came from the south at moderate speeds increasing from 5 to 7 m/s between 14:00 and 16:00. At the time the water level was rising from 0.96 m+CD at 10:30 to 4.38 m+CD at 18:00 (measurements at point Atkinson).

The model has a time lag of about 1 hour with the

Table H- 2 The observed rising tide and predicted rising tide at the FREMP locations on the 18th of July 2016. Tides observed by Erik Balke and Derek Hogan

Location	Observed Time [hh:mm:ss]	Predicted Time [hh:mm:ss]	Difference [hh:mm:ss]
K9	14:27:22	13:25:00	-1:02:22
K8	14:44:43	13:45:00	-0:59:43
K7	14:59:02	14:05:00	-0:54:02
K6	15:05:05	14:00:00	-1:05:05
K5	15:07:15	14:05:00	-1:02:15
K3	15:39:20	14:40:00	-0:59:20
K2	16:00:52	15:10:00	-0:50:52
J7	14:22:00	13:20:00	-1:02:00
J6	14:32:00	13:30:00	-1:02:00
J5	14:57:00	14:00:00	-0:57:00
J4	15:34:00	14:35:00	-0:59:00
J3	15:41:00	14:45:00	-0:56:00
J2	15:59:00	15:05:00	-0:54:00
		Mean error	-58.74 min
		Std. dev.	4.14 min

field measurements. This can easily be explained by the fact that the boundary is not located at the deep end of the Strait of Georgia (100 m depth) but 3 km further onto the flat where water depths are already much smaller (in the order of 3m at MWL).

The time difference between subsequent FREMP location is more important as it shows the progression of the tide over the flats. When these are compared, the model shows good accuracy. The standard deviation between the observed and predicted time of the rising tide is only 4 minutes.

There is a tendency of the time difference decreasing at the more shoreward locations. The tide in the model propagates slightly faster in the

model than in reality. This could again be the result of the difference in location between the boundary and the actual measurements or the bottom roughness being lower in the model than in reality.

Pools at low tide

On the 3rd of July 2016, a large area remained inundated at low tide between 11:00 and 12:00. These findings are described in sections 6.1 and 6.2. Inundation is clearly not only governed by elevation alone. The model should be able to reproduce the longer inundation. The observations of that day are an opportunity to test this.

The wind speed previous to the low tide had been a strong 12 m/s from the north west and was slowly declining during the day. The low tide was one of the lowest of the entire summer at 0.46 m+CD at 10:30. The high water at the end of the day would reach 4.55 m+CD around 18:00 (values at point Atkinson). This day had combination of an exceptionally strong tide and a strong north western wind.

Because the model could only simulate up to a water depth of 7.5 cm it was not possible to determine which areas stay inundated with water depths below this point. Only the bigger pools with depths equal or than 7.5 cm could be predicted. Whenever the water depth goes below this point no flow is calculated and the water depth remains fixed until the next high tide. In Figure H- 2 and Figure H- 4 it can be seen that at the end of the simulation the entire bank still has water depths below the threshold depth. In reality the water would continue to run off at the surface

by the wind or small elevation gradients to collect in ponds.

Validation based on inundation was no longer possible. The model did predict pools deeper than 7.5 cm forming within 500 m from the marsh edge. According to the observations more pools have formed the 3rd of July due to the wind than on an ordinary day. Qualitatively the number of pools should increase most by including wind into the model.

The influence of the wind was compared to the other processes in the model. First a simulation with only the tide was carried out. Then a simulation with a process or combination of processes was carried out. The remaining water depth at low tide from the simulation with a process switched on was subtracted from the tide only simulation. There where water depths had increased by more than 2 cm a contour around the pool is drawn.

Figure H- 2 shows the combination of tide and bathymetry is already responsible for most of the pools forming. By including all processes the big pools still remain and a number of smaller additional pools are predicted (Figure H- 4). Most of these pools were indeed caused by wind (Figure H- 3). Roughness differences only slightly affected the pools seaward of the sand swells. Vegetation was found to redirect the water more efficiently towards the channels in the south and the gaps between the sand swells (the cyan wind + vegetation in Figure H- 3 overlaps almost all green lines of vegetation only).

The combination of wind and vegetation shows most resemblance to the made observations.

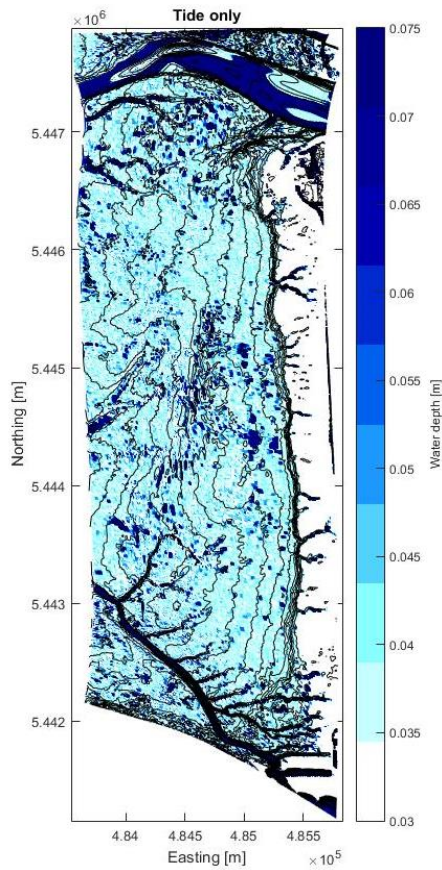


Figure H- 2 Pools when only the tide is simulated

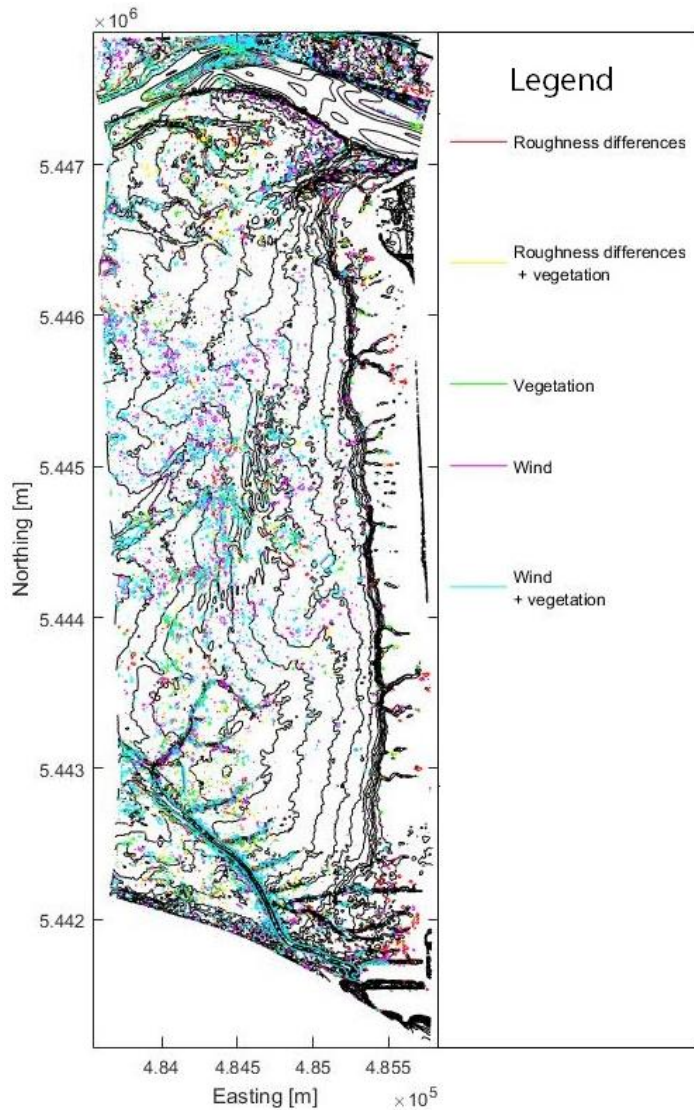


Figure H- 3 Contours of 2cm increased pool depth as a result of including more processes with the tide.

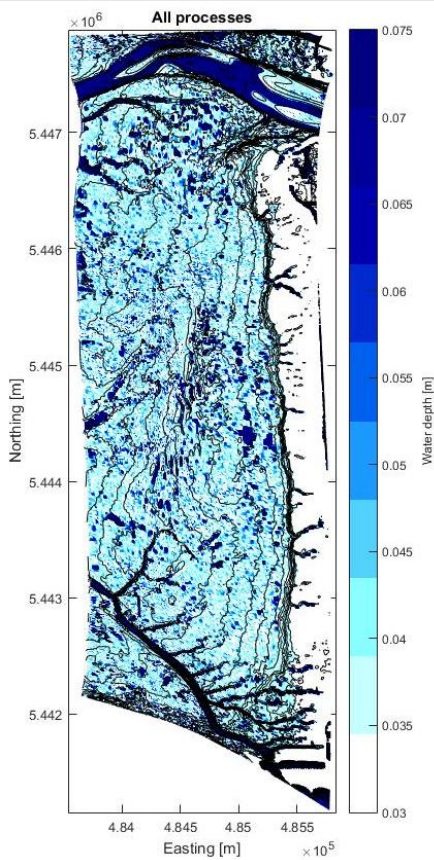


Figure H- 4 Pools when all processes are simulated

Conclusion

The model cannot be validated for inundation. It does show an increase of deeper (>7.5 cm) pools yet this not sufficient for this study to determine actual submergence time of plants. The model does show agreement with field measurements of the incoming tide if the 1-hour time lag between the deep Strait of Georgia and the model boundary 3km further out on the flats is accounted for.

I. APPENDIX 9: WAVE MODEL

Equations

The model calculates the wave height across the bank from the wave energy. The change in wave energy follows from the energy balance equation. When assumed that the waves travel in the same direction across the bottom (i.e. refraction and diffraction are ignored) it is:

$$\text{Eq. I-1} \quad \frac{\partial E}{\partial t} + \frac{\partial c_g E}{\partial x} = D$$

$c_g = \text{wave group velocity} \left[\frac{m}{s} \right]$
 $E = \text{wave energy} \left[\frac{J}{m^2} \right]$
 $D = \text{dissipation rate} \left[\frac{J}{m^2 s} \right]$

When time averaged the equation simplifies to:

$$\text{Eq. I-2} \quad \frac{\partial c_g E}{\partial x} = D$$

From the wave energy the wave height is related through linear wave theory as:

$$\text{Eq. I-3} \quad E = \frac{1}{8} * \rho g * H^2$$

$\rho = \text{density of water} \left[\frac{kg}{m^3} \right]$
 $g = \text{gravitational accelration} \left[\frac{m}{s^2} \right]$
 $H = \text{wave height} [m]$

It is assumed wave energy is dissipated only wave breaking. This dissipation is calculated by:

$$\text{Eq. I-4} \quad D_w = \frac{1}{4} Q_b \alpha \frac{\rho g}{T} H_{max}^2 \quad (\text{Battjes \& Janssen, 1978})$$

$D_w = \text{dissipated energy} \left[\frac{J}{m^2} \right]$
 $Q_b = \text{Fraction of breakers} [-]$

Where:

$$\text{Eq. I-5} \quad H_{max} = \gamma * h$$

$H_{max} = \text{Maximum wave height} [m]$
 $\gamma = \text{Breaking parameter} [-]$
 $h = \text{Water depth} [m]$

$$\text{Eq. I-6} \quad Q_b = \exp \left(- \left(\frac{H_{max}}{H_{rms}} \right)^2 \right) \quad (\text{Baldock et al., 1998})$$

$Q_b = \text{Fraction of breakers} [-]$

Finally, the wave group velocity can be calculated with the formulae from linear wave theory:

$$\text{Eq. I-7} \quad L = \frac{2\pi g}{L} \tanh \left(\frac{2\pi h}{L} \right)$$

$$\text{Eq. I-8} \quad k = \frac{2\pi}{L}$$

$$\text{Eq. I-9} \quad \omega = \frac{2\pi}{T}$$

$$\text{Eq. I-10} \quad c = \frac{\omega}{k}$$

$$\text{Eq. I-11} \quad n = \frac{1}{2} \left(1 + \frac{2kh}{\sinh(2kh)} \right)$$

$$\text{Eq. I-12} \quad c_g = n * c$$

$$L = \text{Wave length} [m]$$

$$k = \text{Wave number} \left[\frac{1}{m} \right]$$

$$\omega = \text{Radial frequency} \left[\frac{1}{s} \right]$$

$$T = \text{Wave period} [s]$$

$$c = \text{Wave celerity} \left[\frac{m}{s} \right]$$

Numerically the equations are implemented as follows. First the domain is defined by the bottom profile. The depth is defined. At the seaward boundary (x=0) the water level, wave height and wave period are defined. The water depth is the difference between the water level and the bottom profile.

Equations I-3 to I-12 are solved first at the point in the domain. Then the wave energy at the next point Δx m further is calculated by schematizing Eq. I-4 according to the midpoint rule:

$$\text{Eq. I-13} \quad E(x + \Delta x) = \frac{\left[E(x)c_g(x) - \frac{D(x + \Delta x) + D(x)}{2} \Delta x \right]}{c_g(x + \Delta x)}$$

When the wave energy is calculated from equation I-13 the wave height is calculated at that point from equation I-4. The process is repeated for each point on the grid until the landward edge is reached.

Input

The model needs the water level, seaward wave height, wave period, bottom profile and breaking

parameter. The water level was taken from the tidal analysis. The wave height and period were taken based on measurements of a wave buoy at Sturgeon Bank in 1976. The bottom profile could readily be imported from a transect of the 2013 Lidar measurement. Finally the breaker parameter was set to 0.55 following considerations in Nelson (1987) for mild slopes.

```
%%
%Script adapted from
https://svn.oss.deltares.nl/repos/openearthtools/trunk/matlab/applications/CoastalMorphology
Modeling/ProfileModel/balance_ld.m
%% Input section
Hrms0=2;
Tp=7;
%water levels;
CD=-3.10;
MWL=3.10+CD;
MHHW=4.48+CD;
MLHW=3.91+CD;
MHLW=2.96+CD;
eta0=[MHHW, MLHW, MWL, MHLW];

TideNames={'MHHW', 'MLHW', 'MWL', 'MHLW'};

gamma=.55; %breaker parameter[-]
rho=1025; %water density [kg/m^3]
hmin=0.01; %minimum calculation depth [m]
Emin=0.1; %minimum wave energy [J/m^2]
%bottom profile from file
INPUT=csvread('LidarProfileJ.csv');
zb=INPUT(:,2);
x=INPUT(:,1);
gamma=ones(length(x),1).*gamma;

%% Loop for each different tide level
for jj=1:length(eta0)
    %% Initialise arrays
    eta=zeros(size(x));
    E=zeros(size(x));
    Hrms=zeros(size(x));
    Qb=zeros(size(x));
    Dw=zeros(size(x));
    eta=zeros(size(x));
    h=zeros(size(x));
    k=zeros(size(x));
    C=zeros(size(x));
    Cg=zeros(size(x));
    Sxx=zeros(size(x));

    %% Set boundary conditions
    eta(1)=eta0(jj);
    h(1)=eta(1)-zb(1);
    E(1)=1/8*rho*9.81*Hrms0^2;
    Hrms(1)=Hrms0;
    %% Step 1
    i=1;
    [k(i), ome(i), c(i), n(i), cg(i), Dw(i)] = WaveChars(h(i), Tp, Hrms(i), gamma(i), rho );
    Sxx(i)=(2*n(i)-0.5)*E(i);

    %% Start loop in x-direction
```

```

for i=2:length(x)
    %First estimate of eta(i+1),E(i+1),Er(i+1)
    eta(i)=eta(i-1);
    E(i)=E(i-1);
    dx=abs(x(i)-x(i-1));
    %% Two-step integration scheme
    for step=1:2;
        h(i)=eta(i)-zb(i);
        %% Check if h>hmin; otherwise leave parameters zero
        if h(i)>hmin && E(i)>Emin
            %local wave parameters
            [k(i), ome(i), c(i), n(i), cg(i), Dw(i)] = WaveChars(h(i), Tp, Hrms(i),
gamma(i), rho );
            % Wave energy
            E(i)=(E(i-1)*cg(i-1)-(Dw(i-1)+Dw(i)*dx)/2)/cg(i);
            Sxx=(2*n-0.5)*E(i);

            %Water level and wave height
            eta(i)=eta(i-1)+(-2/(rho*9.81*(h(i)+h(i-1))))*(Sxx(i)-Sxx(i-1))/dx;
            Hrms(i)=sqrt(8*E(i)/rho/9.81);
        end
    end
end

end
%% Plot results
...
end

```

Figure I- 1 Source code of the wave model

```

function [k, ome, c, n, cg, Dw] = WaveChars(h, T, Hrms, gamma, rho )
%WAVECHARS Summary of this function goes here
% Detailed explanation goes here
%wave parameters
k=dispersion(h,T);
ome=2*pi()/T;
c=ome/k;
n=1/2*(1+(2*k*h)/sinh(2*k*h));
cg=n*c;

%dissipation
Hmax=gamma*h;
Qb=exp(-(Hmax/Hrms)^2);
Dw=0.25*Qb*rho*9.81/T*Hmax^2;
end

```

Figure I- 2 Function to calculate wave group velocity and dissipation

J. APPENDIX 10: SAND SWELLS ON STURGEON BANK

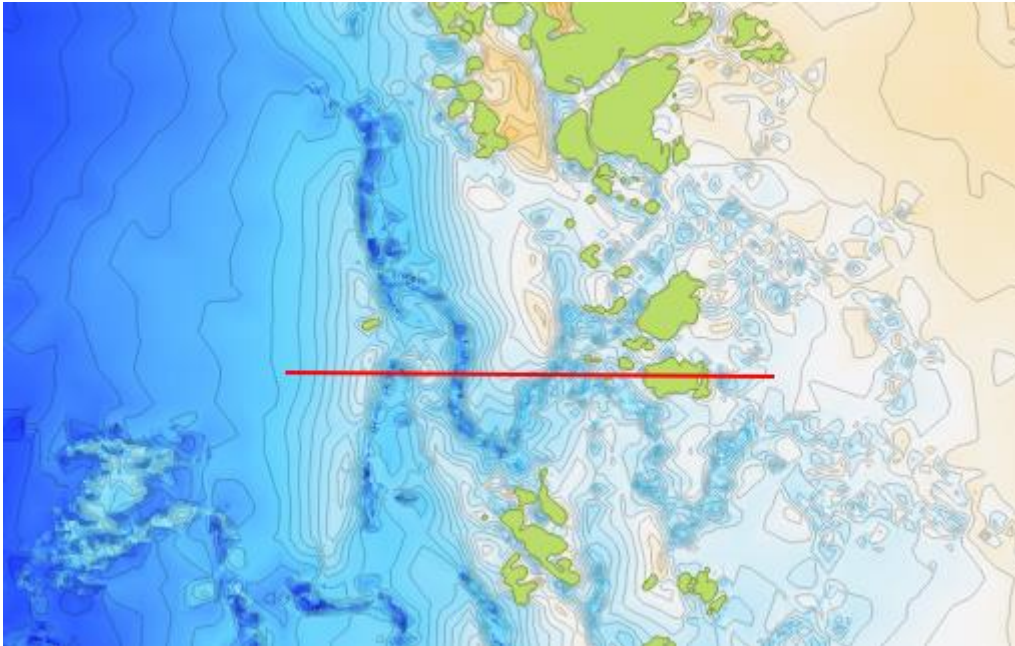


Figure J-1 Sand swells on the bathymetry

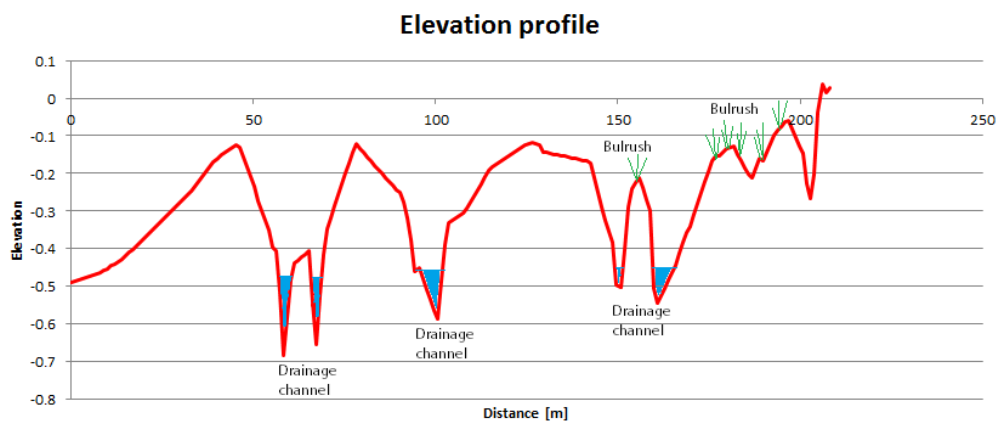


Figure J-2 Elevations on the transect from Figure J-1

Characteristics:

- Asymmetric
- Height: 0.3-0.5m
- Wave length: 50m-70m
- Composed of sand with $D_{50}=210 \mu\text{m}$ and $D_{90}=330 \mu\text{m}$
- Water depth: 0 at low tide, 2-3m at high tide
- Troughs act as drainage channels
- Landward crests colonized by bulrush (type of marsh plant)
- Very stable. Movement only visible on decadal time scale or bigger.

	critical shear velocity	Average flood velocity	Average ebb velocity	Max 1min averaged velocity	Max. velocity (wave +current)	Fraction of measurements $u > u_{cr}$
S12	0.33 m/s	0.18 m/s	0.15 m/s	0.25 m/s (flood)	0.83 m/s	2.5 %
S13	0.57 m/s	0.10 m/s	0.11 m/s	0.11 m/s (ebb)	0.42 m/s	0%
S14	0.69 m/s	0.10 m/s	0.15 m/s	0.20 m/s (ebb)	0.60 m/s	0%

Figure J- 3 Flow measurements in May and June of 1992 from Feeney (1995)

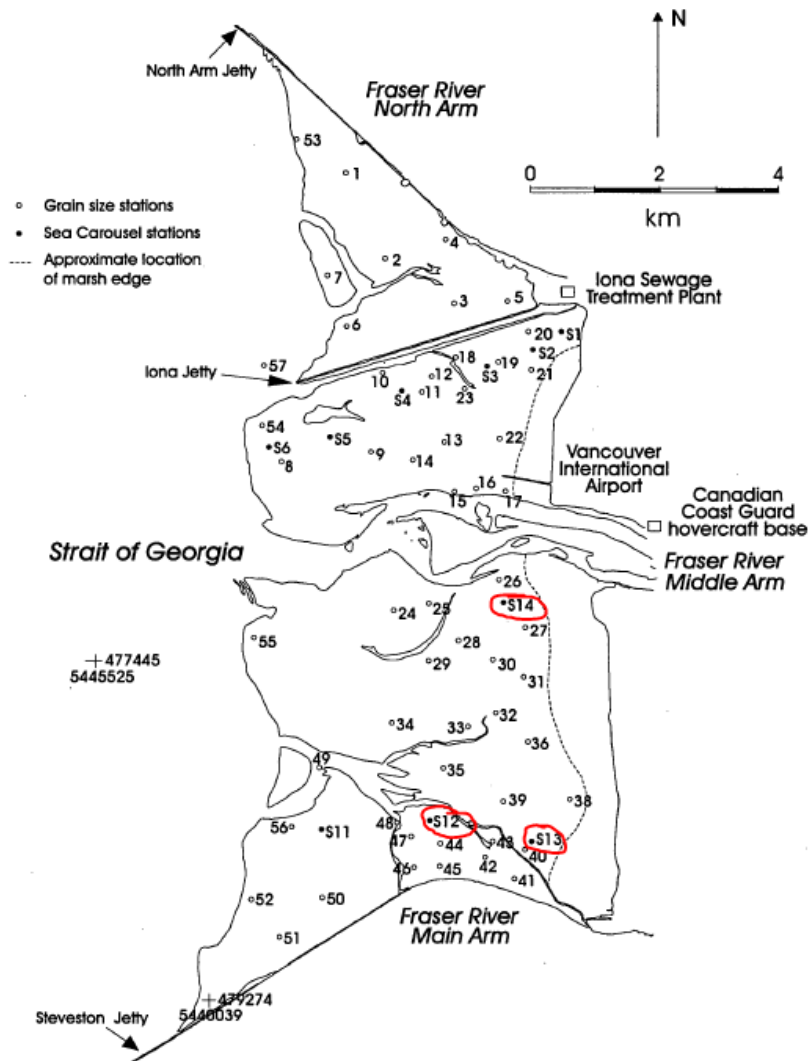


Figure J- 4 Measurement station from(Feeney, 1995)

Classification by van Rijn is based on transport (T) and grainsize (D*):

$$T = \frac{\tau'_{b,c} - \tau_{b,cr}}{\tau_{b,cr}}$$

$$D^* = d_{50} \left[(s - 1) * \frac{g}{\nu^2} \right]^{\frac{1}{3}}$$

Where

$$\tau'_{b,c} = \rho g \left(\frac{\bar{u}}{C'} \right)^2$$

$$C' = 18 \log \left(\frac{12h}{3d_{90}} \right)$$

$$s = \rho_s / \rho$$

Transport regime:		Particle size	
		1 < D* < 10	D* > 10
Lower	0 < T < 3	Mini-ripples	Dunes
	3 < T < 10	Mega-ripples and Dunes	Dunes
	10 < T < 15	Dunes	Dunes
Transition	15 < T < 25	Washed-out dunes, sand waves	
Upper	T > 25 Fr < 0.8	(symmetrical) sand waves	
	T > 25 Fr > 0.8	Plane bed and/or anti-dunes	

Table J- 1 Classification by Van Rijn (1993)

Using typical values for Sturgeon Bank:

$\tau_{b,cr}$	=	1	$\frac{N}{m^2}$	Critical bed-shear stress, estimated from (Feeney, 1995)
\bar{u}	=	Variable	$\frac{m}{s}$	Flow velocity
h	=	Variable	m	Water depth
d_{90}	=	330	μm	90 percentile grain size, sediment sample J5
d_{50}	=	210	μm	50 percentile grain size, sediment sample J5
ρ_s	=	2650	$\frac{kg}{m^3}$	Density of sediment

$$\rho = 1025 \frac{kg}{m^3} \text{ Density of water}$$

$$\nu = 10^{-6} \frac{N}{m^2} \text{ Kinematic viscosity}$$

Doing the calculations with representative values for Sturgeon Bank the following graph is obtained:

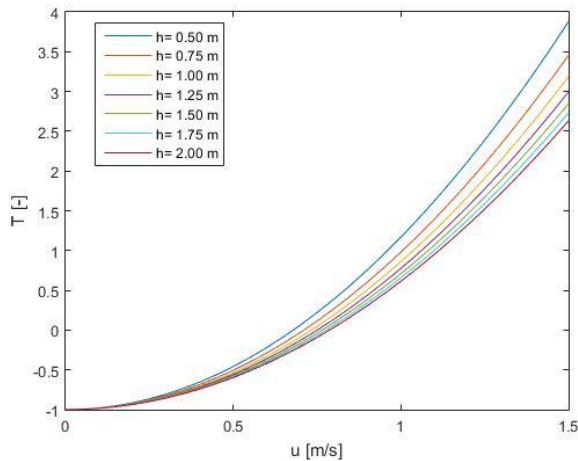


Figure J- 5 Flow velocity plotted against the dimensionless transport parameter T from Van Rijn (1993) for different water depths

From the calculations, it follows that $D^* = 5.24$. The combination of parameters required for the dune or sand wave class as defined in Van Rijn (1993) are never reached. A regime of mini-ripples is far more likely to be induced by the tide in combination with waves. Indeed, these have been encountered during the fieldwork.

The main conclusion is that the sand swells are primarily generated by wave action. Most probably the sand swells are generated during a rare combination of a spring tide and a large storm. Possibly more conditions are required to induce the transport required for large bedforms to form like a strong freshet resulting in turbidity and salinity gradients. Under normal conditions however the tidal flow and wave action are unable to transport the sediment on the sand swells and they remain a fairly stable feature of system.



Figure J- 6 Mini-ripples observed during the fieldwork

Once generated the sand swells are reworked further by drainage through connected troughs and colonization by plants on the crests. More research is needed to understand the conditions required for the generation of these bed forms as well as their interaction with tidal flows and vegetation over time

K. APPENDIX 11: VERTICAL REFERENCE DATUMS

Elevation datasets for Sturgeon Bank and its vicinity were provided in different reference systems. Hence there is a need to convert them to the same vertical datum to avoid errors. The vertical reference systems used are:

- Chart datum (CD)
- CGVD28
- CGVD2013

A passive control network is maintained by Natural Resources Canada which serve as benchmarks. By comparing the benchmarks with published elevations in both CGVD2013 and CGVD28 after the year 2000 the difference in datum was found to be 0.187 m.

Table K- 1 Benchmarks at Sturgeon Bank. Data was made available by Natural Resources Canada (2016)

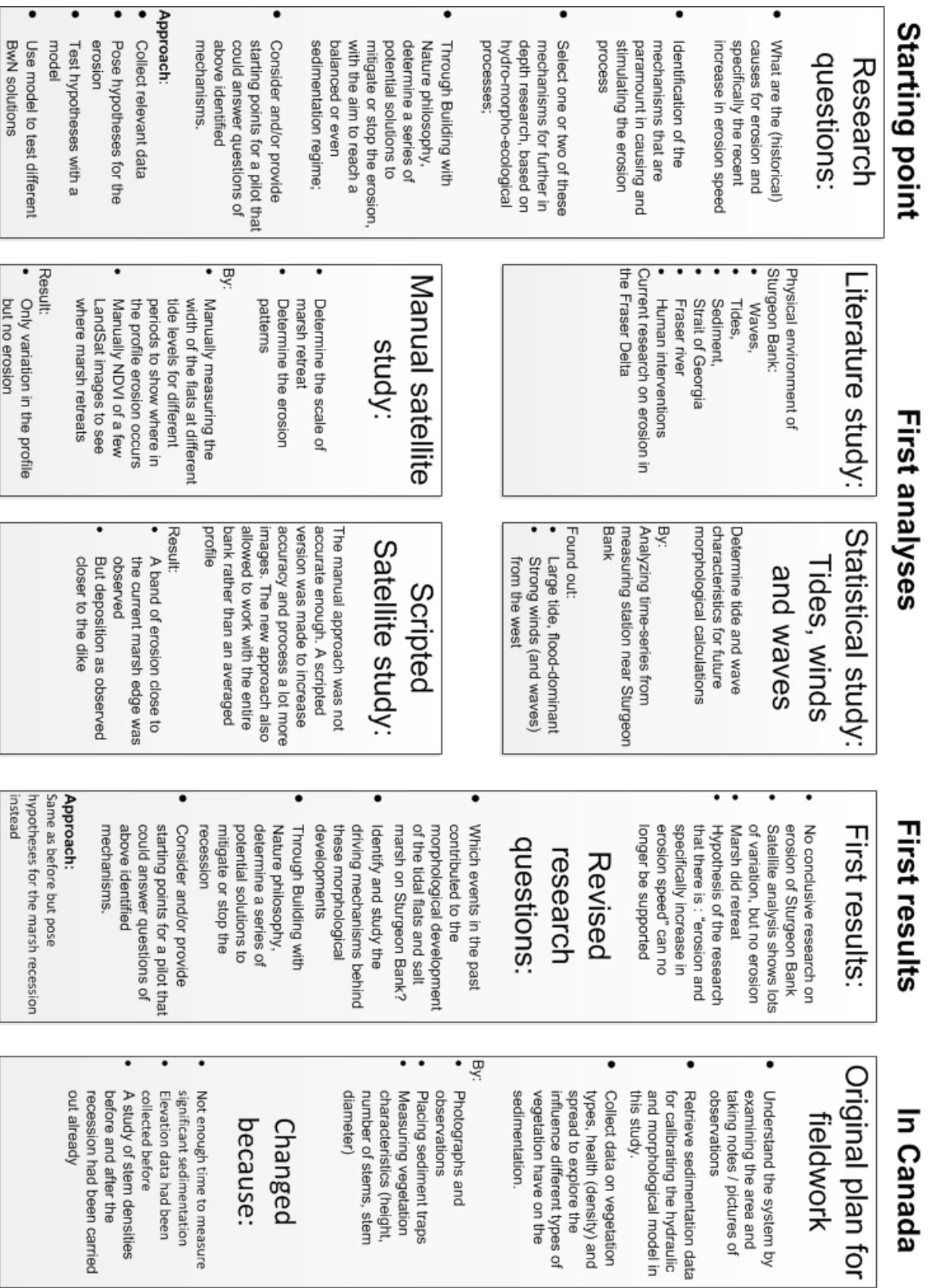
Location	Unique number	CGVD2013 elevation [m]	CGVD28 elevation [m]	Difference [m]
Steveston	19713	3.605	3.419	0.186
Terra Nova	77H4885	1.286	1.103	0.183
Coast guard station	B58081	3.442	3.249	0.193
Average:				0.187

The conversion to chart datum remained unclear. Both CGVD28 and CGVD2013 are defined as 0 at mean water level. CGVD28 bases the 0 on a select amount of reference tide stations while CGVD2013 determines it geodetically from the earth's gravitational field. It is simply assumed that 0 m +CGVD28 equals mean sea level over 0 m+ CGVD2013. However, a field study should be conducted to determine the right conversion between the reference systems.

Table K- 2 Conversion between vertical reference systems for Sturgeon Bank

CD [m]	CGVD28 [m]	CGVD2013 [m]
0	3.10	3.287
-3.10	0	0.187
-3.287	-0.187	0

L. APPENDIX 12: RESEARCH APPROACH



In Canada

Further analyses

Second results

Further analyses

Discussions with local experts

- Find out what has been measured/observed
- Receive new information about Sturgeon Bank and the marsh
- Share and discuss initial results
- Discussions with:
 - Port of Vancouver: Habitat enhancement program
 - Sean Boyd (Environment Canada)
 - Brent Gurd (FLNRO)
 - Rowland Atkins (Golder)
 - Derek Ray (Northwest Hydraulic Consultants)
 - Eric Balke (M.Sc. Student Simon Fraser University)
 - Chris Ilton (PhD. Simon Fraser University)

Process elevation measurements

- Analyze profiles
- Sand swells emerged as a prominent feature
- Compare current elevations with other measurements
- Conversion between reference system needed to established
- Result shows no net erosion in recent years
- Erosion/deposition pattern found suggesting moving sand swells

Results:

- New sources for literature study
- Recently very little net erosion/deposition
- Erosion/deposition pattern suggesting moving sand swells
- The bed near the marsh has become coarser
- Sturgeon Bank has poor drainage (no tidal channels in affected area)

New leading hypotheses:

- Migrating sand swells caused longer inundation resulting in loss of marsh
- Supported by the elevation and sediment analyses
- Excessive amounts of algae lead to the death of marsh plants
- Based on site observations of algae
- Strong winds from the west prevent drainage longer inundation and possibly loss of marsh
- Based on observation during fieldwork

Flow model

Intended as a way to predict drainage patterns and inundation to support/rule out hypotheses. Fieldwork showed areas can remain inundated at low tide due to wind and/or bathymetry while lower areas are dry.

- Very small cells (12x12m) required to capture sand swells and channels
- Flows at very small water depths (<10cm) are beyond the capabilities of the Delft-3D model
- Therefore no conclusion about inundation could be made
- The model does predict general flows on Sturgeon Bank and effects of sand wells and plants during the tide

Wave model

Make a prediction of the behavior of waves on Sturgeon Bank. This ties in with the results from literature about waves

- Setup:
 - No time left for a detailed model after the Delft-3D model failed to meet expectations. Hence only a very simplified model based on breaking was used
- Results:
 - Sand wells induce wave breaking at mean water level, shielding the area directly behind
 - No effect of sand swells at high water levels

Aerial imagery

Aerial imagery was made available by Environment Canada for the study

- Means to test results from the satellite study
- Study drainage feature over time (tidal channels and sand swells)
- Study the position and extent of marsh over time

Fieldwork

- Taking notes / pictures of observations
- Retrieve sediment to for the model and a comparative analyses with other studies
- Measure elevations and compare with previous studies to find erosion/deposition
- Found out that:
 - Sturgeon Bank has poor drainage, especially during strong winds from the west
 - Algae covered large parts of the marsh

Process Sediment

- Determine sediment distribution with methods from earlier studies
- By sieving
- Laser diffraction (not reliable)
- Sedimentation tests
- Compare with results from other studies
- Soil gets coarser

Setup model

Prepare a grid and bathymetry

Additional literature study

- Consult literature for:
 - Marsh growth/recession mechanisms
 - Particularly if algae can be a threat
 - Implement new sources from the time in Canada
- Found out:
 - Waves are important in marsh dynamics
 - Marsh behaviour is cyclic with many interlinking processes

Review satellite study

- Adjusted some parameters to match results on aerial imager.
- Reanalyzed results with new insights

Final hypotheses

Define mechanisms

There are many interactions that shape the system. A selection of the most important ones that could affect the marsh was made based on insights from all analyses and literature

Formulate hypotheses

Within the framework of defined interactions, promising hypotheses were formulated:

- Sediment deficit
- Sea-level rise
- Migrating sand swells
- Ponding (algae)

Discussions about causes

- With the committee the connections and hypotheses were extensively discussed
- The matter was discussed with a leading ecologist, Peter Herman

- Insight in the plausibility of mechanisms was gained:
- Algae not a cause of recession
 - Importance of inundation and elevation on plants

Final results

Evaluation of hypotheses

Based on the information of the analyses and literature an evaluation was made of each hypothesis.

- Result
- No hypothesis can fully explain the marsh recession
 - The big role of feedback between mechanisms became apparent

Conclusions

- No cause could be identified
- There is a need to integrate the hypotheses and feedbacks within the system in order to reach a conclusion for the marsh recession

Evaluation of feedbacks

Because feedback emerged as an important mechanisms these were reviewed as a new hypothesis.

- Results:
- Feedback mechanisms corroborate with most results
 - It gives no indication about the actual cause of the recession

Recommendations

- Studies to better quantify the identified mechanisms:
- Practical with a pilot
 - Theoretical with interaction between morphology and marsh

